MINERAL AGES AND METAMORPHISM

by
Stanley Robert Hart

S.B., Massachusetts Institute of Technology
(1956)
M.S., California Institute of Technology
(1957)

submitted in partial fulfillment
of the requirements for the
degree of Doctor of
Philosophy

at the
Massachusetts Institute of Technology
September, 1960

Signature of Author _____
Department of Geology and Geophysics, Aug. 19, 1960

Certified by _____
Thesis Supervisor

Accepted by _____
Chairman, Departmental Committee on Graduate Students

Mineral Ages and Metamorphism

Stanley R. Hart

submitted to
The Department of Geology and Geophysics
in partial fulfillment of the requirements for
the degree of Doctor of Philosophy

August 22, 1960

A general investigation of the effects of thermal metamorphism on isotopic mineral ages has been carried out. The diffusion rates of radiogenic argon have been determined by mass spectrometric measurements. The diffusion rates of argon in feldspar were determined both by this mass spectrometric method and by a radioactive argon 41 counting method. The difference between the two methods was marked, and suggests a limited usefulness for data obtained by radioactive argon counting techniques. The existence of two or more radiogenic argon phases in each mineral was established. The effective diffusion radius for argon in hornblende was shown to be fifteen times smaller than the average physical grain size. Muscovite heated in vacuum gave an argon diffusion coefficient 80% higher than muscovite heated under one kilobar of water pressure.

K-Ar ages on muscovite from a metamorphic area were found to be proportional to grain size. From the diffusion results obtained on this muscovite, a minimum temperature of 400° C can be assigned to the metamorphism.

Rb-Sr, K-Ar and U-Pb analyses of biotite, feldspar, hornblende, whole rock, and monazite samples from two contact metamorphic zones show age discordancies which can be related to parameters of the contact metamorphism. The shape and displacement of the various "mineral age" versus "contact distance" curves can be related to the relative daughter product diffusion parameters of the minerals. A simple model is presented which interprets discordant age patterns in terms of time, temperature and the mineral diffusion parameters.

Hornblende was shown in the contact study to have excellent argon retentivity. To test the general applicability of a hornblende K-Ar method, ten hornblendes and three pyroxenes,

ranging in age from 100 m.y. to 2600 m.y., were analyzed for K and Ar. The calculated ages are in excellent agreement with ages determined by other method s on associated minerals. The average potassium content of these hornblendes suggests that most hornblendes of Paleozoic age or older can be accurately dated by the K-Ar method.

Thesis Supervisor: P. M. Hurley
Professor of Geology

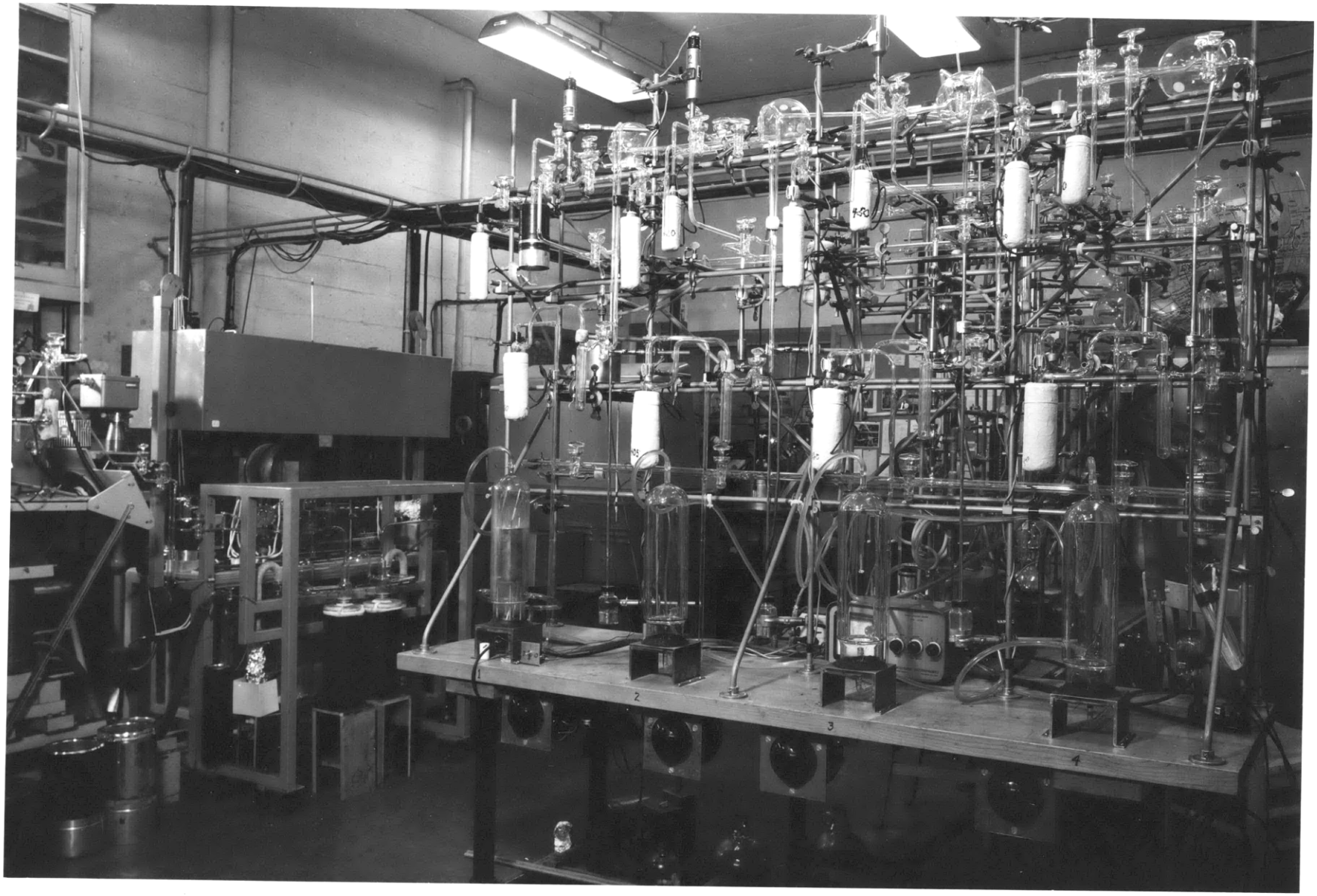
1
2
3
4

Table of Contents

Part Two

Illustrations

Part I

Chapter I

Chapter II

Chapter III

Part II

PART I

I. Some Diffusion Measurements Relating to the K-Ar Dating Method

Abstract

The diffusion rates of argon in muscovite, hornblende and pyroxene were determined by mass spectrometric measurement of the natural radiogenic argon released during isothermal heating. Diffusion rates of argon in a feldspar were determined both by this mass spectrometric method and a radioactive argon 41 method. The difference between the two methods was marked, and suggest a limited usefulness for data obtained by radioactive argon counting techniques. The existence of two or more argon phases in each mineral was established. The effective diffusion radius for argon in a hornblende was shown to be 15 times smaller than the average physical grain size. The diffusion coefficients for argon in muscovite heated in vacuum, and under 1 kilobar water pressure, were only 80% different. K-Ar ages on muscovite from a metamorphic area were found to vary in proportion to the grain size. From the diffusion results on this muscovite, a minimum temperature of 400° C can be assigned to the metamorphism.

Introduction

In the past five years over fifteen papers have been published dealing with the diffusion of argon in natural minerals. There is very little general agreement between different investigators, qualitative or quantitative. Many

basic questions remain unresolved and the existence of such disagreement makes any geologic application of the data meaningless.

The results of some diffusion measurements made on muscovite, feldspar, hornblende and pyroxene are reported in this paper. They are admittedly incomplete but serve to define some of the basic issues involved in the application of argon diffusion data to geologic systems.

Procedures

Two different methods were used. One involved the artificial production of argon 41 in potassium minerals by fast neutron irradiation, followed by counting measurements of the time-dependent discharge of radioactive argon during isothermal heating. The other involved mass spectrometric measurement of the natural radiogenic argon discharged from the minerals during isothermal heating.

Radioactive Argon Experiments

Eleven grams of orthoclase perthite from Massey, Ontario were sealed in a Plasticene tube and irradiated for ten minutes with fast neutrons in the M.I.T. cyclotron. The activity was allowed to decay for two hours, then the sample was transferred to an Inconel tube and sealed on to a vacuum system. The externally heated Inconel tube was brought to a temperature of 795° C in 15 minutes. The temperature was held at 795±10° C and the released activity measured with an external

G-M tube surrounded cylindrically by a glass counting volume. The counting volume was shielded with two to four inches of lead brick and the background counting rate was about 50 cpm. The gas activity during the run varied from background to 600 cpm. The background counting rate was checked periodically by pulling the gas out of the counting volume onto liquid nitrogen cooled charcoal. After 80 minutes of heating at 795° the temperature was increased to 1040° and heating continued until the decay rate equalled the diffusion rate. The sample was then fused to insure complete release, and the decay of the activity followed for two hours to demonstrate that the activity was argon 41. Extrapolation of this final decay curve to time zero allowed computation of the fractional amount of argon released at any given time.

Radiogenic Argon Experiments

The apparatus used for these measurements consisted of a Kanthal wound furnace which was enclosed in a water jacketed bell jar and connected to a high vacuum purification train. A sample charge of two to ten grams, contained in an alundum crucible, was placed in the furnace and the furnace evacuated overnight. The samples were outgassed for several hours at 250 to 350° C. The furnace was then isolated from the pumps, about 1×10^{-5} cc stp of enriched argon 38 was added, and the temperature raised as quickly as possible to the desired level. As soon as this temperature was reached, a cut of the gas in the furnace was obtained by expansion into

a large volume. The gas remaining in the furnace was pumped out (one to two minutes), another spike added and collection continued. The furnace temperature was maintained during all these procedures. The cut of gas in the expansion volume was purified on hot copper oxide and titanium. The isotope ratios were measured with a Reynolds-type glass tube mass spectrometer which is connected to the purification system. All succeeding sample cuts were measured in the same way. Heating was continued for twelve to thirty-six hours, with from four to six cuts of gas measured. The sample was finally fused to release the remaining argon and this was purified and measured as above. The temperatures were held constant to within ten degrees, and the platinum and platinum-10% rhodium thermocouples frequently calibrated at the melting point of pure copper. The accuracy of the radiogenic argon measurements varied from ±2% to perhaps ±50%, depending on the amount of air contamination. The air corrections were 50 to 90% for the muscovite runs, 3 to 50% for the feldspar runs and 30 to 98% for the hornblende runs.

Treatment of Data *

The cumulative fraction of argon released for each heating interval was computed. Then for each value of F a corresponding value of Bt was calculated from

$$F = 1 - \frac{6}{\pi^2} \sum_{n=1}^{\infty} \left[\frac{1}{n^2} \exp(-n^2 Bt) \right] \qquad 1.$$

where $Bt = \frac{\pi^2 D t}{a^2}$, and a is the radius of the sphere.

* See also Page 119.

This is the solution of Fick's law for diffusion from a homogeneous sphere with initial uniform concentration of argon, and uniform concentration of argon at the surface at all times (taken equal to zero). The equations for diffusion from a cylinder or a slab could be used with equal facility and justification. Reichenberg (1953) gives a tabulation of numerical values for the spherical diffusion equation solution.

The values of Bt determined from equation 1 were plotted versus time on linear graph paper. For diffusion of argon at a single value of the diffusion coefficient the experimental points should fall on a straight line intersecting the origin; the slope of the line being proportional to the diffusion coefficient of the argon. However, the experimental values were found to invariably define two or more intersecting straight lines. This was interpreted (after Gerling, 1957, and Amirkhanov et al., 1959b) as independent diffusion of two or more argon phases, each with a characteristic activation energy. In order to calculate a diffusion coefficient for a given straight line segment, an extrapolation and subtraction of the argon from the preceeding and the following segments must be made. By successive corrections the diffusion coefficient for each argon phase can be calculated, as well as the proportion of argon making up each phase. Identification of the various phases at each temperature can be made from this proportion of total argon that they represent. The experimental curves are consistent with this inter-

pretation of non-coupled volume diffusion from different structural sites. However, this interpretation could not be proven unique.

Results

The analytical data for the diffusion runs is tabulated in Tables 1 to 3 and plotted as values of Bt versus t in Figures 1 to 5.

Feldspar Results

Orthoclase crypto-perthite from Massey, Ontario, with a median grain size of about 200 microns, was used for both radioactive and radiogenic argon diffusion measurements. The radioactive argon 41 results are shown in Fig. 1, the radiogenic argon 40 results are shown in Fig. 2. Segment A in Fig. 1, 795° and 1040° C, shows loss of argon at a single value of the diffusion coefficient. Segment B cannot be assigned to diffusion from a second site, as this can only take place with a smaller value of B (slope). The segment B must be related to a change, or changing of structure and could be caused by mixing of the two phase feldspar. However, the absence of a similar increased slope for the radiogenic argon, Fig. 2, indicates that segment B is probably related to effects caused by the neutron irradiation, rather than a homogenizing of the perthite. As a test of possible mixing, samples of this feldspar were heated at 810°, 900° and 1050° C for times up to forty-five minutes. X-ray diffraction measurements of

Table1

Analytical Data for Feldspar Diffusion Runs

Temp. °C.	Cut No.	Σt(min.)	Radiogenic Ar^{40} (cc stp/g)	ΣAr^{40r}	Fraction of Total	Bt (spherical)
300-810	1	35	1.40×10^{-4}	1.40×10^{-4}	0.293	0.088
815	2	82	0.360	1.76	0.368	0.147
815	3	238	0.210	1.98	0.413	0.191
815	4	378	0.0966	2.07	0.433	0.214
815	5	638	0.131	2.20	0.461	0.247
1110	Fusion	(30)	2.58	4.78	1.0	—
2 gram sample						
400-940	1	19	relative ratios measured		0.450	0.234
960	2	75	only - no absolute stan-		0.525	0.340
960	3	184	dard used.		0.620	0.522
960	4	330			0.720	0.798
960	5	584			0.837	1.32
960	6	1318			0.885	1.67
1120	Fusion	(30)			1.0	—
~10 gram sample						

Table 2

Analytical Data for Hornblende Diffusion Runs

Temp. °C.	Cut No.	Σt(min.)	Radiogenic Ar^{40} (cc stp/g)	ΣAr^{40r}	Fraction of Total	Bt (spherical)
300-650	1	60	1.05×10^{-6}	1.05×10^{-6}	0.0158	0.000215
645	2	326	0.116	1.17	0.01753	0.000265
645	3	1261	0.295	1.46	0.0220	0.000417
645	4	1603	< 0.180	< 1.64	< 0.0246	< 0.000522
845	5	1723	0.258	1.90	0.0388	0.00133
1150	Fusion	(20)	62.9	64.8	1.0	—
8 gram sample						
200-855	1	30	2.70×10^{-6}	2.70×10^{-6}	0.0439	0.00171
870	2	152	0.257	2.96	0.0481	0.00204
870	3	309	0.492	3.45	0.0561	0.00281
870	4	384	0.120	3.57	0.0580	0.00300
870	5	586	0.697	4.27	0.0694	0.00433
870	6	1466	1.00	5.27	0.0855	0.00660
1140	Fusion	(16)	56.5	61.5	1.0	—
6 gram sample						
300-840	1	50	2.19×10^{-6}	2.19×10^{-6}	0.0360	0.00115
855	2	140	0.292	2.482	0.0408	0.00147
855	3	244	0.356	2.838	0.0467	0.00193
855	4	354	0.0372	2.875	0.0472	0.00197
855	5	697	0.830	3.705	0.0610	0.00332
1130	Fusion	(14)	57.1	60.8	1.0	—
4 gram sample						

Table 3

Analytical Data for Muscovite & Pyroxene Diffusion Runs

Temp. °C.	Cut No.	Σt(min.)	Radiogenic Ar^{40}(cc stp/g)	ΣAr^{40r}	Fraction of Total	Bt (spherical)
0-270	1	(40)	$< 5x10^{-8}$	—	< 0.0005	—
270-600	2	142	$3.27x10^{-6}$	$3.27x10^{-6}$	0.0319	0.00087
615	3	524	5.40	8.67	0.0846	0.0064
615	4	1329	2.98	11.65	0.114	0.0118
615	5	1995	1.81	13.46	0.131	0.0159
615	6	2865	0.84	14.30	0.139	0.0180
1190	Fusion	(30)	86.7	101.0	1.0	—
2 gram sample - muscovite						
230-755	1	65	$1.52x10^{-5}$	$1.52x10^{-5}$	0.140	0.0183
750	2	145	1.00	2.52	0.231	0.0525
750	3	265	0.779	3.30	0.303	0.0949
750	4	509	0.677	3.97	0.365	0.144
750	5	781	0.715	4.69	0.432	0.212
750	6	1381	0.848	5.54	0.510	0.316
1200	Fusion	(30)	5.33	10.8	1.0	—
2 gram sample - muscovite						
250-890	1	36	$1.52x10^{-6}$	$1.52x10^{-6}$	0.165	0.0257
905	2	249	4.30	5.82	0.630	0.545
910	3	581	(.145-.78)	(6.0-6.6)	(0.65-.715)	(0.594-0.78)
1190	Fusion	(10)	2.32	9.23*	1.0	—
4 gram sample - pyroxene						

* value obtained in a previous run used because of uncertainty introduced by large air correction on Cut No. 3.

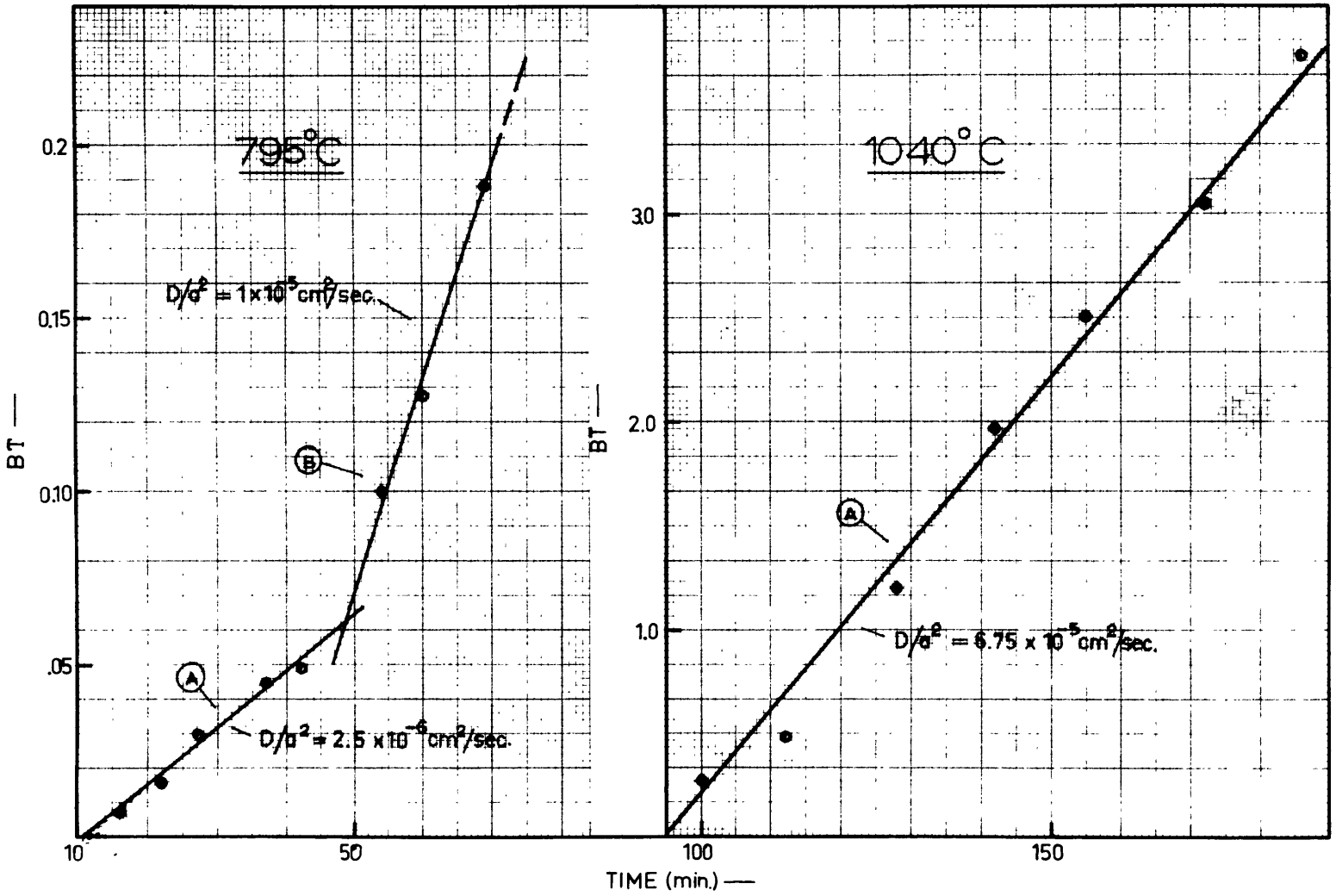

FIG. 1 - POINTS FROM DIFFUSION EQUATION SOLUTION

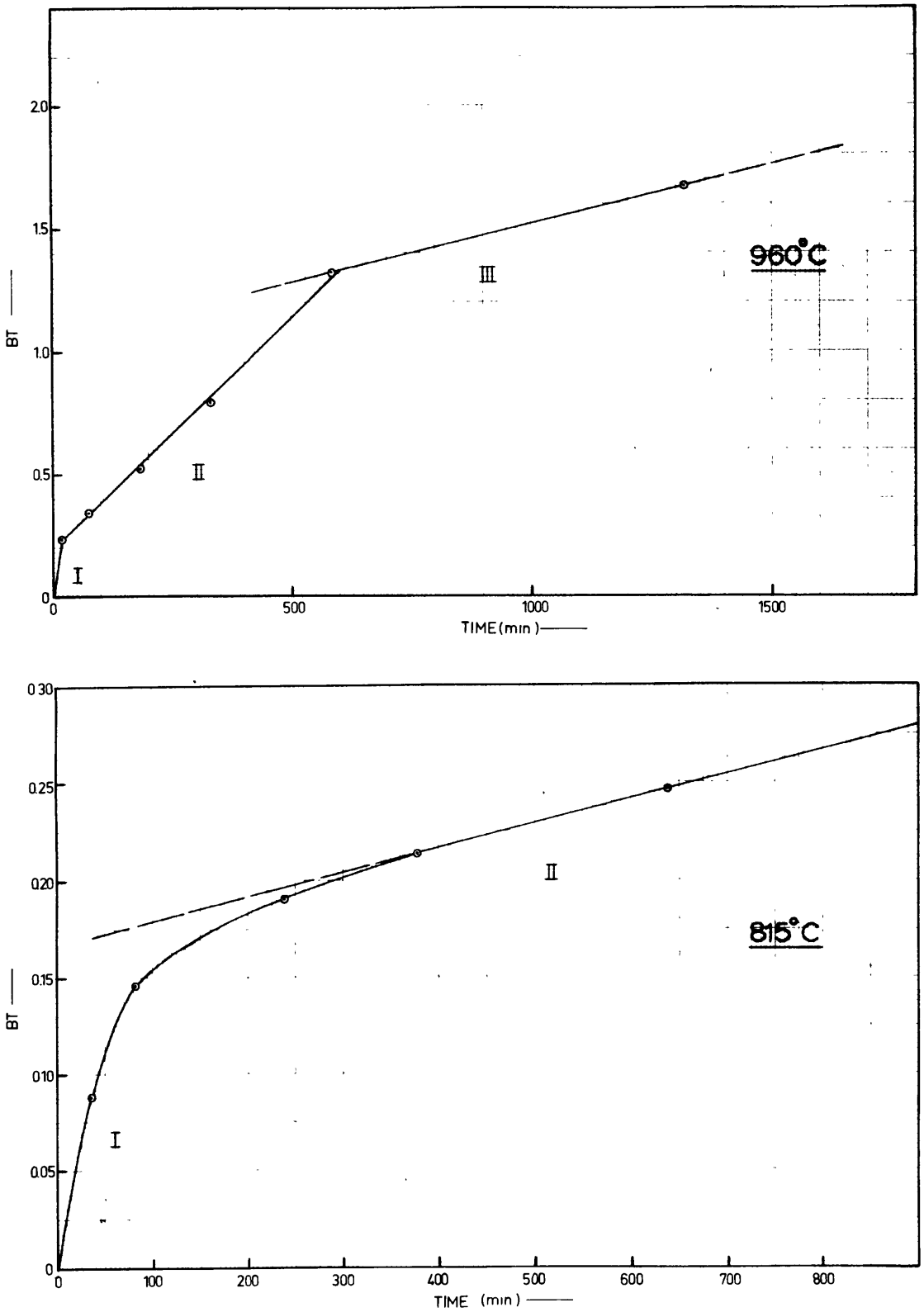

FIG. 2 — FELDSPAR DIFFUSION CURVES, 815°C, 960°C.

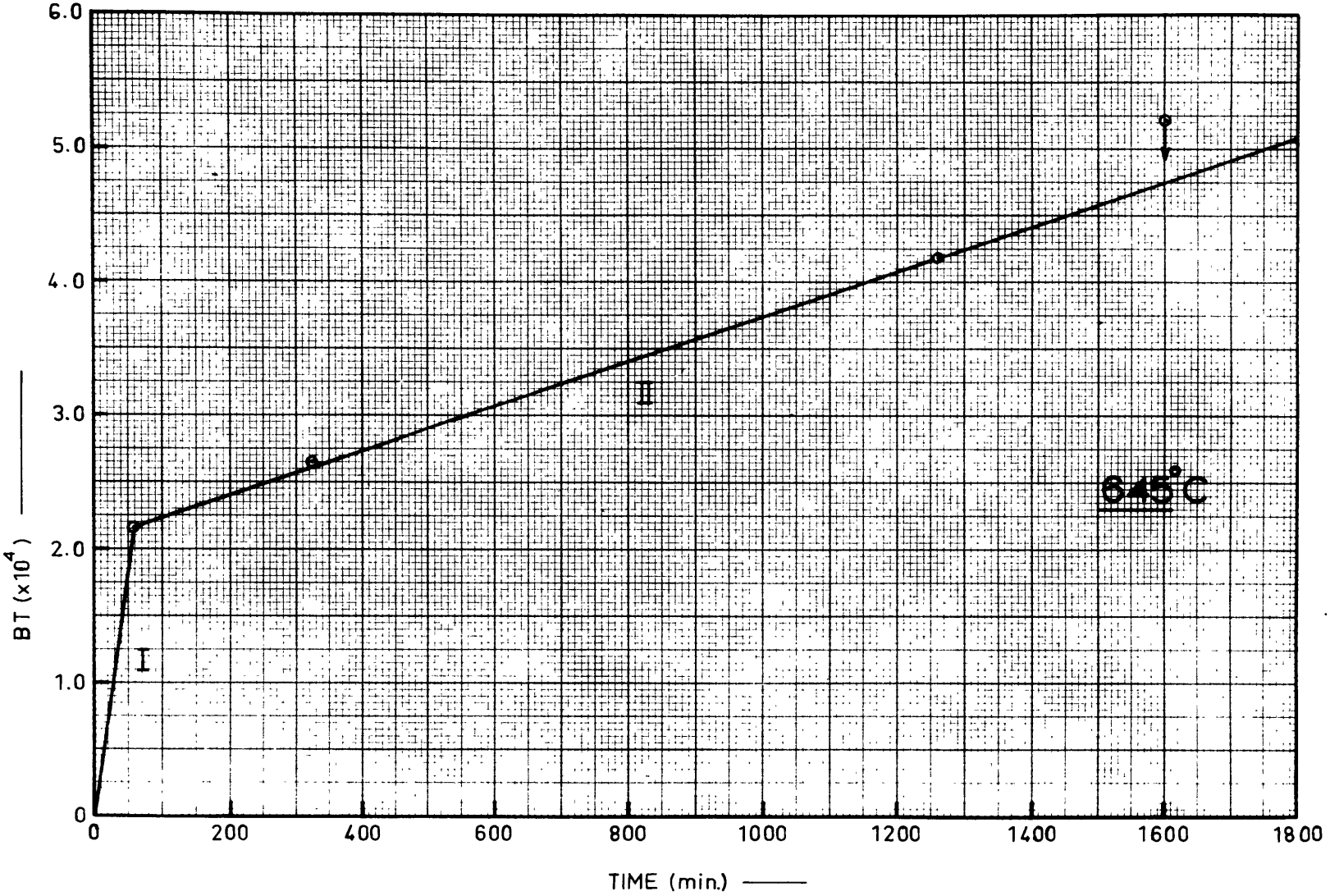

FIG.3 — HORNBLENDE DIFFUSION CURVE

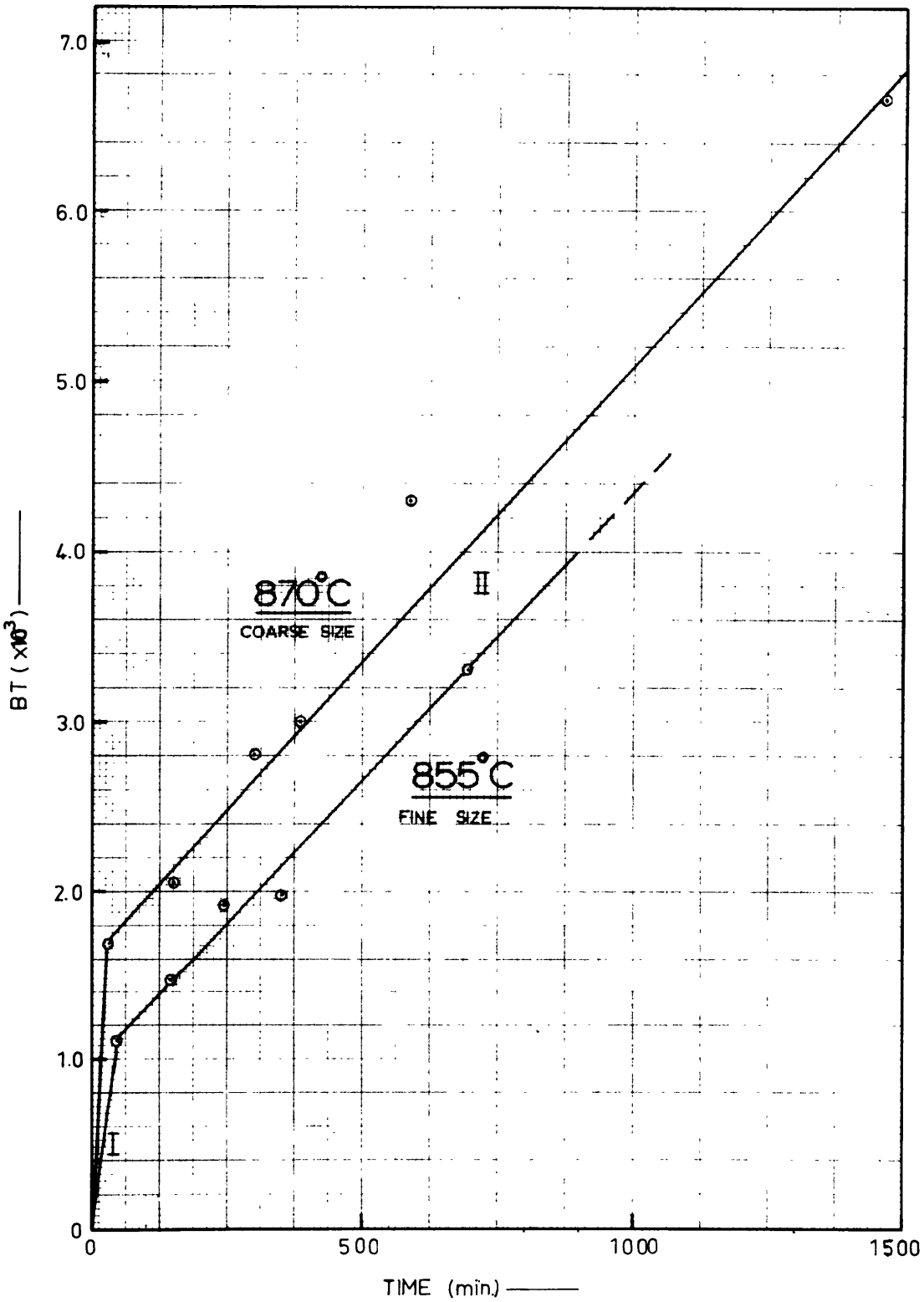

FIG. 4 – HORNBLENDE DIFFUSION CURVES

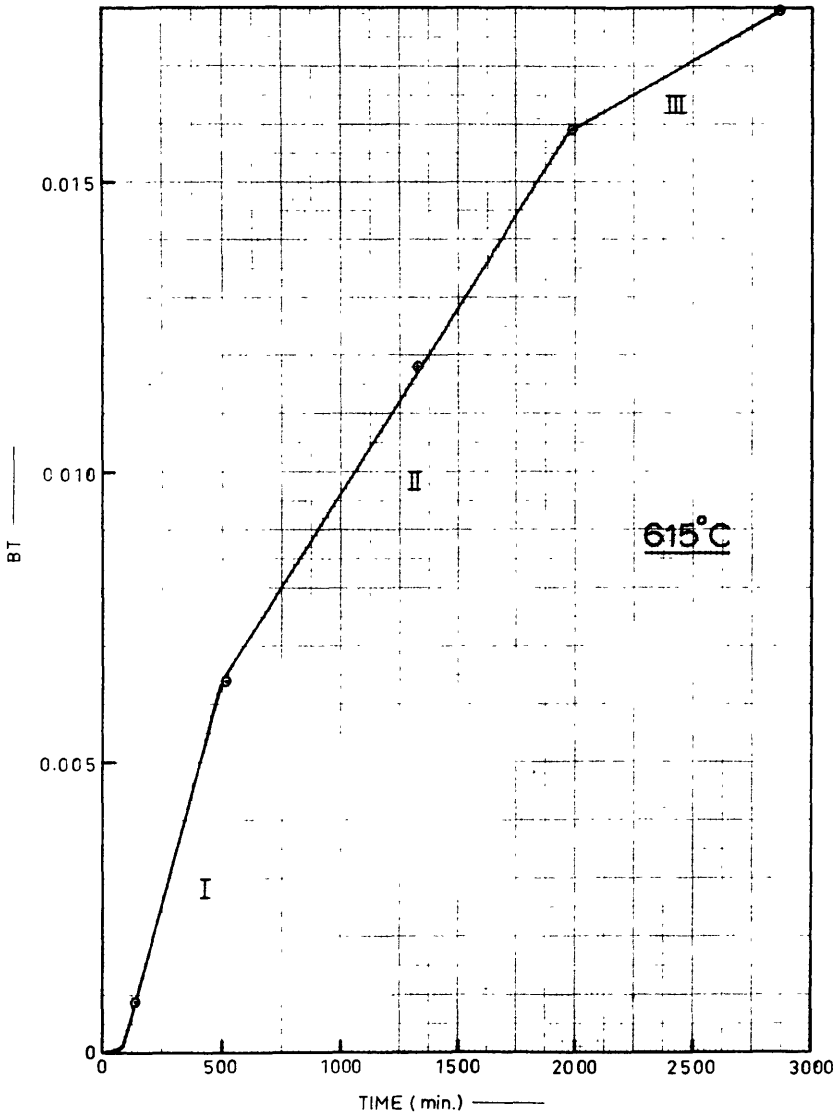

FIG. 5 - MUSCOVITE DIFFUSION CURVE

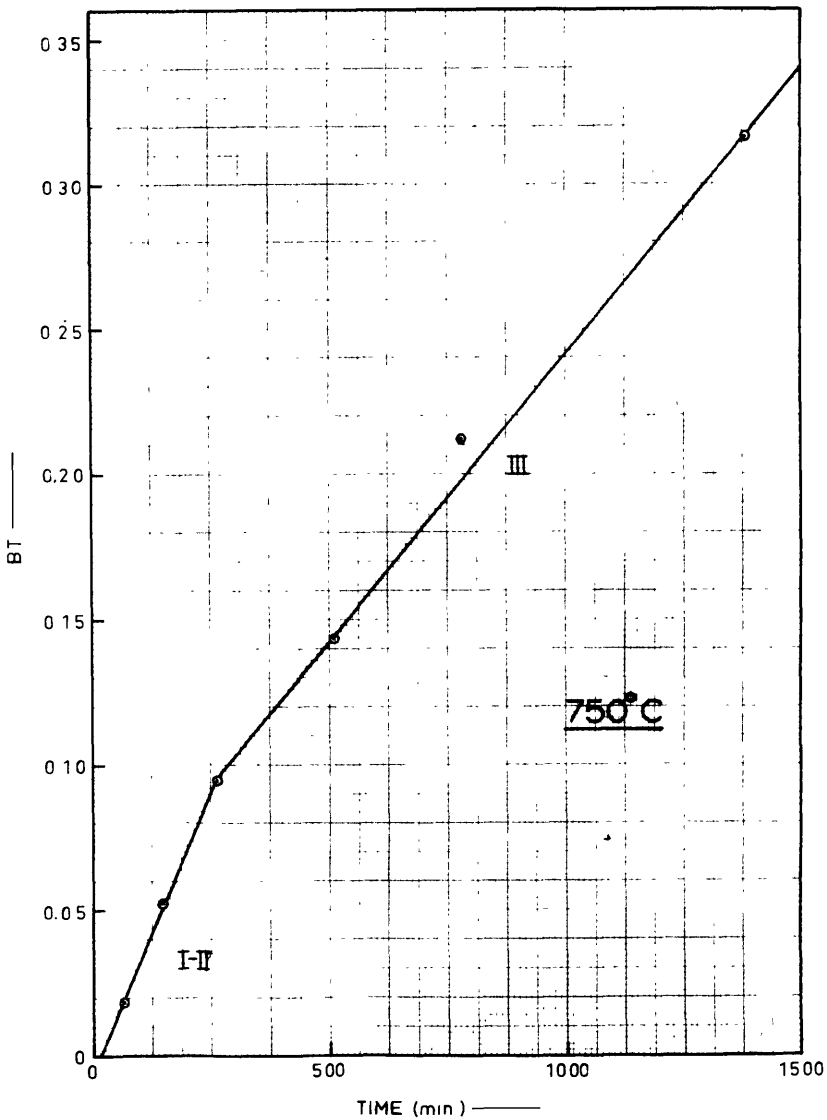

FIG. 5 - MUSCOVITE DIFFUSION CURVE

the ($\bar{2}01$) albite and orthoclase reflections indicated no measurable change in composition.

The radiogenic argon curves of Fig. 2 indicate the presence of three distinct argon phases. The calculated diffusion coefficients and activation energies* for the three phases are presented in Table 4.

Table 4: Feldspar Diffusion Parameters

	815°		960°		Activation Energy (per mole)
Phase	Fraction	D/a^2	Fraction	D/a^2	
I	31%	$5.6\times10^{-5}\,sec^{-1}$	32%	$>2.2\times10^{-5}\,sec^{-1}$	
II	~50%	$2.5\times10^{-7}\,sec^{-1}$	48%	$3.2\times10^{-6}\,sec^{-1}$	46 Kcal
III	not observed		<20%	$<4.7\times10^{-7}\,sec^{-1}$	

The diffusion curves for radioactive argon and radiogenic argon are basically different. There is no indication of more than a single radioactive argon phase whereas there are at least three radiogenic argon phases. Disregarding radiogenic phaseI which does not represent true volume diffusion, the diffusion coefficients of radiogenic phase II are an order of magnitude smaller than the diffusion coefficients of the radioactive argon. The activation energy is the same, however. It would appear that the neutron irradiation has caused an increase of the diffusion coefficient of the radioactive argon. This could be accounted for by the increased

* The term "activation energy" as used throughout this paper is defined by the relation $\mathcal{D}=D_0\exp(-Q/RT)$, where D_0 and R are constants, and Q is the activation energy.

number of defects, i.e. a decrease in the effective radius for diffusion. Diffusion results obtained by neutron activation procedures would seem to have little direct application to natural systems. Fechtig et al. (1960) measured the diffusion coefficients of radioactive argon 37 in four calcium minerals. They state, "since the series of measurements were reproducible several times, one can suspect that radiation damage effects do not occur to a large extent." Geological interpretations based on this a priori proof are difficult to justify.

This one feldspar run represents the only diffusion measurements made using radioactive argon 41. The method was explored because of its inherent sensitivity but was discontinued for the reasons stated above. The following results were obtained using natural radiogenic argon.

Hornblende Results

The sample used for these measurements was obtained from an amphibolite layer in the Precambrian Idaho Springs formation of Colorado. X-ray and microscopic examination revealed no biotite impurity. The sample did contain a few percent diopside. Two sizes were prepared by crushing and sieving. One had a grain size of 140 to 300 microns, the other a grain size of 44 to 53 microns. The analytical data (Table 2) is plotted in Figs. 3 and 4 as values of Bt versus t. The low argon content of this hornblende, coupled with very small diffusion coefficients, resulted in low accuracy for many of the measurements.

The curves indicate the presence of at least two argon phases. Phase I corresponds to a relatively rapid loss of a few percent. It is not possible to rule out the existence of higher activation energy phases, since less than 8% of the total argon was released during any of the heatings. The D/a^2 value determined for the fine size sample at 855° C was only 50% higher than that determined for the coarse size sample, while the two size fractions differed by a factor of twenty in their physical (a^2) value. This is considered proof that the effective radius for argon diffusion in this hornblende is less than 30 microns. The average physical radius measured in thin section is about 500 microns. Table 5 summarizes the diffusion parameters for this hornblende.

Table 5: Hornblende Diffusion Parameters

	645°	855° Fine	870° Coarse
Fraction in Phase I	1.4%	2.3%	3.3%
D/a^2 phase I	$>4.8\times10^{-9}$ sec^{-1}	$>2.6\times10^{-8}$ sec^{-1}	$>2.6\times10^{-8}$ sec^{-1}
D/a^2 phase II	7.4×10^{-11} sec^{-1}	2.8×10^{-9} sec^{-1}	3.6×10^{-9} sec^{-1}

Activation Energy, phase I ~15 Kcal/mole, phase II ~34 Kcal/mole.

Muscovite Results

Results of an age variation versus grain size study of a muscovite from Clarendon, Vermont are reported in the next section. The 74-140 micron size fraction of that suite was used for these diffusion measurements. This sample contained

about 10% calcite and chlorite. impurities. The analytical data is presented in Table 3 and plotted in Fig. 5. Three argon phases are distinguished. The first phase does not exhibit the rapid loss which is characteristic of phase I in the feldspar and hornblende. The first two phases are unresolved in the 750° C run. Table 6 summarizes the diffusion parameters measured for muscovite.

Table 6: Muscovite Diffusion Parameters

	615° C		750° C		Activation Energy (per mole)
Phase	Fraction	D/a^2	Fraction	D/a^2	
I	9%	$2.4 \times 10^{-8}\ sec^{-1}$	17%	$6.4 \times 10^{-7}\ sec^{-1}$	47 Kcal
II	3%	$1.0 \times 10^{-8}\ sec^{-1}$			
III		$< 3.1 \times 10^{-9}\ sec^{-1}$	~70%	$3.4 \times 10^{-7}\ sec^{-1}$	>63 Kcal

Hydrous minerals heated under vacuum are clearly unstable. Before argon diffusion results on hornblende, muscovite, etc. can be used to interpret geological phenomena, the effect of water loss in vacuum should be established. Evernden et al. (1960) found that the diffusion coefficients measured for argon in glauconite heated under vacuum were 1000 times larger than for argon in glauconite heated under 1000 to 10,000 p.s.i. water pressure. To test muscovite in the same way, a two gram charge was heated in a Tuttle-type cold seal bomb under 1 kilobar water pressure. The temperature was held at 710° C for seventy-two hours and the argon remaining at that time extracted and measured. The sample was found to have lost 32% of its argon during this treatment, compared to approximately

52% loss for comparable vacuum heating. This corresponds to a difference of 80% in the diffusion coefficients. The difference between this and the factor of 1000 observed by Evernden for glauconite probably reflects the greater stability of muscovite with respect to water loss. The magnitude of this effect is not predictable though, and diffusion data obtained on hydrous minerals in vacuo cannot be given direct geologic application. The data is valid only as a maximum limit.

Pyroxene Results

To test the retentivity of pyroxene for argon, a sample of pure pyroxene from the Sudbury gabbro was heated at 905° C for ten hours. The grain size of the sample was 140 to 300 microns. The analytical data is given in Table 3. The argon occurs in at least two phases. The first phase contains 45% of the total argon and gives a D/a^2 value of $4 \times 10^{-6} sec^{-1}$. The second phase has a D/a^2 value of less than $2 \times 10^{-6} sec^{-1}$.

Discussion of Diffusion Results

The results of all the diffusion measurements are shown plotted in Fig. 6 as values of D/a^2 versus 1000/T K. Straight line joins between various temperatures are assumed though there is no proof that the join is not curved or even discontinuous. The slope of the joins is proportional to the activation energy. Fig. 7 [illegible] shows a comparison of this data with data published by Amirkhanov et al. (1958, 1959a,b,c,d).

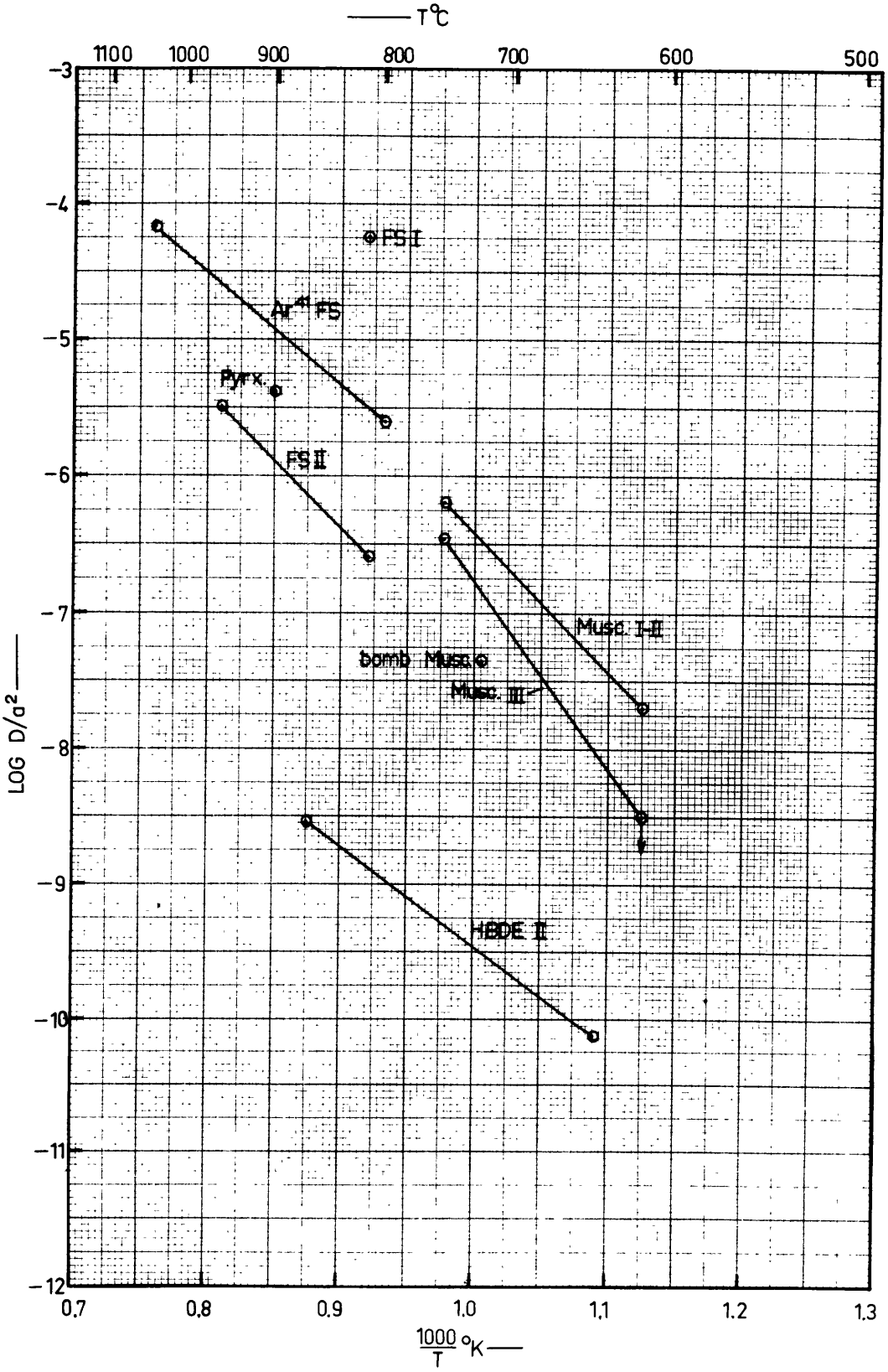

FIG. 6 — DIFFUSION COEFFICIENTS VS. TEMPERATURE

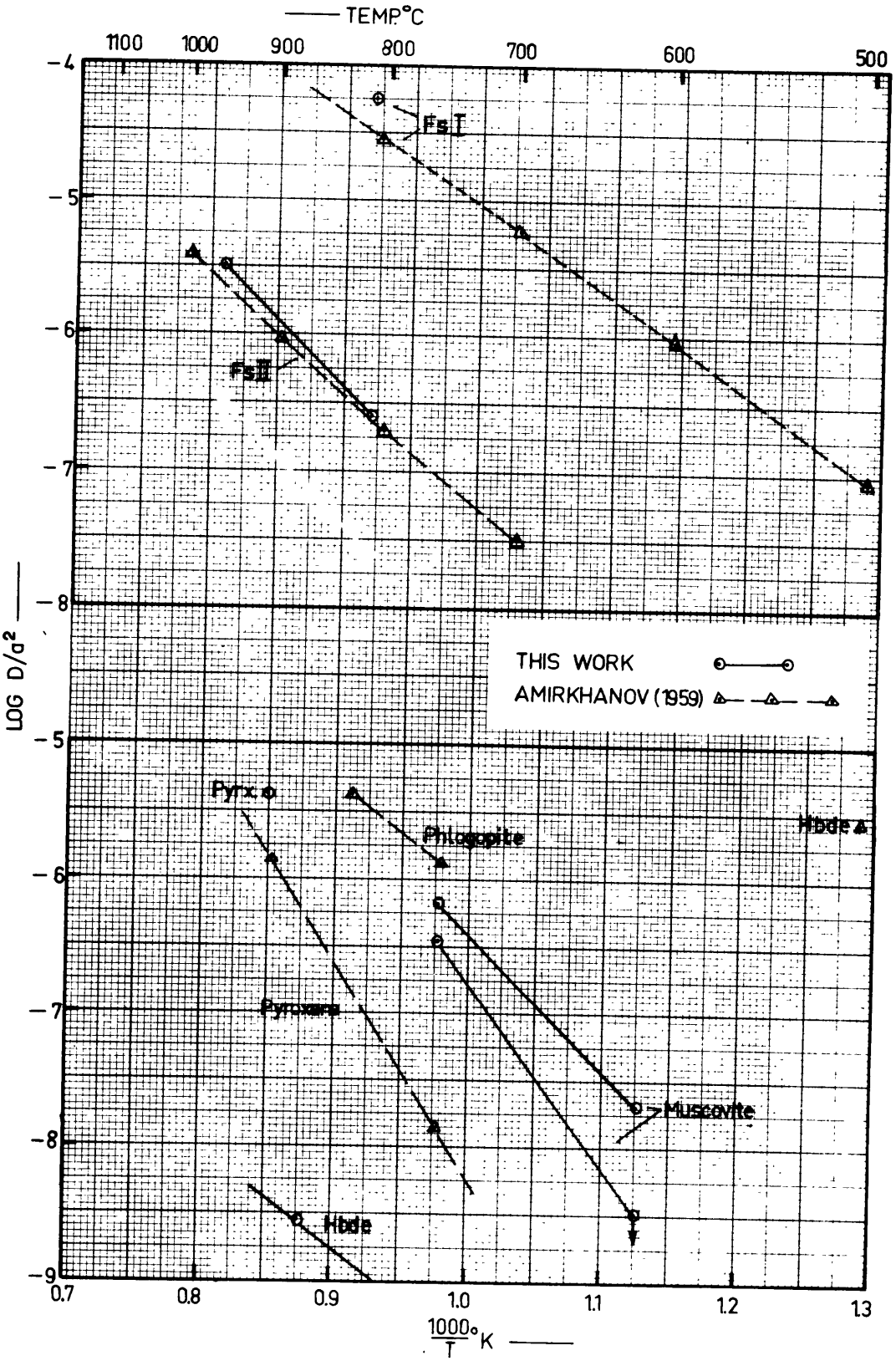

FIG. 7 —COMPARISON OF DIFFUSION RESULTS

The agreement is excellent except for the hornblende points. His hornblende was from a pegmatite and it is possible that the effective radius for diffusion was much smaller. Regarding the number of argon phases and their relative proportions, the data of this paper is also in general accord with that of Amirkhanov (above) and Gerling (1957, 1958). Evernden et al. (1960) recognized only a single position for argon in phlogopite, glauconite and feldspar. Their data unfortunately was obtained in such a way that it was impossible to resolve the argon into phases. The knees which they observe in their D versus 1/T curves are no doubt caused by these argon phases in different activation states, as are those observed by Fechtig et al. (1960). Both these investigators measured only a single release of argon at each temperature. To properly resolve the argon from different sites it is necessary to follow the complete release of argon at a single temperature.

Variation of Apparent Age with Grain Size

Diffusion loss of argon in minerals is in part a function of the term D/a^2, where a is the effective radius of diffusion. In some minerals the effective diffusion size may be the same as the physical grain size. The diffusion results on hornblende, presented earlier, indicated a diffusion size which was much smaller than the physical size. Evernden et al. (1960) demonstrated the same thing for sanidine. They also suggested that micas might have a diffusion radius approaching

that of the physical radius. If so, the argon loss from micas during a metamorphism should depend strongly on the grain size of the mica.

To test this possibility, muscovite from a Precambrian marble which had undergone metamorphism during the Paleozoic was separated on the basis of grain size and the age of each grain size fraction determined. The marble was collected by W. H. Pinson from the Precambrian Mount Holly series near Clarendon, Vermont. The marble was crushed and screened into five size fractions. Muscovite was separated from these size fractions by magnetic and heavy liquid methods. Sample splits for Rb-Sr analysis were washed in cold 6NHCl for thirty minutes. The analytical data is presented in Table 7.

Table 7: Analytical Data for Muscovite Grain Size Analyses

Sample Number	Grain Size	K%	$*Ar^{40}$ (in 10^{-4} cc stp/g	$*Ar^{40}$ / Total Ar^{40}	Rb (ppm by wt)	$*Sr^{87}$ (ppm by wt)	$*Sr^{87}$ / Total Sr^{87}
—	4mm-10mm	8.26	2.67	0.96			
C	-10+20	8.93	2.25	0.94			
D	-28+40	7.81	1.56	0.85			
B	-50+100	5.29	0.816	0.92	274	0.489	0.156
A	-100+200	6.26	1.02	0.82	282	0.485	0.140

* Radiogenic

The calculated ages and the estimated median grain radii are given in Table 8.

Table 8

Calculated Muscovite Ages and Grain Radii

Sample Number	Approximate Median Radius (microns)	K-Ar Age (m.y.)	Rb-Sr Age (m.y.)
—	3500	675±25	
C	690	545±20	
D	250	440±15	
B	110	350±10	430±30
A	55	360±10	410±30

The K-Ar ages show a consistent decrease with decreasing grain size. The two smallest sizes A and B are interpreted as having undergone complete loss of argon at 355 m.y., the time of metamorphism. The Rb-Sr ages may indicate complete loss at a different time, or an age variation may exist which is masked by the experimental error. A factor of four in the grain radius should theoretically be sufficient to produce the observed K-Ar age variation from 675 m.y. to 355 m.y. The variation instead occurs over a range of grain size of about a factor of thirty-five. This may be accounted for by the presence of considerable ground-down coarse material in the finer fractions. It is clear that an age variation exists. The problem is to determine over what range of grain size it occurs. It is also clear that the effective diffusion radius is larger than 690 microns, possibly much larger.

Several cases have been reported in the literature where muscovite from a pegmatite shows an older age than muscovite in

the country rock cut by the pegmatite (Gerling, 1957; Wasserburg et al., 1959). These can be explained by the relatively greater diffusion loss from the finer country rock muscovite during a post-crystallization metamorphism.

Using the age data of Table 8, and extrapolated muscovite diffusion data from Fig. 6 it is possible to calculate the time-temperature history of Paleozoic metamorphism at Clarendon, Vermont. The calculated temperature is relatively insensitive to the estimated duration of metamorphism, changing only 30° C for a change in time interval from 5 m.y. to 50 m.y. A factor of two error in the D/a^2 value only changes the temperature by 10 to 15° C. For a 10 m.y. metamorphism, the temperature is calculated to be 425° C. If a knee occurs in the Fig. 6 muscovite extrapolation, the temperature would be higher. This study shows then that the temperature of Paleozoic metamorphism at Clarendon, Vermont, was almost certainly greater than 400° C. This is a reasonable estimate.

Acknowledgments

The author wishes to thank W. H. Pinson for providing the sample of Mount Holly series marble. H. W. Krueger provided much help in the preparation of the muscovite suite. G. H. Curtis of the University of California, Berkeley, kindly provided the author with preprints of their diffusion data. H. Faul of the U.S. Geological Survey, furnished the author with several muscovite samples and age data from

Vermont. Special thanks are due P. M. Hurley, without whose help and encouragement this work would not have been possible.

References Cited

Amirkhanov, Kh. I., S. B. Brandt, E. N. Bartnitskii, V. S. Gurvich, and SA. Gasanov, 1958, "On the Question of the Preservation of Radiogenic Argon in Glauconite", Doklady, ANSSSR, vol. 118, No. 2, Geochemistry series.

Amirkhanov, Kh. I., E. N. Bartnitskii, S. B. Brandt, and G. V. Voitkevich, 1959a, "On the Migration of Argon and Helium in Several Rocks and Minerals", Doklady, ANSSSR, vol. 126, No. 1, Geochemistry series.

Amirkhanov, Kh. I., S. B. Brandt and E. N. Bartnitskii, 1959b, Diffusion of Radiogenic Argon in Feldspars", Doklady, ANSSSR, vol. 125, No. 6, Geochemistry series.

Amirkhanov, Kh. I., S. B. Brandt, E. N. Bartnitskii, S.A. Gassanov, and V. S. Gurvich, 1959c, "On the Mechanism of losses of Radiogenic Argon in Micas", Izvestiia, ANSSSR No. 3, Geological Series.

Amirkhanov, Kh. I., S. B. Brandt, E. N. Bartnitskii, and S. N. Voronovskiia, 1959d, "Diffusion of Radiogenic Argon in Sylvite", Geokhimiia, ANSSSR, No. 6.

Evernden, J. F, G. H. Curtis, R. W. Kistler, and J. Obradovich, 1960, "Argon Diffusion in Glauconite, Microcline, Sanidine, Leucite, and Phlogopite", in press.

Fechtig, H., W. Gentner, and J. Zahringer, 1960, "Argon Determinations on Potassium Minerals, VII, Diffusion of Argon in Minerals and its Effect on Potassium-Argon Age Determinations", Geochim, et Cosmochim. Acta, Vol 19.

Gerling, E. K., 1957, "Argon Method of Age Determination and its Application in Precambrian Geology", UNESCO Int. Conf. on Radioisotopes in Sc. Research, Paris.

Gerling, E. K., and I. M. Morozova, 1958, "Determination of the Activation Energy of Liberation of Argon from Micas", Geokhimiia, No. 4

Reichenberg, D., 1953, Properties of Ion-Exchange Resin in Relation to their Structure, III, Kinetics of Exchange", J. Amer. Chem. Soc., Vol 75.

Wasserburg, G. J., and G. W. Wetherill, "Ages in the Precambrian of Death Valley, California", 1959, annual meetings, A.G.U. Abstract.

II A Study of Mineral Ages in a Contact Metamorphic Zone

Abstract

Rb-Sr, K-Ar and U-Pb analyses of biotite, feldspar, hornblende, whole rock and monazite samples from two contact metamorphic zones show age discordancies which can be related to parameters of the contact metamorphism. The shape and displacement of the various "mineral age" versus "contact distance" curves can be related to the relative diffusion parameters of the minerals. A simple model is presented which interprets discordant age patterns in terms of time, temperature and mineral diffusion parameters.

Introduction

Almost a complete range of mineral age discordancies has been observed in certain "mixed-age" or "noisy" areas. Ages by the same method on different minerals and by different methods on the same mineral may all be discordant. The discordancies may even vary in sign from area to area. Most of the mixed-age areas which have been previously encountered are the result of regional metamorphism. In these areas it is not generally possible to relate age discordancies to specific environmental factors. A study of mineral ages in a contact metamorphic zone should permit a correlation of observed age discordancies with at least one variable, the temperature.

Contact zones where the country rock is markedly older than the intrusive and yet not affected by regional metamorphism contemporaneous with the intrusive are somewhat uncommon. The best area which could be found is in the Front Range of Colorado where Laramide stocks cut rocks which retain a Precambrian age of 1200 to 1400 m.y. (Aldrich et al., 1958b). The Monteregian intrusives of Quebec, Canada, and the Paleozoic intrusives in the Green Mountains of Vermont are other possibilities. Sample collections were made across contact zones of two of the Laramide stocks in the Front Range. A discussion of preliminary results has been given previously (Hart, 1960).

Geology

The crystalline core of the Front Range is composed essentially of Precambrian granite, schist and gneiss. The oldest of these is the quartz-biotite and quartz-biotite-sillimanite schist of the Idaho Springs formation. These schists are cut by an extensive series of Precambrian granitic batholiths. These granitic rocks are in order of decreasing age, Quartz monzonite gneiss, Granite gneiss, Boulder creek granite, Pikes Peak granite, and the Silver Plume granite.

Cutting these Precambrian rocks of the Front Range is a series of about ten major stocks, Paleocene or Eocene in age. These stocks occupy a narrow belt extending southwestward across the Front Range. This belt is paralleled some miles

to the south by a highly mineralized zone containing most of the early Tertiary ore deposits of the Front Range. Most of the stocks have been intruded upward at a steep angle and some undoubtedly represent old volcanic throats. There is no evidence in the area for any significant thermal regional metamorphism since the Precambrian.

Sample Description and Location

Two contact localities were sampled in August, 1959. The Audubon-Albion stock, five miles west of Ward, Colorado and about seven square miles in surface area, intrudes both the Idaho Springs formation and the Silver Plume granite. Fig. 1 is a sample location map for samples collected across the western contact zone, near Lake Isabelle. Thirteen samples of schist were taken over a distance of 300 feet, and six samples of granite were taken over a distance of 150 feet. The only macroscopic contact effect observed was an absence of sillimanite in the schist in a fifty foot zone near the contact. The contact itself is exposed and knife sharp.

The Eldora stock, one mile west of Eldora, Colorado, has a tabular projection one-half mile long and 1000 feet wide in contact with the Idaho Springs formation. Fig. 2 is a location map for nine samples which were collected here over a distance of 250 feet. The contact is gradational over a ten foot zone, and many xenoliths and ghost structures of

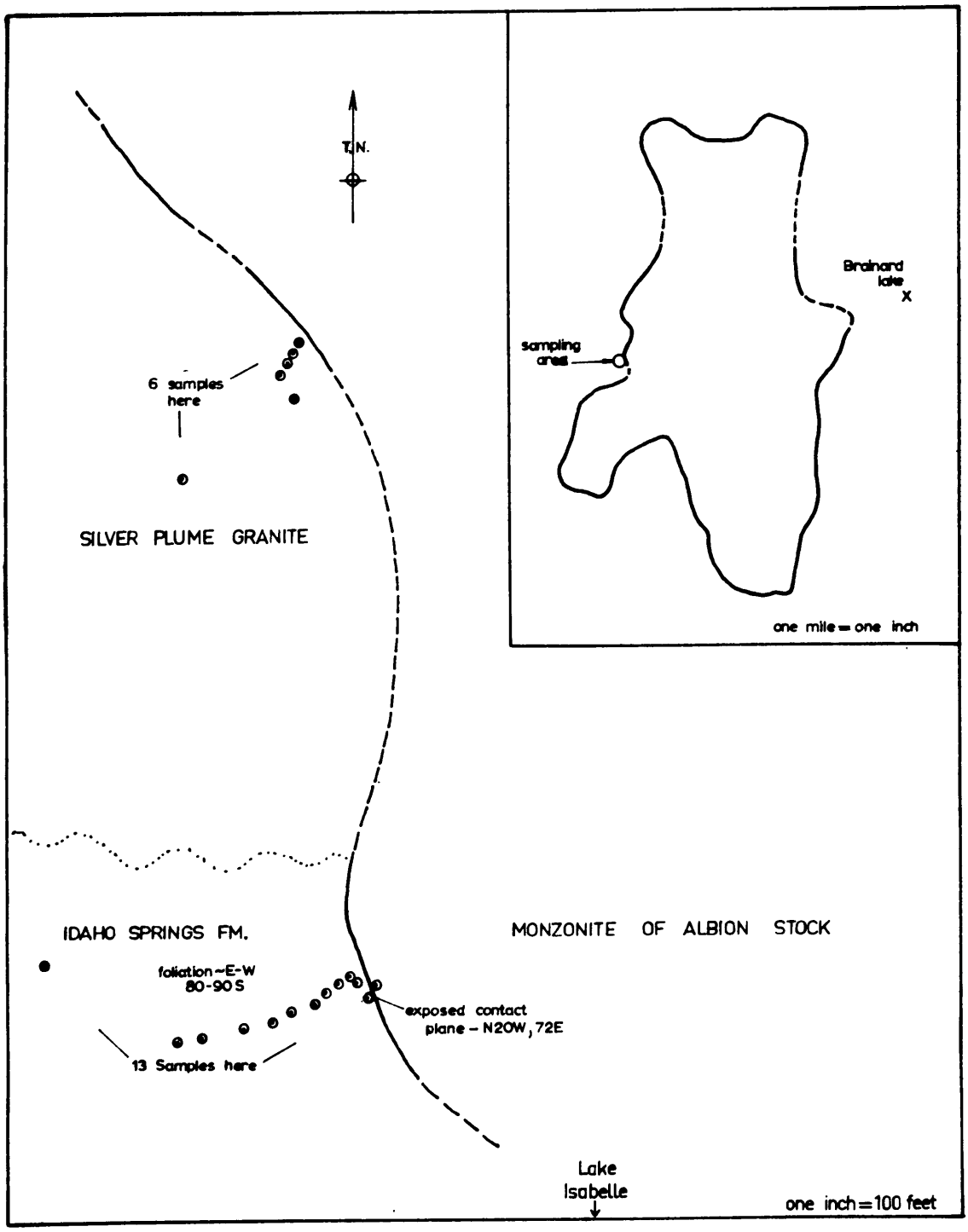

FIG. 1 —SAMPLE MAP, AUDUBON-ALBION AREA, FRONT RANGE, COLORADO.

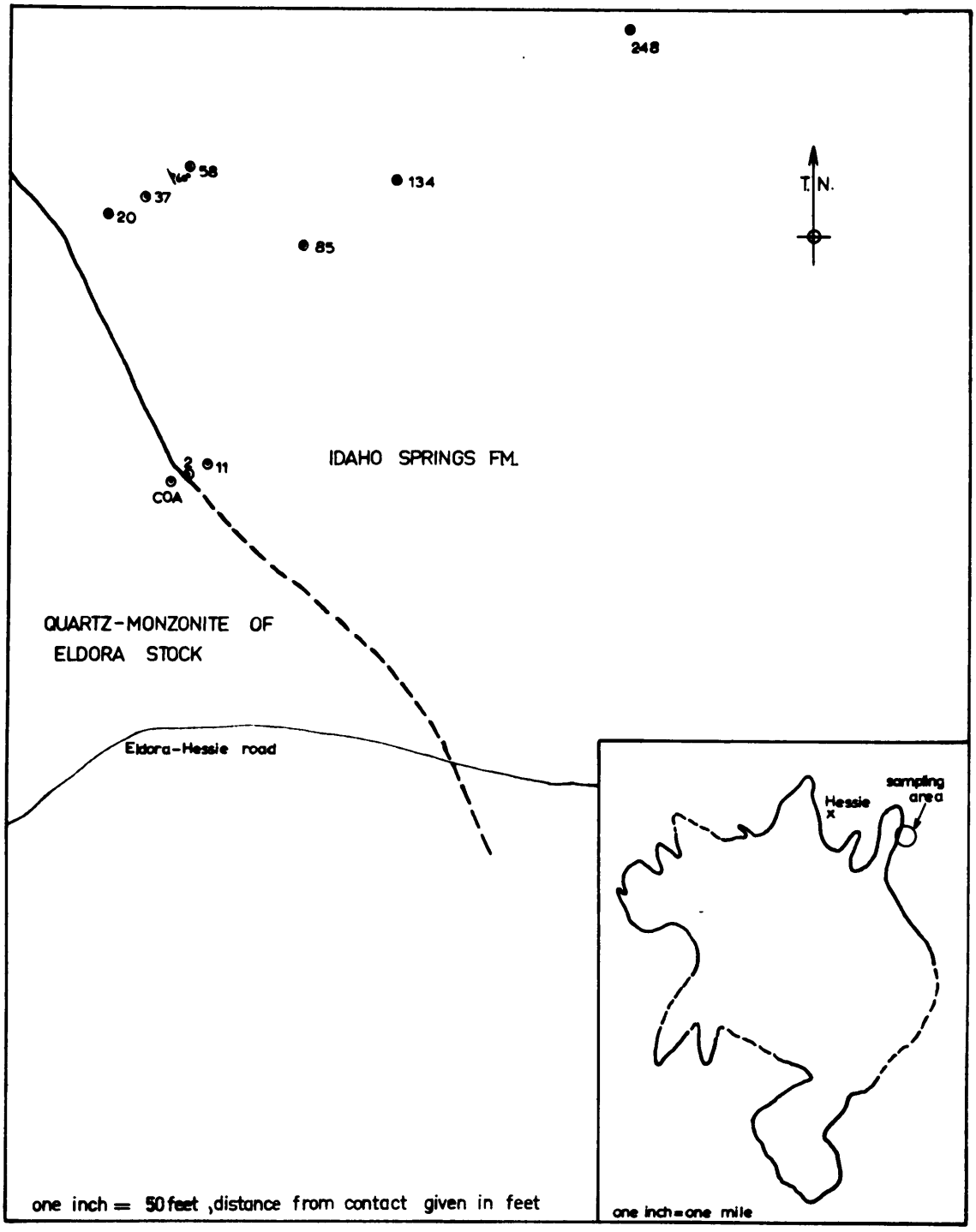

FIG. 2 —SAMPLE MAP, ELDORA AREA, FRONT RANGE, COLORADO

schist are present in the quartz monzonite intrusive. The foliation in the schist is irregular for a distance of fifty feet from the contact, and many pegmatitic stringers and quartz veins are present in this zone. This contact zone is markedly different from the Audubon-Albion contact zone. The difference may be accounted for by the more salic nature of the Eldora stock, more fluids associated with the intrusion, a higher intrusive temperature, or emplacement earlier in the orogenic cycle. The lateral variation of the schist in this contact zone allowed several rock types to be collected at each location; usually a pegmatitic phase, and an amphibolitic segregation.

The following table gives the sample number (distance from contact) and the mineral assemblages observed in thin section. The phases are listed in order of decreasing abundance in the section.

A0A	Oligoclase, orthoclase, quartz, hornblende, biotite, magnetite and sphene
A6A	orthoclase, quartz, albite, biotite, magnetite and garnet
A12A	biotite, quartz, orthoclase, garnet, magnetite and albite
A18A	same as A12A
A23A	quartz, biotite, albite, orthoclase, magnetite, garnet, chlorite, chloritoid.
A38A	quartz, orthoclase, albite, biotite, magnetite and garnet
A51A	quartz, albite, biotite, orthoclase, magnetite and garnet
A74A	Sillimanite, quartz, orthoclase, biotite, albite, magnetite and chlorite

A88A Quartz, sillimanite, biotite, albite, orthoclase and magnetite

A122A Quartz, orthoclase, sillimanite, biotite, magnetite and chlorite

A152A Quartz, orthoclase, sillimanite, biotite, albite, magnetite and chlorite

A169A Albite, quartz, orthoclase, biotite, magnetite and sillimanite

A300A Orthoclase, quartz, albite, biotite, magnetite, garnet, muscovite and sillimanite

C0A Oligoclase, quartz, orthoclase, hornblende, biotite, epidote, sphene and magnetite

C2A Oligoclase, hornblende, epidote, magnetite, sphene, biotite, quartz and orthoclase

C11A Hornblende, oligoclase, traces of magnetite and biotite

C20A Feldspar, quartz and biotite (pegmatite lens)

C37A Same as C20A

C58A Same as C20A

C85A Same as C20A

C134A Hornblende, oligoclase, diopside, magnetite and quartz

C248A Hornblende, andesine, diopside, magnetite, epidote and quartz

4088 Sample of Idaho Springs formation from junction of Routes 6 and 40, five miles east of Idaho Springs. Biotite quartz schist with coarse feldspar-quartz stringers.

Discussion of Petrography

In the Audubon-Albion contact suite there are two distinct assemblages. Up to sample A74A the rocks contain garnet but no sillimanite; beyond that, sillimanite but no garnet. It is believed that this is a retrograde reaction,

sillimanite (plus other phases) →Garnet, related to thermal contact effects. The "coexistence" of garnet, muscovite orthoclase and sillimanite in sample A300A clearly indicates another reaction of the same type. This suggests the presence of a second thermal source some distance beyond, and unrelated to the exposed contact itself.

The abundance of rimmed plagioclase, sphene, and biotite alteration of hornblende in sample C2A (Eldora) is an indication of the gradational nature of the contact. The absence of pyroxene from C11A, and the traces of biotite alteration of hornblende suggests a retrograde reaction related to the contact metamorphism.

Analytical Techniques

Concentrates of biotite and hornblende were obtained from the ground samples by a combination of magnetic and heavy liquid treatments. The hornblende samples other than C2A were quite pure, containing only traces of pyroxene. The hornblende from C2A contained appreciable (5 to 10%) biotite impurity. The varying potassium content of the biotites largely reflects varying sample purity. The main impurity was sillimanite with unliberated magnetite inclusions.

Two to ten gram samples for argon analysis were outgassed in vacuum for one-half hour at 300 to 375° C. Tests indicate that no argon loss occurs during this treatment. The samples were then fused to a glass, without flux, in a resistance-wound vacuum furnace. Enriched argon 38 was used as the

isotope dilution spike. The released gases were purified on hot copper oxide and titanium sponge. The pure argon sample was then run on a Reynolds-type mass spectrometer which is directly coupled to the purification line. The background peak at mass 36 accounted for 2 to 10% of the total mass 36 gas peak. Extensive tests have shown that this 36 background is not appreciably affected by the introduced gases as long as they are free of hydrogen. Precision of the argon analyses in the biotite age range of 50 to 150 m.y. is 2 to 3%, and somewhat better for older samples. Accuracy is on the order of 1%, as indicated by a comparison of results obtained on an interlaboratory standard biotite.

The potassium analyses were made using a Perkin-Elmer flame photometer, with lithium internal standard. Duplicate solutions were made up in all but two cases. Reproducibility, as indicated by these duplicate analyses, is about 1% for the biotites and 1.5% for the hornblendes. The accuracy of the biotite potassium analyses is believed to be better than 1%, as indicated by analyses of standards. The hornblende potassium analyses may be systematically high by as much as 4%. A comparison with isotope dilution analyses on several samples proved ambiguous.

The rubidium and strontium analyses were made using isotope dilution techniques. The precision and accuracy of the rubidium analyses is better than 2%, as indicated by replicate analyses on an interlaboratory shelf solution.

Separate strontium isotope ratio measurements were made on the whole rock samples. The overall error for the determination of the radiogenic strontium content in the whole rocks is estimated to be about 6%. In the biotites, the error is about 4%.

Results and Discussion

The analytical data for all the measurements which were made is presented in Table 1.

Audubon-Albion Contact Zone

With the exception of biotites A88A and A122A, the average of the other five is 66.3 m.y. with a standard deviation of 4% and a standard error of 1.7%. This is about the spread which would be expected from experimental error. These five biotites are interpreted as having lost all their argon at the time of intrusion, and serve to date the Audubon-Albion stock at 66.3 ± 2 m.y. Biotites A88A and A122A have retained some argon. Their position in between samples which show complete loss suggests the presence of an unexposed heat source beyond 300 feet or so. It was previously mentioned that the mineral assemblage in A300A also suggested a secondary thermal source. The Rb-Sr age of 89 m.y. on Biotite A300A is changed to 78 m.y. when the intersection point of the biotite-whole rock radiogenic growth lines is used. The experimental error very nearly overlaps the biotite argon age on this sample, and indicates very little if any retention of radiogenic strontium.

Table 1.

Analytical Data for Colorado Contact Suites

Sample Number	Grain Size	Mineral	K %	*Ar^{40} (10^{-5} cc Stp/g)	*Ar^{40} / Total Ar^{40}	Rb (ppm wt.)	*Sr^{87} (ppm wt)	*Sr^{87} / Total Sr^{87}	K-Ar Age (m.y.)	Rb-Sr Age (m.y.)
A0A	-50+100	Biotite	4.84, 5.15	1.42	0.69				70±2	
A38A	+50	Biotite	7.52	2.04	0.77				66±3	
A74A	-50+100	Biotite	7.49, 7.59	2.02	0.47				65±2	
A88A	-50+100	Biotite 1	5.68, 5.85	2.70	0.73				114±4	
	-50+100	Biotite 2	5.59, 5.78	2.48	0.71				106±4	
	-100+200	Feldspar	9.77, 10.22	1.90	0.86				40±1	
	-50	Whole Rock				342	2.25(I.R.) 2.18(I.D.)	0.138(I.R.)		1650±120
A122A	-50+100	Biotite	6.55, 6.58	2.34	0.56				87±2	
A152A	-28+40	Biotite	5.82, 5.83	1.64	0.72				69±2	
	-50	Whole Rock				392	1.45(I.R.) 1.14(I.D.)	0.208(I.R.)		940±75
A169A	-100+200	Biotite	7.25, 7.24, 7.31	1.88	0.41				63±2	
A300A	-50+100	Biotite	6.83, 6.92	1.82	0.68	1240	0.457(I.D.)	0.174(I.D.)	65±3	89±7
	-50	Whole Rock				284	1.51(I.R.) 1.65(I.D.)	0.101(I.R.)		1340±60
C2A	-100+200	Hornblende	1.18	0.553	0.60				114 (unfused)	
				0.598	0.40				123±5	
C11A	-50+100	Hornblende	0.77, 0.79	3.84	0.91				950±35	
C58A	2-10 m.m.	Biotite	7.34, 7.48	2.06	0.83	907	1.15(I.D.)	0.31(I.D.)	68±2	305±15
C134A	-50+100	Hornblende	1.02, 1.07	6.65	0.94				1160±40	
C248A	5-10 m.m.	Biotite	7.34, 7.46	2.43	0.69	888	1.52(I.D.)	0.37(I.D.)	80±2	410±20
	-50+100	Hornblende	1.01, 1.06	6.56	0.85				1150±40	
4088	+50	Biotite	7.39, 7.61	38.3	0.98				970±30	

* Radiogenic

The three whole rock Rb-Sr ages are widely scattered and show that the chemical system represented by the samples collected was not a closed system. The ages are therefore not necessarily meaningful, though they do illustrate the range of mobility of radiogenic strontium during metamorphism.

Table 2 shows the analytical data and calculated ages for a U-Pb analysis of monazite from sample A169A.

Table 2

Analytical Data and Ages for Monazite Analysis

Concentration in wt.%			Atom Percent Abundances			
U	Th	Pb	Pb^{204}	Pb^{206}	Pb^{207}	Pb^{208}
0.580	5.46	0.396	0	0.272	0.0252	0.703

Age in million years	$\frac{U^{238}}{Pb^{206}}$	$\frac{U^{235}}{Pb^{207}}$	$\frac{Pb^{207}}{Pb^{206}}$	$\frac{Th^{232}}{Pb^{208}}$
	1260	1360	1500	1100

The analyses were performed at the Geophysical Laboratory and the Department of Terrestrial Magnetism, Washington, D.C., under the supervision of Dr. G. R. Tilton. The Pb^{204} observed was attributed to laboratory contamination. The measured Pb^{206}/Pb^{204} ratio was 2700. The procedures of Tilton et al. (1957, 1957a) were used, with some modifications. These ages, while clearly discordant, show that monazite, like zircon, is quite resistant to thermal events. The monazite is undoubtedly detrital and may have experienced three or more metamorphic episodes. In any event, regardless of the number or age of the metamorphic episodes, if each episode

resulted in only a net loss of lead or a net gain of uranium the true age must be in excess of 1550 m.y.

Composition of Audubon Contact Zone Biotites

The composition of the biotite in the mineral assemblages observed in the Audubon contact zone is a function of temperature, activity of water, and activity of oxygen, and is independent of bulk compositional changes. If the contact rocks represent a chemical system open to water and oxygen, variations in the iron to magnesium ratio in biotites reflect only variations in the temperature. The total iron to magnesium ratios of six of the biotites were determined on the optical spectrograph, using two chemically analysed biotites as absolute standards. The averages of triplicate analyses on each biotite are shown plotted in Fig. 3. The standard error for the analyses ranged from 1% to 6%.

Data given by Wones (1959) indicates that the ratio of Fe/Mg in biotite in an assemblage feldspar-magnetite-biotite will decrease with increasing temperature or activity of oxygen. The Fe/Mg ratios of biotites in the garnet-bearing assemblages are not directly comparable with those in the sillimanite assemblages but should be larger, all other things being equal. The compositions of the first four biotites in Fig. 3 are consistent with a negative temperature gradient. The fifth sample indicates a possible reversal of the temperature gradient, in accordance with other observations previously

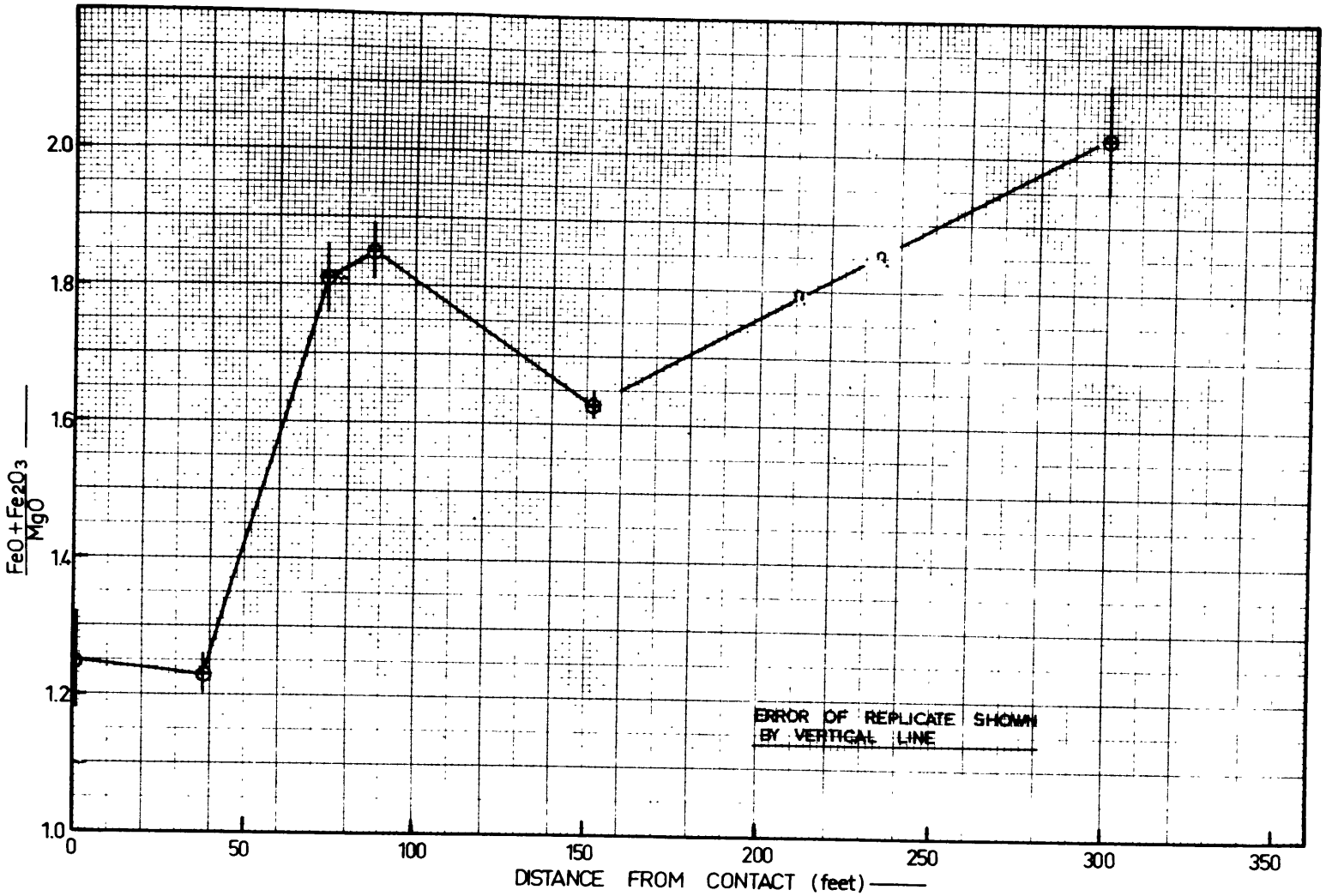

FIG 3 —IRON-MAGNESIUM RATIOS IN CONTACT BIOTITES

discussed. The biotite at 300 feet shows the highest Fe/Mg ratio of all, and either indicates a low temperature or an environment with different activities of oxygen or water. A choice cannot be made from the limited data available.

Eldora Contact Zone

The ages determined on minerals from the Eldore contact zone are presented in Table 1, and illustrated in Fig. 4. There is no evidence in this zone for a secondary heat source. The hornblendes show striking argon retentivity compared to the biotites. The ages of 1160 m.y. and 1150 m.y. at 134 and 248 feet are believed to represent the general age level of unaffected Precambrian rocks in the district. The biotite argon age of 68 m.y. at 58 feet probably represents complete loss of argon and is identical with the age shown by the Audubon stock. The biotite at 248 feet shows slight retention of argon. The difference in the distances at Audubon and Eldora over which argon retention in biotite occurs is probably related to the effects previously proposed as causes of the gradational contact at Eldora.

A calculation of the time-temperature history at distances of 11, 88 and 300 feet has been made using a theoretical heat flow model.* Hypothetical diffusion loss curves were computed from these time-temperature curves by graphical integration and application of the appropriate diffusion equations. The results demonstrate that the parameter which governs the distance interval over which complete loss occurs from different

* For details of these calculations, see page 194.

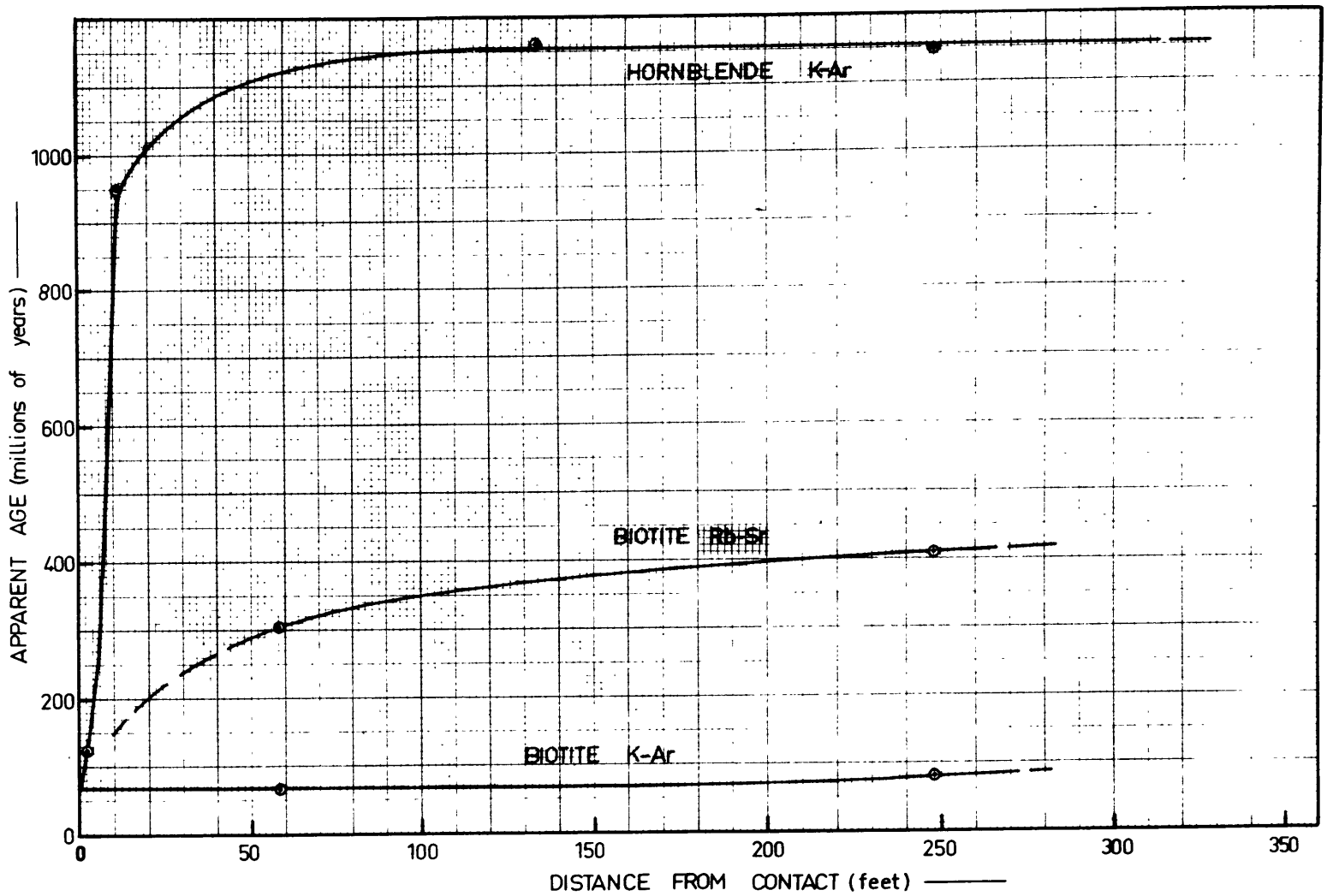

FIG. 4 — CONTACT ZONE AGES, ELDORA STOCK, FRONT RANGE, COLORADO

minerals is the activation energy for diffusion of the given daughter element. It is apparent from Fig. 4 that the distance interval over which loss of strontium in biotite occurs is much larger than the interval over which loss of argon from hornblende occurs. This infers a much larger activation energy for argon in hornblende. The relative vertical displacement of the curves in Fig. 4 is a function both of the activation energies and the relative values of the diffusion coefficients. If the activation energy is constant, a change in D/a^2 of 10^4 will displace the curve from zero loss to complete loss.

Discordant-Age Theory

Consideration of the results from this contact study, especially the indication of a low activation energy for strontium in biotite, has led to the formulation of a "discordant-age model". It is believed that this model explains in a general way many of the discordant age patterns which have been reported in the literature. Fig. 5 illustrates hypothetical "model" D/a^2 versus 1000/T relationships for various daughter products in various minerals.* If the minerals are heated at a given temperature, their relative daughter product diffusion losses will be proportional to the relative values of D/a^2 at that temperature. Three cases are considered, represented by T_1, T_2 and T_3. In order for some retention to occur at each temperature, the heating times must decrease with increasing temperature. Thus T_3 might correspond to the high temperatures of contact metamorphism (10^5 yrs), T_2 to the moderate temperatures of regional metamorphism (10^7 yrs) and

* The temperature scale here is arbitrary. The lines are positioned empirically by consideration of the three cases discussed. See also page 200.

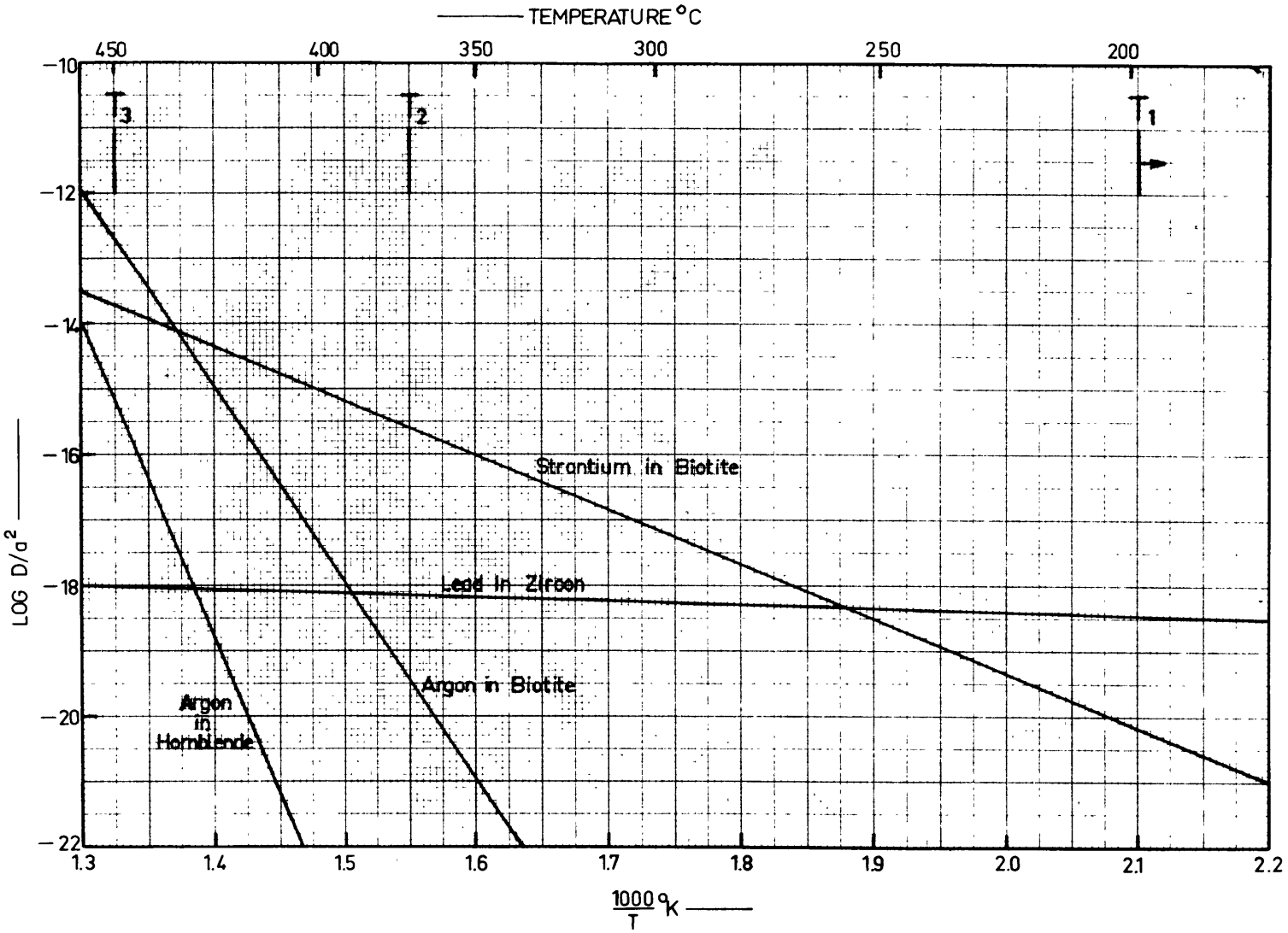

FIG. 5 — GENERALIZED MODEL FOR DISCORDANT AGE THEORY

T_1 to the ambient surface temperatures of very old stable shield areas (3×10^9 yrs). The contact results of this study represent case $3(T_3)$, with no loss of argon from hornblende, no loss of lead from monazite, partial loss of strontium from biotite and complete loss of argon from biotite. Case $2(T_2)$ is represented by results from Sudbury, Ontario, and the Baltimore gneiss province, where complete loss of strontium from biotite has occurred, no loss of argon from biotite or hornblende, and little or no loss of lead from zircon. (Fairbairn, 1960; Tilton, 1958). Case $1(T_1)$ is represented by various results from the oldest shield areas where argon and strontium ages on biotite and hornblende seldom show appreciable loss, but where zircon ages are frequently discordant. Tilton (1960) has suggested continuous lead loss by diffusion as the most reasonable interpretation of these discordant zircon ages. He first recognized that this process must infer a very low activation energy for lead in zircon. The writer has extended this idea to the above generalized model, on the basis of results obtained from this contact study. It is obvious that many deviations will occur and the discordant age patterns observed will not always fit the model. The discordant relationships inferred from Fig. 5 are unique only so long as the (a^2) values of the minerals remain in the given proportions.

Geological Time Scale

The K-Ar age of 66 ± 2 m.y. for the time of emplacement of the Laramide stocks in the Front Range porphyry belt is be-

lieved to be the first reliable measurement of this event. Andesitic pebbles thought to have come from lavas erupted from the volcanic throat of the Audubon stock (Lovering et al., 1950) are found at the base of the Upper Cretaceous-Paleocene Denver formation. A time of 66 m.y. then can be assigned to the time scale somewhere around the Cretaceous-Paleocene boundary.

Summary

Twenty-four independent age analyses have been made on samples of biotite, feldspar, hornblende, whole rock, and monazite from two contact metamorphic zones bordering Laramide stocks in the Front Range, Colorado. The age discordancies which were found can be related to the presumed temperature distribution in the contact zone, the mineral paragenesis, and compositional variations of the biotite. A low activation energy for strontium in biotite and a high activation energy for argon in hornblende can be inferred from the shape of the "apparent age" versus "contact distance" curves. Using these estimates a comprehensive model has been proposed which relates discordant age patterns to time, temperature, and the diffusion parameters of the minerals.

Acknowledgments

The author wishes to thank L. T. Aldrich for making possible a week's visit to the Department of Terrestrial Mangentism, and G. R. Tilton for instruction and supervision

in the techniques of Uranium-Lead analysis during the week's visit. The author also acknowledges the assistance of D. G. Brookins in the optical spectrographic analyses of biotites and of H. W. Krueger for help in building and maintaining equipment. Finally, the author is grateful to P. M. Hurley, whose support and encouragement made this study possible.

References

Aldrich, L. T., G. W. Wetherill, G. L. Davis, G. R. Tilton, 1958, "Radioactive Ages of Micas from Granitic Rocks by Rb-Sr and K-Ar Methods", Trans, A.G.U., v. 39, p. 1124.

Fairbairn, H. W., P. M. Hurley and W. H. Pinson, 1960, "Mineral and Rock Ages at Sudbury-Blind River, Ontario", in press.

Hart, S. R., 1960, "Mineral Ages and Metamorphism", Proceedings of Conference on "Geochronology of Rock Systems", Annals of the N.Y. Acad. of Sci., in press.

Lovering, T. S., E. N. Goddard, "Geology and Ore Deposits of the Front Range, Colorado", U.S.G.S. Prof. Paper 223.

Tilton, G. R., G. L. Davis, G. W. Wetherill, L. T. Aldrich, 1957a, "Isotopic Ages of Zircon from Granites and Pegmatites", Trans. A. G. U., V. 38, p. 360.

Tilton, G. R., and G. L. Davis, "Solid Diffusion as a Mechanism for Discordant Lead Ages", Abstract, A.G.U. Annual Meeting, Washington, D. C., 1960

Tilton, G. R., L.O. Nicolaysen, 1957b, "The Use of Monazites for Age Determination", Geochim. et Cosmochim. Acta, Vol. 11, pp. 28.

Wones, D. R., 1959, "Biotites on the Join Phlogopite-Annite", Annual Report, Director of the Geophysical Laboratory, Carnegie Institution of Washington Yearbook.

III The Use of Amphiboles and Pyroxenes for K-Ar Dating

Introduction

Micas have long provided the basis for most K-Ar and Rb-Sr isotopic mineral ages. Their use has become accepted almost to the exclusion of other possible minerals. Pinson et al. (1958) analyzed three hornblendes for rubidium and strontium. One of these had a Rb/Sr ratio favorable for age calculation. Hayden et al. (1960) obtained a geologically reasonable K-Ar age on an amphibole from Montana. Damon(1957) measured the K-Ar age on a hornblende from the Storm King pegmatite and obtained an age in excess of that measured on coexisting biotite. Excess original argon in the hornblende is given as the most likely explanation by Damon. A study of ages across a contact metamorphic zone (Hart, 1960) indicates that hornblende retains argon much better than biotite. Amirkhanov et al. (1959a) have measured the diffusion coefficient of argon in pyroxene and find it to be very small at geologic temperatures. It is suggested that these minerals may prove useful for dating purposes, especially in metamorphic areas. To determine the applicability of these minerals for K-Ar dating, the potassium and argon content of ten hornblendes and three pyroxenes has been measured.

Sample Description

Because of the low potassium contents of hornblende and pyroxene, it is essential that all biotite and feldspar impurities be removed from the sample. Table 1 gives a description

of the samples with an estimate of the biotite impurity. This estimate was made by grain counts and X-ray diffraction measurements of all the samples, using hornblende-biotite mixtures as standards. Several samples showed no free biotite, but fine intergrowths were detected by the X-ray examination.

Table 1.

Description of Hornblende and Pyroxene Samples

Sample Number	Locality	Rock Unit	Biotite Impurity
H-B47*	Wheaton, Maryland	Tonalite	1 %
H-B21*	Ellicott City, Maryland	Granite	3 %
H-P20*	Devault, Penna.	Baltimore gneiss	0.5%
H-Sk*	Bear Mountain, N.Y.	Storm King granite	0.2%
H-G15*	Crossnore, N.C.	Granite gneiss	1 %
H3006	Rockport, Mass.	Cape Ann granite	1.5%
P3069	Mont Royal, Quebec	Tinguaite dike	0.2%
H3070	Chicoutimi, Quebec	Syenite	5 %
P3073	Kenogami, Quebec	Gabbro	0.2%
H3089	Dill Station, Ontario	Gneiss	0.2%
H3136	Oak Bay, New Brunswick	Granite	0.2%
P3426	Neelon Twp., Ontario	Sudbury gabbro	0.2%
H3451	Dryden, Western Ontario	Amphibolite	4 %
H4068	Eldora, Colorado	Idaho Springs Fm., schist	0.2%

* These samples were obtained through the courtesy of G. R. Tilton and G. L. Davis of the Geophysical Laboratory.

H – Hornblende

P – Pyroxene

Analytical Techniques

The argon analyses were made by isotope dilution, using enriched argon 38 as a spike. Sample weights of from three to five grams were used for the argon analyses. The argon 36 component was used to calculate the air correction. Potassium analyses were made using a Perkin-Elmer flame photometer with lithium internal standard. Isotope dilution analyses for potassium were made on several samples as checks. The analytical errors vary with the potassium and argon content, and are estimated for each individual analysis. Decay constants used are $\lambda_e = .585 \times 10^{-10}\text{yr.}^{-1}$, $\lambda = 5.30 \times 10^{-10}\text{yr}^{-1}$, $K^{40} = 1.22 \times 10^{-4}$ g/g of K.

Results and Discussion

The analytical results are shown in Table 2, along with an estimate of the fraction of potassium actually contributed by the hornblende or pyroxene.

There is a lack of agreement between the flame photometer potassium determinations and the few isotope dilution potassium analyses. Until more of the samples can be checked by isotope dilution, the flame photometer values will be used. From the range of potassium values shown, it is likely that most hornblendes, as well as many pyroxenes of Paleozoic age or older can be accurately dated by present techniques.

Table 2.

Analytical Data for K-Ar Measurements on Hornblendes and Pyroxene

Sample Number	K% F.P.	K% I.D.	K HBDE, Pyrx. / K Total	$*Ar^{40}$ (in 10^{-5} cc stp/g)	$*Ar^{40}$ / Total Ar^{40}	Ar^{40}/K^{40}	Age (m.y.)
H-B47	0.394 0.403		~0.83	0.543	0.29	0.0200	310±15
H-B21	2.12		~0.90	2.65	0.71	0.0184	290±10
H-P20	1.35		~0.98	6.65	0.83	0.0722	950±50
H-SK	1.66 1.69		>0.99	7.82	0.82	0.0687	910±40
H-G15	0.53 0.54	0.547	>0.87	2.20	0.62	0.0605	820±30
H3006	1.49		~0.93	2.26	0.56	0.0223	345±15
P3069	0.112		>0.91	0.046	0.05	0.0060	100±80
H3070	1.05 1.15		~0.68	4.58	0.80	0.0610	820±30
P3073	0.155		>0.94	1.04	0.50	0.0983	1200±60
H3089	1.31		>0.99	6.31	0.87	0.0707	1000±40
H3136	0.482		>0.98	0.740	0.28	0.0226	350±20
P3426	0.0914	0.0941	>0.90	0.925	0.26	0.148	1610±70
H3451	0.663		~0.58	15.7	0.92	0.347	2680±60
H4068	1.01 1.06	0.942	>0.99	6.56	0.85	0.0926	1150±40

* Radiogenic

Table 3

Comparison of Hornblende-Pyroxene Ages with Ages of Associated Minerals

Sample Number	K-Ar Ages This Work	Biotite K-Ar	Biotite Rb-Sr	Zircon $\frac{238}{206}$	Zircon $\frac{235}{207}$	Zircon $\frac{207}{206}$	Zircon $\frac{232}{208}$	Miscellaneous
H-B47*	310			500	510	570	490	
H-B21*	290	315	290	355	370	450	310	
H-P20*	950	1000	495					
H-SK *	910	845	940	960	990	1060	850	
H-G15*	820			690	720	800	680	
H3006	345							Zircon Pbα -260 a.
P3069	~100							Brome Mt., Biotite K-Ar, 125 m.y. b.
H3070	820							Fs Rb-Sr 940 c. HBDE Rb-Sr 960 c.
P3073	1200							Grenville locality
H3089	1000	1000[d]	860[d]					
H3136	350							Feldspar Rb-Sr[d] 300±60
P3426	1610	1780[d, e]	1245[d, e]					
H3451	2680							Superior Province locality
H4068	1150	80	410					

* The biotite and zircon ages on these samples were determined previously by staff at the Geophysical Laboratory and Department of Terrestrial Magnetism. The results were reported by personal communication from G. R. Tilton.

a. Webber et al. (1956)
b. "Age Determinations by the Geol. Survey of Canada" (1960)
c. Pinson et al. (1958)
d. Hurley et al (1958), recomputed values
e. These ages were on a biotite-bearing sample of the same gabbro, but from a different locality.

Table 3 is a comparison of these hornblende and pyroxene ages with ages determined on other minerals from the same rock. In every case there is marked concordance between the hornblende and pyroxene ages and the original or metamorphic age inferred from these comparison age analyses. The low argon content of several of these samples makes their measured age especially sensitive to the presence of excess argon. No evidence is found for the possible general existence of "excess" or "trapped" radiogenic argon in hornblendes (or pyroxenes).

Acknowledgments

The writers are especially grateful to Dr. G. R. Tilton and Dr. G. L. Davis, of the Geophysical Laboratory, for providing five hornblende samples from well-dated localities. The continued support of this laboratory by the Division of Research of the Atomic Energy Commission is also gratefully acknowledged.

References Cited

Amirkhanov, Kh. I., E. N. Bartnitskii, S. B. Brandt, and G. V. Voitkevich, 1959a, "On the Migration of Argon and Helium in Several Rocks and Minerals", Doklady, Ac. Sci. USSR, vol. 126, No. 1, Geochemistry Series.

Damon, P. E., 1957, "Helium and Argon in the Lithosphere and Atmosphere", Doctoral Dissertaion, Columbia University, N.Y.

Hart, S. R., 1960, "Mineral Ages and Metamorphism", Proceedings of the Conference of Geochronology of Rock Systems, Annals of the New York Academy of Science, in press.

Hayden, R. J., and J. P Wehrenberg, 1960, "A^{40}-K^{40} Dating of Igneous and Metamorphic Rocks in Western Montana", J. Geol. Vol. 68, No. 1.

Hurley, P. M., et al., 1958, M.I.T. Fifth Annual Progress Report, U.S.A.E.C. NYO-3938.

Pinson, W. H., H. W. Fairbairn, R. F. Cormier, 1958, "Sr/Rb Age Measurements on Hornblende and Feldspar and the Age of Syenite at Chicoutimi, Quebec, Canada", Bull. G.S.A., Vol. 69, p. 599.

Webber, G. R., P. M. Hurley, and H. W. Fairbairn, 1956, "Relative Ages of Eastern Massacusetts Granites by Total Lead Ratios in Zircon", Am. J. Sci. Vol. 254.

PART II

Appendix I

Apparatus and Experimental Techniques

A. Sample Preparation and Purification

From the five to fifteen pounds of collected sample, a representative hand specimen and thin section chip were set aside. The remainder was first pulverized with a jaw crusher and disc grinder and then sieved with a 50 mesh screen. The oversize was reground until everything passed the 50 mesh screen. Occasionally an oversize of concentrated biotite could not be reduced. The minus 50 fraction was passed through a sample splitter until a hundred gram portion was obtained and bottled as a whole rock fraction. Any oversize biotite concentrate was mixed in before splitting the sample. The remaining sample was screened at 50, 100 and 200 and the -50+100 or -100+200 fraction taken for mineral separation. This fraction was run through a Carpco magnetic separator. The magnetite and tramp iron were pulled out by a moving belt-permanent magnet arrangement on the Carpco feed. The Carpco magnetic fraction was separated in bromoform. A potassium-rich feldspar fraction was obtained from the float of carefully adjusted bromoform. A biotite-hornblende rich fraction was obtained from the sink portion of regular bromoform. Final purification of the biotite was made on a Frantz Isodynamic magnetic separator. After purification of the hornblende on the Frantz, the remaining biotite impurity was floated out in carefully adjusted methylene iodide. Estimated hornblende

purity is given in Table 1, chapter 3, part I. The variable potassium content of the biotite is chiefly a function of sample purity. The biotite samples range from 70% to 99% purity. In most cases the principal impurity in the biotite is sillimanite with unliberated magnetite inclusions.

B. Measurement of Radiogenic Argon

1. Gas Release and Purification System

Fig. 1 is a schematic diagram of the argon purification line constructed and used in this research.

Stopcocks

The circled crosses represent Corning two-way 4 m.m. mercury seal evacuated bulb stop-cocks. The use of these made it impossible to bake out the purification system. However, the system was kept under vacuum at all times and the air argon blank from just the purification train was insignificant ($\sim 5 \times 10^{-7}$ cc stp) compared to the sample blank ($\sim 2 \times 10^{-5}$ cc stp). The stopcocks were found to have a finite leakage rate across them when there was a large pressure gradient from one stem to the other. The leakage rate in from the atmosphere, however, was found to be completely negligible. The change in 40/38 ratio in the routine spike bulb was less than 3% in three years and this establishes a maximum leakage rate through the spike bulb stopcock. The stopcocks generally took several weeks to degas initially.

Copper Oxide

The copper oxide traps are used to oxidize hydrogen. From one to four std.cc of hydrogen may be formed during a normal fusion by reduction of water vapor on hot metal or sample. The pyrex copper oxide traps are permanently maintained at 400 to 450° C.

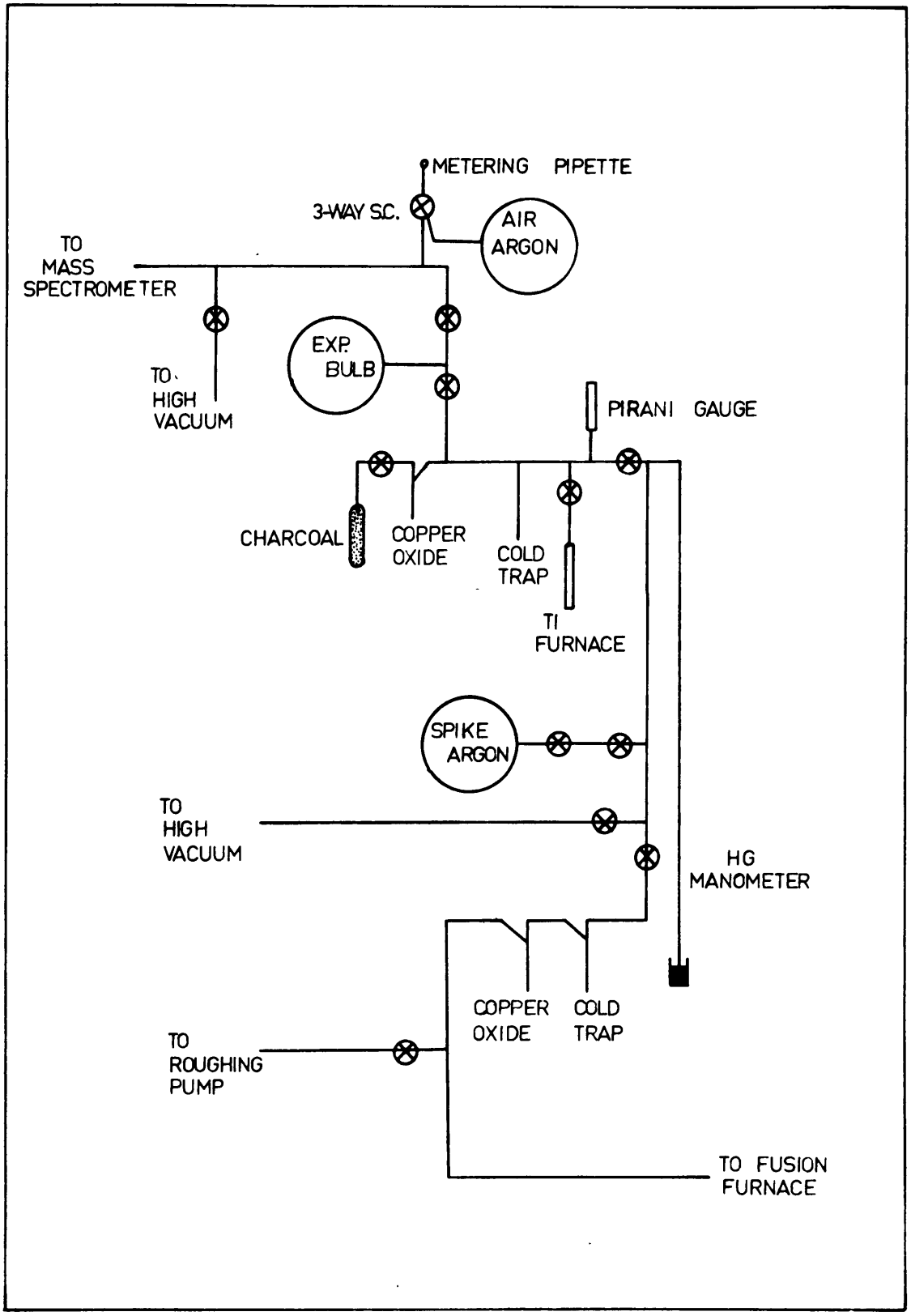

FIG. —ARGON EXTRACTION AND PURIFICATION TRAINS

Vacuum System

The roughing pump is a Welch Duo-Seal Model 1400 forepump and is used to evacuate the furnace initially, after a sample is loaded. The high vacuum is obtained with a model 1400 forepump and single stage mercury diffusion pump. There is a large cold trap between the diffusion pump and the purification line.

Titanium Furnace

This consists of a molybdenum crucible containing ten to fifteen grams of titanium sponge suspended at the bottom end of a Vycor tube. The Vycor tube is heated externally with a Kanthal wound resistance furnace capable of reaching 1300° C.

Air Argon Release System

This metering system consists of a 500 cc bulb, a three-way stopcock, and a pipette. The volume of the pipette plus lower bore of the stopcock is 1.125 cc. The bulb is filled with spectroscopic air argon, and the half life of the pressure is about 308 releases. The initial releases contained about 3×10^{-4} cc stp of air argon with less than 1% impurity. About 20 to 30 releases were made during this research.

Spike Release System (Low Level)

This metering system consists of a 1093.2 cc bulb, and a 2.628 cc manifold included between two stopcocks. The inner

stopcock bore is 0.2601 cc, the outer stopcock bore is 0.2830 cc. The decay constant is 2.40×10^{-3} release^{-1} and the half life is about 289 releases. The volume measurements were made by duplicate fillings of mercury or water; then weighing of the mercury, and filling of a graduated cylinder with the water.

This spike bulb was filled with about 4×10^{-3} cc stp of enriched argon 38 spike obtained in 1955 from Oak Ridge. Spike calibrations were made by admitting five to eight cm of air into a 3.4327 cc pipette, expanding the air once or twice (expansion ratio = .157), and mixing it with a spike release. Fig. 2 shows the spike calibration curves for this 'low-level spike' (Betty) and for the 'routine Spike' (Alice). The isotope ratios of the two spikes are also given in Fig. 2. In this research sixty-three 'low level' spike releases and forty-seven 'routine spike' releases were used.

Fusion Furnace

Fig. 3 is a scale drawing of the fusion furnace constructed for this research. It was designed especially for constant temperature diffusion runs but was found to be satisfactory for normal fusions as well. A double-walled water cooled bell jar encloses the furnace and is sealed to the base plate with Apiezon Q vacuum wax. The leakage rate of air argon into the furnace was measured to be about 7×10^{-13} liters/sec. In a normal one hour fusion this would amount to 2×10^{-6} cc stp of air argon.

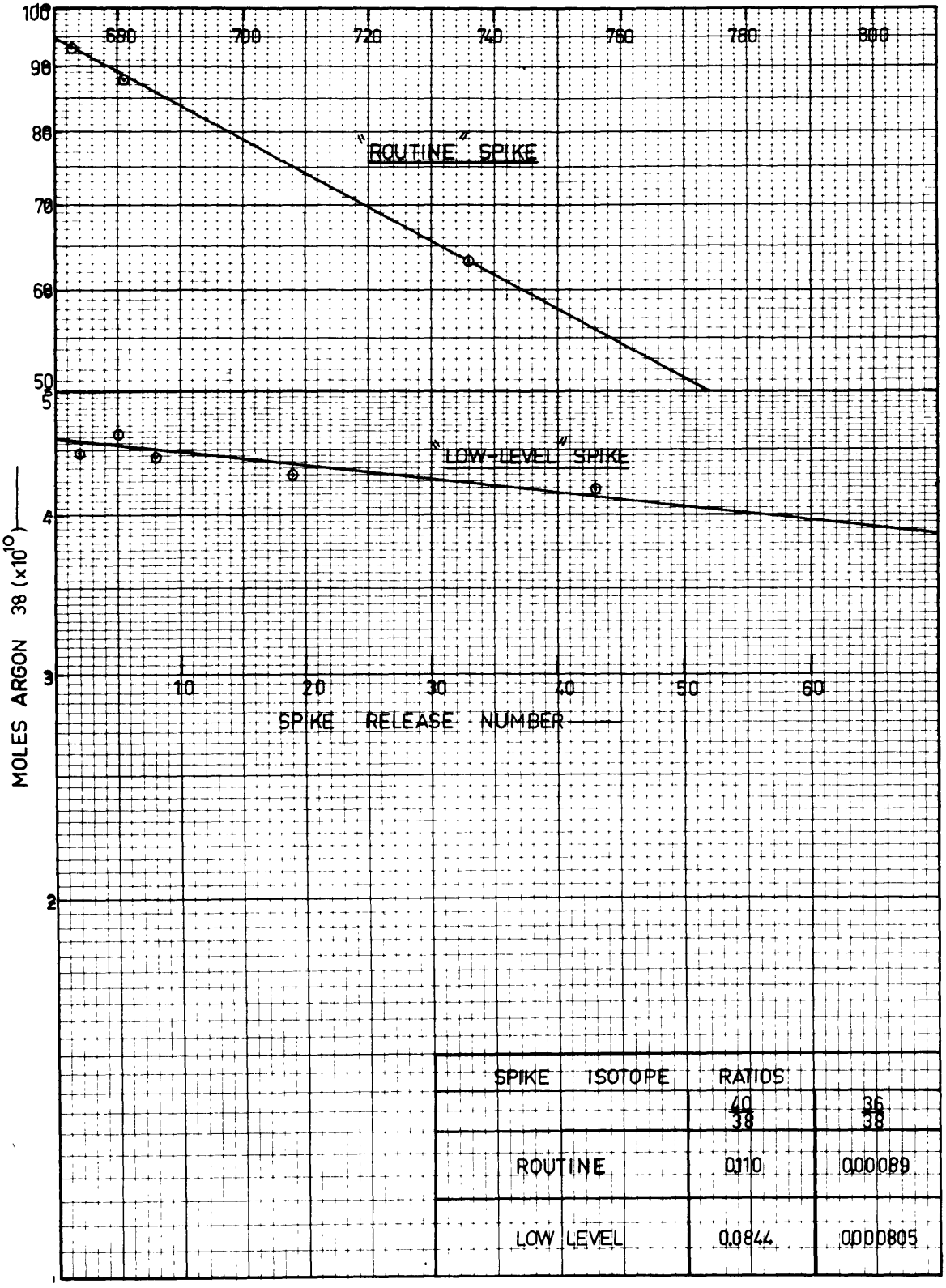

FIG. —ARGON 38 SPIKE RELEASE CURVES

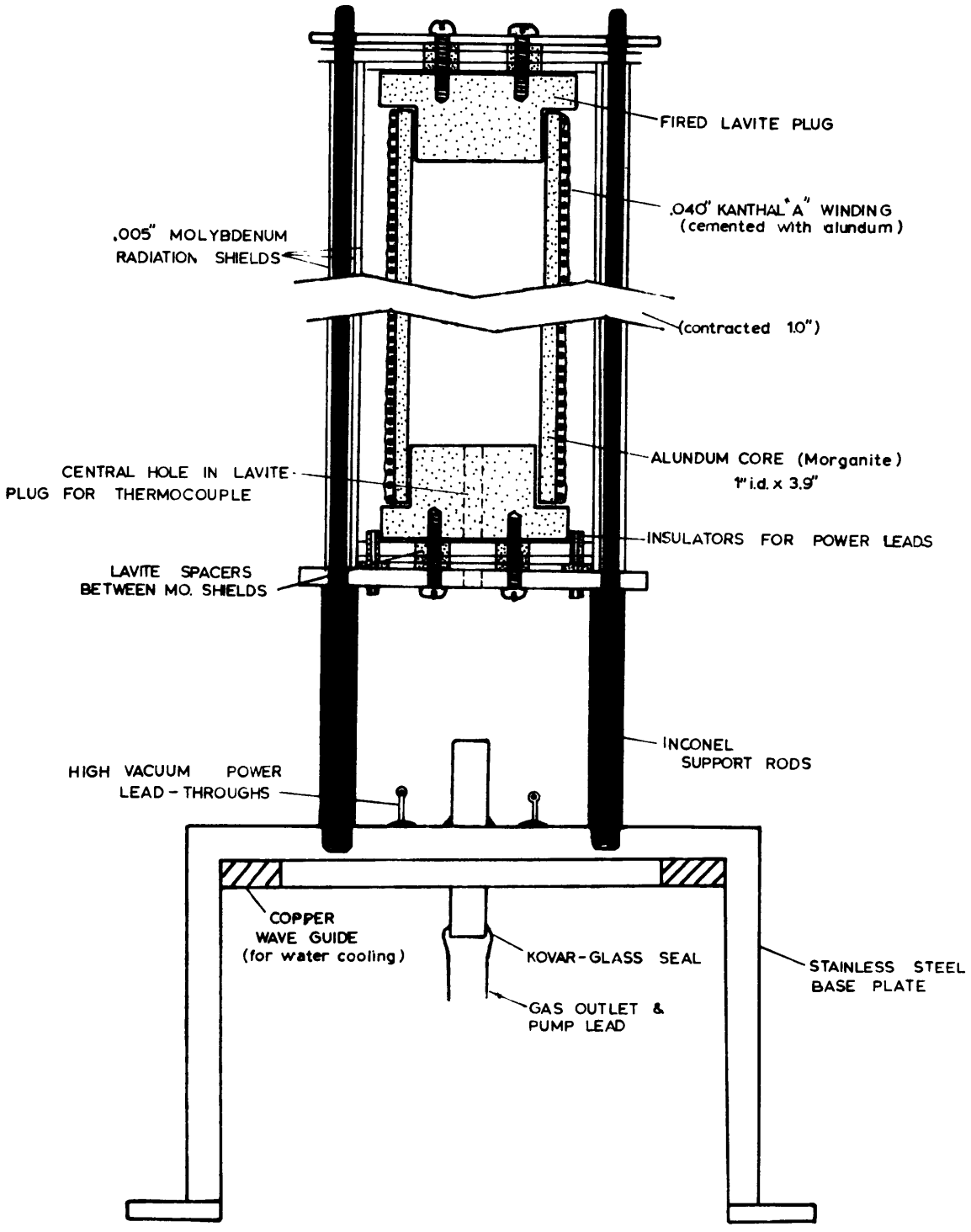

FIG. – HIGH TEMPERATURE FUSION FURNACE
(approx. to scale – vacuum bell jar not shown.)

The central two inch portion of the furnace was found to have a vertical temperature gradient of less than 10° C at 1000° C. The sample crucibles were usually supported in this zone on a 22 m.m. cylinder of alundum with a 1 m.m. wall thickness. Two platinum-platinum, 10% rhodium thermocouples were used during diffusion runs; one above and one below the sample. The thermocouples were calibrated by suspending a loop of pure .010" copper wire near them and watching for the continuity break in the circuit during heating. The thermocouples deteriorated with use; new ones calibrated to within 10° C, while old ones were frequently 20 to 30° C off. To insure accurate readings, the insulated vacuum lead-throughs had to be cleaned frequently.

The Morganite alundum core was wound with ten ohms of 40 mil Kanthal A wire. With new molybdenum shields, the furnace would reach 1200° C at 400 watts. The reflecting properties of the shields deteriorated rapidly and after ten fusions it would take 600 to 650 watts to reach 1200° C. 1200° C was sufficient to completely fuse all the minerals used in this research. This type of furnace was found to have two major disadvantages. First, the air argon blank from it was two or three times larger than from the induction-heated furnace (Alice) and ranged from 7×10^{-6} cc stp to 2×10^{-5} cc stp in mock no-sample runs. Also, sample charges larger than six grams had a tendency to overrun the crucible during fusion and cement the furnace together.

Run Procedure

One to six grams of sample are weighed to the nearest milligram. The sample is poured into a 22 m.m. x 34 m.m. Morganite alundum crucible. This is inserted in the furnace, the furnace cap is put on, the thermocouples adjusted and the bell jar put in place and sealed. A vacuum of $< 1/2$ cm is pulled with the roughing pump and then the high vacuum pump is cut in. The sample, purification line and baking charcoal are pumped on overnight. In the morning all stopcocks are rotated several times and the bores pumped out. The titanium is baked out at 950 to 1050° C until the pressure is less than five microns. The heater is taken off the charcoal and the charcoal, titanium and purification section stopcocks closed. The spike manifold is pumped and the spike prepared. The furnace is outgassed by passing six to seven amps through the windings. In five minutes or so the sample temperature will reach 100 to 200° C and the power is turned down. The temperature will coast to 300 to 400° C and the sample is outgassed at that temperature for thirty to sixty minutes.

This outgassing procedure allows a higher temperature to be reached in the windings and cement. Because of the exponential nature of air argon desorption, outgassing for more than one hour does little additional good. The following table gives the results of some outgassing experiments made to demonstrate that no radiogenic argon was being lost by these procedures.

Outgassing Experiments

Mineral	Time (min.)	Temperature °C	Fraction Radiogenic Released
Muscovite	40	270°	$<0.05\%$
Muscovite	6	625-575°	$\sim 1.0\%$
Feldspar	30	350°	$\sim 0.06\%$
Biotite	60	400°	$<0.1\%$
Hornblende	30	425°	$<0.2\%$

After the sample is outgassed, the pump stopcock is closed and the spike added. Liquid nitrogen is put on the cold traps. The temperature is raised slowly through the sample decrepitation point (biotite 400 to 500°, muscovite 600°, hornblende ~700° and pyroxene about 850° C). The sample is then brought quickly to the desired temperature (1150 to 1200° C) and held for ten to thirty minutes. The higher temperatures are necessary for fusion of pyroxene and muscovite, while hornblende and biotite will fuse at the lower temperatures. Occasionally a few pellets of NaOH are added to the muscovite samples to insure fusion. After fusion, the cold trap is warmed up and the gases allowed to equilibrate for ten minutes. The condensibles are then refrozen, and the remaining gas is pulled onto the purification train charcoal. Onehalf hour is sufficient to adsorb all the argon, though the hydrogen pressure will still be high. The purification train stopcock is closed and the charcoal warmed to 200° C. The hydrogen is allowed to burn on the copper oxide for thirty to sixty minutes.

The titanium is heated to 900 to 950° C and the gas admitted. Take-up of gas down to about 10 microns pressure is very rapid. The charcoal trap is closed off and the titanium cooled slowly for ten minutes. The heater is then removed and the titanium cooled for an additional ten to fifteen minutes. This is about the optimum period; longer cooling may result in the release of some of the hydrogen. The purified argon is allowed to expand into the connecting line and the sample system of the mass spectrometer for five minutes, then the titanium furnace is closed off. The sample system consists of a baked charcoal, a trap cooled with liquid nitrogen, and a 550° C Vycor copper oxide furnace. The mass spectrometer run normally takes about one half hour.

2. Mass-Spectrometry

Three mass spectrometers are available for argon analyses. A cycloidal focussing instrument, model 620, made by Consolidated Electrodynamics, a standard Nier-type metal tube instrument, and a glass tube Reynolds-type instrument obtained from Atomic Laboratories, Berkeley, California. The 620 is not sensitive enough to measure argon 36, but it has no mass discrimination and has very stable characteristics. It is ideal for measuring argon 38 and 40 ratios, testing for leaks, monitoring outgassing procedures and checking the hydrogen content of gas samples. The Nier-type instrument has an appreciable background at mass 36 and is used chiefly for determining the

argon 36 content of Precambrian samples. The Reynolds-type instrument was used for nearly all of this research.

Reynolds-type Mass Spectrometer (See Reynolds, 1956)

Assembly of this instrument was begun in February, 1959. Low vacuum was not achieved until several stopcocks on the inlet side were replaced with Granville-Phillips metal valves in early June. Initial sweeps at pressures of 4 to 6×10^{-7} m.m. showed poor sensitivity and large background in 36 to 40 region. The pumping speed was increased by tripling the size of the pump lead. Addition of source magnets (100 to 200 gauss) resulted in a factor of 10 increase in sensitivity and virtual elimination of all background except at mass 28 and 44. Accidents were frequent in the early months but continual improvements in performance were made. The instrument operated with only seven days down-time from January 1 to August 1, 1960.

Operating Specifications

Pressure: 2×10^{-9} m.m. after bakeout, 2×10^{-8} m.m. "steady-state".

Trap Current: Usually run at 1.5 ma, maximum about 2.5 ma.

Total Emission Current: Usually 12 ma, maximum off meter scale.

Noise level on V.R.E.: .05-.1 mv.

Sensitivity: Under normal conditions, one ion per 4000 atoms. best sensitivity, one ion per 1000 atoms.

Output Resistor: 10^{11} ohms Victoreen

Background: Normal conditions, 38 and 40 ~0.2-0.5 mv, 36 ~0.1 mv

Bakeout Procedure: First cycle, 200° C for twelve hours, ion gauge and filament on when $p < 5 \times 10^{-6}$ m.m. Ion gauge and filament off, oven cooled. Glassware torched and cold traps cycled while oven is cooling. Ion gauge degassed. Oven heated 200° C for another twelve hours. Ion gauge and filament on when $p < 5 \times 10^{-6}$ m.m. Oven slowly cooled, final pressure 2 to 5×10^{-9} m.m.

Source magnet position: Not too critical when tube is clean. Adjust for maximum trap current and minimum background.

Accelerating voltage: ~+2500 volts.

Leak: Granville-Phillips metal valve.

Operation: Dynamic flow. Static runs seldom made.

Magnet: Linear from 50 ma (1700 gauss) to 220 ma (6000 gauss).

Mass Discrimination: Variable, 2 to 3% (Mass 38 to 40).

Deflection Plates: 135v (for vertical beam deflecdon)

Focussing: Beam intensity relatively insensitive to focussing adjustments.

Special Problems

Discrimination

Repeated measurements of air argon isotope ratios indicated a significant and slightly variable mass discrimination. The discrimination increases with an increase of emission current. An air argon metering system was constructed (described earlier)

so that the discrimination could be determined after all critical argon analyses (high air correction runs, etc.) The measured 40/36 ratios of 22 air argon runs varied from 293 to 300. After a 5.14% correction for leak fractionation, these ratios correspond to a discrimination in the 38/40 ratios of from 2.1% to 3.0%.

Fractionation

Graham's law leak fractionation was assumed.* For dynamic runs of essentially infinite halflife, the fractionation correction is -2.5% of the 38/40 ratio. For runs of shorter halflife, curves were constructed giving the percent change of ratio in ten minutes versus gas pressure halflife. The measured ratios were plotted versus time and a line of the slope given by the theoretical curves was passed through the points. The ratio at the zero time intercept was then corrected by -2.5%. In general, the measured points agreed very well with the theoretical slope.

Mass 36 Background

A considerable effort was made to insure that the argon 36 measurements were accurate. Comparison of argon 36/argon 38 ratios determined initially on both the Nier-type and the Reynolds-type spectrometers showed large differences. The discrepancies were traced to 36 background enhancement effects caused by hydrogen in the argon sample. Since the ratio of the gas 36 peak to background 36 peak on the Reynolds instrument is

* i.e., flow rates assumed to be inversely proportional to the square root of the atomic weights.

about 100 times that of the Nier instrument, the enhancement effect was naturally more serious on the latter spectrometer. Quantitative measurements of this effect were made by determining the mass 36 increment caused by introducing various amounts of hydrogen. Fig. 4 shows the increment of mass 36 and 37 on both instruments versus the quantity of hydrogen. The hydrogen content of argon samples after routine purification varied between 1×10^{-6} and 1×10^{-5} cc stp. This could cause a doubling of the normal gas 36 peak on the Nier instrument and a 10 to 20% effect on the Reynolds instrument. Fig. 4 also shows that monitoring of the mass 37 peak is of little use, since the effect of hydrogen at mass 37 is a factor of ten smaller than at mass 36. The only ideal solution to the problem is complete removal of the hydrogen.

Fig. 5 shows the behavior of samples of argon and hydrogen on liquid nitrogen cooled charcoal (2 grams of 8 to 14 mesh activated charcoal). With accurate timing, most of the hydrgen can be pumped away as soon as the argon is adsorbed. The difference between sections (A) and (B) of the curve suggests that hydrogen is being pumped off the charcoal at (A). This is a method frequently used for removal of hydrogen from gas samples. Rather than use this method, however, a copper oxide trap was installed in the sample system and run at 550° C. At this temperature traces of hydrogen are rapidly cleaned up. The temperature is not high enough however to produce a significant equilibrium pressure of oxygen. Above

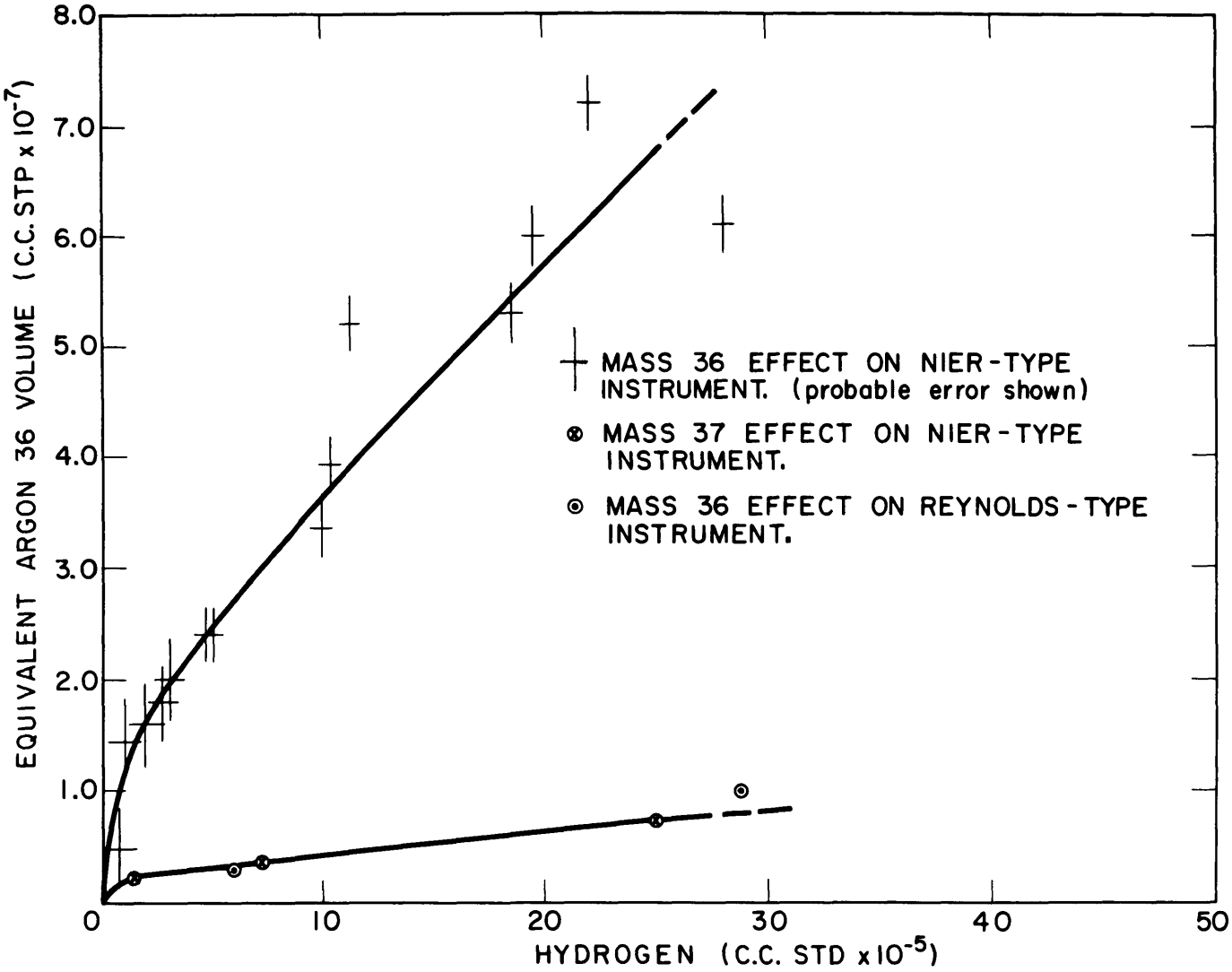

FIG. 4 HYDROGEN PRESSURE VERSUS BACKGROUND EFFECT

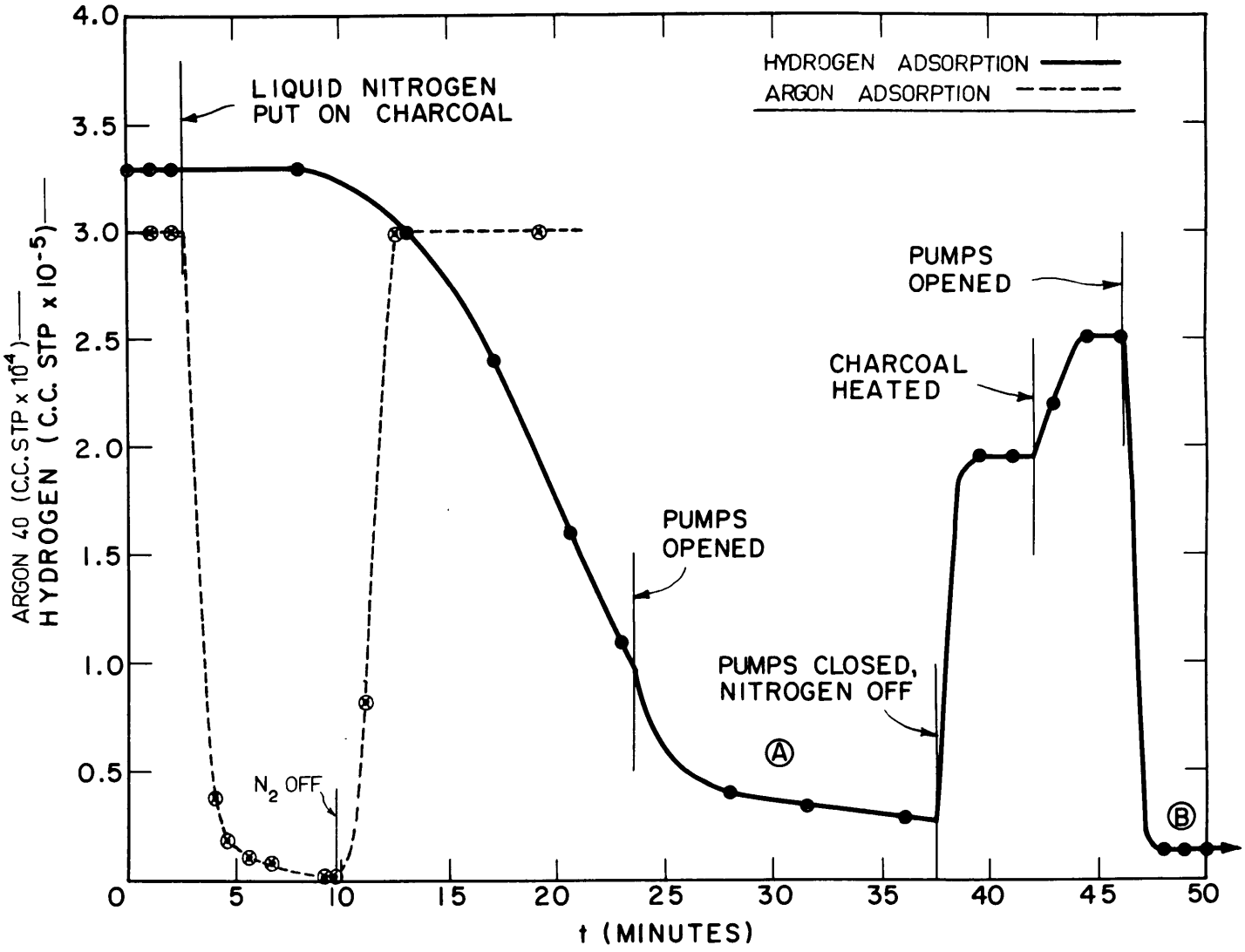

FIG. 5 —ADSORPTION OF ARGON & HYDROGEN ON CHARCOAL

600° C, the oxygen content in the system becomes appreciable and at 700° C the theoretical dissociation pressure is about 2×10^{-4} m.m.

Another test of 36 enhancement on the Reynolds-type instrument was made by running a sample of nitrogen gas (<0.1% argon) at different flow rates, corresponding to tube pressures of 5×10^{-7} m.m. and 1×10^{-6} m.m. (Normal pressure during a run is never allowed to exceed 1×10^{-6} m.m.). The net 36 increase for these two flow rates was .025 mv and .035 mv respectively. The 38 and 40 peaks also increased during this test, indicating the effect to be similar to a memory effect. The 36/38 and 38/40 ratios of these mass increments were similar to the argon ratios of the previous days run. The effect, while finite, is less than 0.2% of the argon quantities measured during a normal run.

A third test of argon 36 measurement accuracy was made by running a sample of air argon at two different flow rates. In one case the 36 background accounted for 6% of the gas peak, in the other case only 1%. The measured 40/36 ratios were exactly the same in each case.

In a final test, the argon ratios froma normal run were measured, then the argon was pulled onto a charcoal and pumped on for forty-five minutes to remove any hydrogen. The ratios were remeasured and found to be identical with the initial ratios.

It is concluded that accurate argon 36 measurements are possible as long as the argon sample is free of all other gas, especially hydrogen. (See also, "Discussion of Errors", Appendix I D).

C. Measurement of Potassium, Rubidium and Strontium

1. Chemical Procedures

Potassium was determined chiefly by flame photometry and occasionally by isotope dilution. Strontium and rubidium were determined solely by isotope dilution.

The reagents used are : water, hydrofluoric acid, hydrochloric acid, nitric acid, ammonia solution, and ammonium oxalate. Pure water is obtained by passing tap distilled water through a Barnstead Bantam demineralizer column. Pure ammonia, hydrochloric acid and nitric acid are prepared by distillation in a Vycor still. No purification of the hydrofluoric acid or ammonium oxalate is necessary.

Isotope dilution Procedures

1. 0.2 to 1.0 grams of sample are weighed and transferred to a large platinum dish.
2. Add appropriate amounts of K^{41}, Rb^{87} and Sr^{84} spikes.
3. Add ~1 ml of 1:1 H_2SO_4 and 10 ml of HF.
4. Digest on steam bath down to H_2SO_4. Add 5 to 10 ml more HF, take down to mush.
5. Add 50 ml demineralized water, heat until in solution, take down to sulfuric acid. Add 50 ml more demineralized water.
6. As this boils down, slowly add 2NHCl until 25 ml of 2NHCl solution is obtained.
7. Filter this solution and add ~10 ml of Sr^{85} tracer.

8. Put this solution carefully on the ion exchange columns, using a pipette. The columns are 1" x 20" Vycor, filled with Dowey 50,8% cross-linked, 200-400 mesh hydrogen ion cation exchange resin. The columns are washed beforehand, twice with 6NHCL and once with water.

9. After the solution has soaked in, carefully wash down the walls with 2NHCl and allow this to sink in.

10. Elute with 2NHCl. Fe and Al come through first, then Na and K. The K is detected by flame test. The best rubidium will be in a 20 ml portion following the last trace of potassium.

11. The K and Rb solutions are evaporated to dryness and converted to nitrates. They are evaporated onto the tantalum filament as nitrates.

12. The strontium is monitored by the Sr^{85} activity. It is collected in 10 to 20 ml portions and evaporated to dryness. The 50 ml containing the highest activity is transferred to a 50 ml Vycor dish and evaporated to dryness.

13. For application to the filament, the $SrCl_2$ is converted to $SrC_2O_4H_2O$. This is done by adding a few drops of HCl and 1 ml of water to the $SrCl_2$ residue. A few crystals of ammonium oxalate are dissolved in this. An excess of ammonia is added (1 ml) and the solution evaporated to dryness. The dish is cooled, and a few ml of ice-cold water carefully added. The solution is pipetted off, and the strontium oxalate residue washed several more times with ice cold water. (This dissolves any of the

rubidium which is present). The oxalate residue is taken up in a small pipette and applied to the filament.

Potassium Flame Photometer Procedure

1. Same as steps 1, 3, 4 and 5 for isotope dilution procedure.
2. Transfer to 500 ml volumetric flasks and dilute to volume.
3. Pipette 50 ml of #2 and 5 ml of Lithium standard (16,000 μgm/ml) into a 100 ml volumetric flask. Dilute to volume.
4. Filter into a polyethylene bottle.
5. Analyze on Perkin Elmer model 146 flame photometer, using appropriate standards containing the same concentration lithium as the unknowns (~800 μgm/ml). The standards are read three times each, setting the high standard to 90 in between each reading. The unknowns are also read three times, this time setting the nearest standard to the triplicate average each time.

Contamination Blanks

One isotope dilution potassium blank showed 10.5 μgm of contamination. A flame photometer potassium blank showed about 23 μgm contamination. The difference is attributed mainly to the use of distilled but not demineralized water in the flame photometer analyses. A rubidium and strontium blank run by Professor W. H. Pinson using 100 ml of HF during the "Digestion" showed 0.2 μgms and 0.3 μgms respectively.

Spike Calibration Procedures

The K^{41} spike was calibrated against the same shelf solution from which the flame photometer standards were made. It was found to have increased in concentration from about 46.0 μgm/ml (1956 calibration) to 56.7 μgm/ml (July 1960 calibration). Two calibrations gave 56.1 and 57.1 μgm/ml.

The rubidium 87 and strontium 84 spikes had been calibrated as follows by Prof. W. H. Pinson. The 85 milligram rubidium spike was diluted to 59.6 μgm/ml by weighing as RbCl. It was also calibrated against a shelf solution which was made up by purifying normal RbCl on an ion exchange column, weighing 0.2 grams into solution, and correcting for 0.5% K impurity. A gravimetric analysis of the shelf solution as the perchlorate, with ethyl acetate extraction of impurities, agreed to about 1.2% with the weighing and dilution value. Calibration of the spike against this shelf solution gave 64.2 μgm/ml by mass spectrometery and 63.6 μgm/ml by flame photometry. The discrepancy of these with the gravimetric value is attributed to anion impurities in the chloride salt, probably rubidium oxide.

The strontium 84 spike gave good agreement between the weighing and dilution value and that obtained by calibration against a shelf solution.

Condensed U-Th-Pb Procedure

This is the procedure used for a monazite analysis made at the Geophysical Laboratory.

1. About 3 grams of borax, which has been purified of lead by dithizone extraction, is melted in a platinum crucible. Fifty milligrams of monazite are added and fused for fifteen minutes at about 1000° C over a Meeker burner with air blast.
2. The glass is dissolved in less than 100 ml of 3NHCl.
3. Aliquots of this solution are pipetted and spiked for Uranium, lead and thorium concentration analysis. An unspiked portion is taken for lead ratio determination.
4. The lead solutions, 10% in citrate and adjusted to pH 8.5, are extracted into dithizone. The lead and iron are stripped back into 10 ml of 2% HNO_3. The iron is complexed with 10 ml of NH_4OH-KCN solution. The lead is extracted back into dithizone, and then stripped back into 2% HNO_3. It is then washed with chloroform, and evaporated to dryness. This is taken up in 1 ml of 2% HNO_3, adjusted tp pH 4.5 with ammonia, and the lead precipitated as sulfide by bubbling H_2S into the warmed solution. The lead sulfide, after centrifuging, is pipetted onto the tantalum filament.
5. Hydroxides are precipitated from the uranium solution by bubbling ammonia gas through it and centrifuging. The precipitate is taken up in a few drops of concentrated HNO_3, 15 ml of $Al(NO_3)_3$ solution added, and the uranium extracted into hexone. Strip the uranium from the hexone with water.

Evaporate the water solution just short of dryness. add 15 ml of 10M NH_4NO_3. Extract with hexone again. Backwash the hexone with water. Evaporate the water down, and heat well to destroy the ammonium nitrate. The nitrate residue is then pipetted onto the tantalum filament.

6. The same procedure is used for thorium as for uranium except that the aluminum nitrate hexone extraction can be eliminated if there is a lot of thorium present. If the concentrations of uranium and thorium are equivalent they are treated together as in step five.

2. Mass Spectrometric Procedures

The mass spectrometer is a standard 6" 60° Nier-type. A high capcity diffusion pump (Martin) allows the tube to be pumped down to 1×10^{-5} mm in about one half hour. In several hours the pressure may be 1 to 2×10^{-6} mm. The tube is baked only infrequently. A vibrating reed electrometer is used for the ion current amplification. The tantalum ribbon filaments are cleaned and checked in the spectrometer before each sample is applied. A single filament can frequently be used for five to ten strontium runs. Filaments for K and Rb are replaced and cleaned for each new sample.

Rubidium and potassium runs are usually made on the 100 or 1000 mv scales. The strontium runs are usually made on the 10 and 100 mv scales. Conditioning the strontium samples for several hours at a temperature just below where the strontium emits helps to burn off any rubidium and seems to improve the ultimate strontium emission. In strontium isotope ratio runs 50 to 75 sets of peaks are scanned; for Rb, K, and Sr concentration runs, 25 to 40 sets are taken.

During the course of a run the strontium ratios often show a systematic variation. The 86/88 ratios may show cycles of up to 0.5% amplitude, while the 87/86 ratios commonly follow mirror image cycles of one half that amplitude. This is very likely due to filament fractionation. The rubidium ratios commonly show equivalent variation but it is usually of a more random nature.

D. Discussion of Errors

In the following sections, consideration is given to the sources and probable magnitudes of errors involved in the various analytical techniques used in this thesis investigation.

1. Argon Analyses

The following are possible sources of gross errors.

Incomplete Argon Release: It is impossible to state any adequate criteria for the complete release of argon except complete fusion.

Although some unfused samples may give quantitative release, most do not. Sintered, cemented, but unfused samples of muscovite, biotite and pyroxene have yielded up to 25% additional argon on complete fusion. One sample which was initially fused to a glass was refused in the presence of NaOH flux, with less than (.1%) additional argon released. As a general procedure, fusion to a glass seems to be necessary and sufficient.

Incomplete Mixing of Spike Argon

In one run where the spike was given only 10 minutes to mix with the radiogenic argon, 65% more radiogenic was measured than in a subsequent run using normal procedures. This particular error could only be explained by lack of equilibration of spike and radiogenic argon. (In normal runs this problem is avoided by a quantitative adsorption of all the argon on liquid nitrogen cooled charcoal.)

Adsorption of Non-representative Mixtures of Radiogenic and Spike Argon on Cold Traps, Stopcock Grease, etc.

All cold traps are cycled (warmed to room temperature and cooled again) before the gas is expanded to a different part of the purification train. This is done as routine practice, although a specific instance of argon being trapped by condensing gases was never noted. Carr and Kulp (1957) showed that quantities of argon as small as 10^{-9} cc could be circulated in a system containing molten rock sample, mercury diffusion pump, hot calcium, charcoal traps, and stopcocks with less than 2% loss by absorption.

Contamination by "Memory" Argon

According to some investigators memory effects in a Reynolds type glass spectrometer are a serious problem. This effect shows up as a variation in isotope ratios after the gas is admitted. No serious memory effects were ever observed in the Reynolds-type tube used in this research. Memory can be observed under special conditions but is negligible in a normal run. For example, the best test of memory effects is to follow a run of high 38/40 ratio with a run of low 38/40 ratio. This was done many times as part of the normal calibration of the discrimination of the ion source. Following all runs where large air corrections were expected, an air argon sample was run to precisely determine this discrimination correction. The normal run might have a 38/40 ratio of one, whereas air has a 38/40 ratio of 0.00063. The 38 measured in these air runs was always in excess of the air ratio and is probably a memory effect.

The amount of this excess varies depending on the pump down interval. When the pump down time is only one half hour, the measured air 38/40 ratio might be ~ .002 (after correcting for 38 bkgnd). When several hours pump down time is allowed following the previous run, the 38/40 air ratios average about .0008. At worst then, this memory would cause a 3% effect in the isotope ratios of a run with low 38/40 ratio (.03), and would normally be less than 0.1%. Two routine procedures probably contributed to the lack of memory trouble. One was an arbitrary limit of 1×10^{-6} mm placed on the maximum pressure of gas allowed in the tube during a run. The other was adjustment of the weight of sample used so as to have a 38/40 ratio greater than 0.3.

In addition to the above errors which might be called "accidental", there are measurement errors associated with the isotope ratios, and "systematic" errors associated with the electronics, fractionation correction, mass 36 background correction, spike calibration, etc.

Isotope Ratio Measurements on Gas Source Spectrometer

For the argon runs presented in this thesis, six to eight sets of peaks (36-38-40) are normally measured, spread over a flow time of about 25 minutes. The 38 and 40 peaks are invariably larger than 300 mv, with a 38/40 ratio ranging from 1 to .03. The precision of this measured ratio is determined largely by the stability of the emission regulator. The calculated standard error of the mean of six to eight sets ranges from 0.05% to 0.2%, with an average of about 0.07%.

Measurement of the 36 peak is made on the 10 or 30 mv scale, with electronic noise barely visible on the 30 mv scale. The precision of the 36/38 or 36/40 ratio is directly affected by the peak height on account of this electronic noise. When the 36 peak is greater than 3 mv, the standard error of 6 sets of 36/38 ratios averages about 0.3%. For the smallest 36 peaks normally encountered (1 mv), the standard error is not worse than 1%. Occasional runs may have much worse precision due to instability of the emission regulator or magnet supply.

Source Discrimination

The mass discrimination of the Reynolds type instrument was found to vary with time due to unknown drift, usually changing after a bakeout period. It was also a function of the value of the total emission current. For this reason the discrimination was measured frequently using air argon as a standard (see Appendix IB). Discrimination corrections ranging from 2% to 3.5% were applied to all measured ratios. Duplicate discrimination measurements made at one half hour intervals without change of instrument settings showed better than 0.2% precision. Without measuring discrimination after every run, the general drift rate indicates the correction for discrimination to be precise to about 0.5%.

Fractionation Correction

Corrections for flow fractionation due to the molecular leak were always made on a theoretical basis. When there was appreciable resevoir depletion the plotted ratios almost always agreed with a

theoretical curve. Corrections made in this way showed the precision for ratio measurements mentioned above. It is possible that this correction, while precise, is systematically in error, e.g., while two lines of different slopes can be fitted to the experimental points with equal precision, the extrapolation to "time zero" may result in a finite difference. This is estimated to be less than 0.2%.

Electronic Variables

The attenuator ratios on the vibrating Reed electrometer were within 0.1-0.2% of face value when measured, but these were not systematically calibrated or corrected for.

The Brown recorder was checked and calibrated at the start of the investigation. Experience indicates these to maintain their accuracy over long periods of time. There is evidence from many of the rapidly decaying runs, however, which indicates that peaks of less than several inches in height are consistently recorded smaller than actual size. In general this can be accounted for by keeping the peaks large. This is not possible with the 36 peaks, and there may be up to a 1% systematic error in many cases. Attempts to define this error by running air argon at different flow rates were ambiguous.

Mass 36 Background Correction

A background peak at mass 36 ranging in size from 2% to 15% of the total gas 36 peak was always measured before each run and

corrected for. This correction can be made with considerable accuracy, providing the background doesn't change when the sample is introduced. The investigation of possible background increases described earlier in Appendix IB rules out any gross effects (>5%). Several very young samples have been run which give zero ages, whereas negative ages would be expected if a 36 background increase took place. It is very difficult however to prove that increases of 1% to 2% do not ever occur.

Spike Calibration

Two spike systems were used; a "routine" spike and a "low range" spike. Reproducibility of calibrations of the "routine" spike, using air as a primary standard, is about 0.3%. The accuracy of the calibrated values as indicated by analysis of a standard biotite is not worse than 1%.

The reproducibility of calibrations of the "low range" spike is about 0.9%. Consideration of results from runs on the standard biotite and a comparison of duplicate runs made using both spikes indicate the calibration of this spike to be 4 to 5% low, and variable. This discrepancy was not satisfactorily resolved, and the low range spike was used only in diffusion runs where relative rather than absolute values were necessary.

Overall Argon Precision

The overall error in the isotope ratios due to all random errors is taken as 0.5% for 38/40 and 1% for 36/38. The value of total argon (no air correction) involves the error in the 38/40 ratio

and the spike uncertainty. A total error of 0.6%, then, should represent the precision of zero air correction argon measurements. Five analyses of the standard biotite (Sixth Annual Report, 1958) show a standard deviation of 0.54%. Consideration of other zero air correction replicates indicates the usual precision to be nearer 1%.

For runs with a finite air correction, the error in determining the proportion which is radiogenic may be written as:

$$\sigma^* = \frac{\sigma^{36}(\%\,\text{AIR})}{(\%\,\text{Radiogenic})}$$

Where σ 36 is the error in the 36/38 measurement - about 1%.

Fig. 6 is a plot of σ^* versus % Air for several values of σ 36. Fig. 7 shows the minimum age which can be measured to a precision of 5% (σ^*) versus absolute amounts of air contamination (for two values of σ 36 and for a hypothetical 5 gram sample of 7% K mineral). In the present research, air contamination averaged 4×10^{-5} std cc, and this limits measurements of 5% precision to samples 7 million years or older.

Most of the argon age analyses made had air corrections ranging from 30% to 60%. If σ36 = 1%, then σ^* = 1%, which is an overall precision of 1.2% (combination of 0.6% ratio error and 1% air correction error). No suitable replicates are available for comparison.

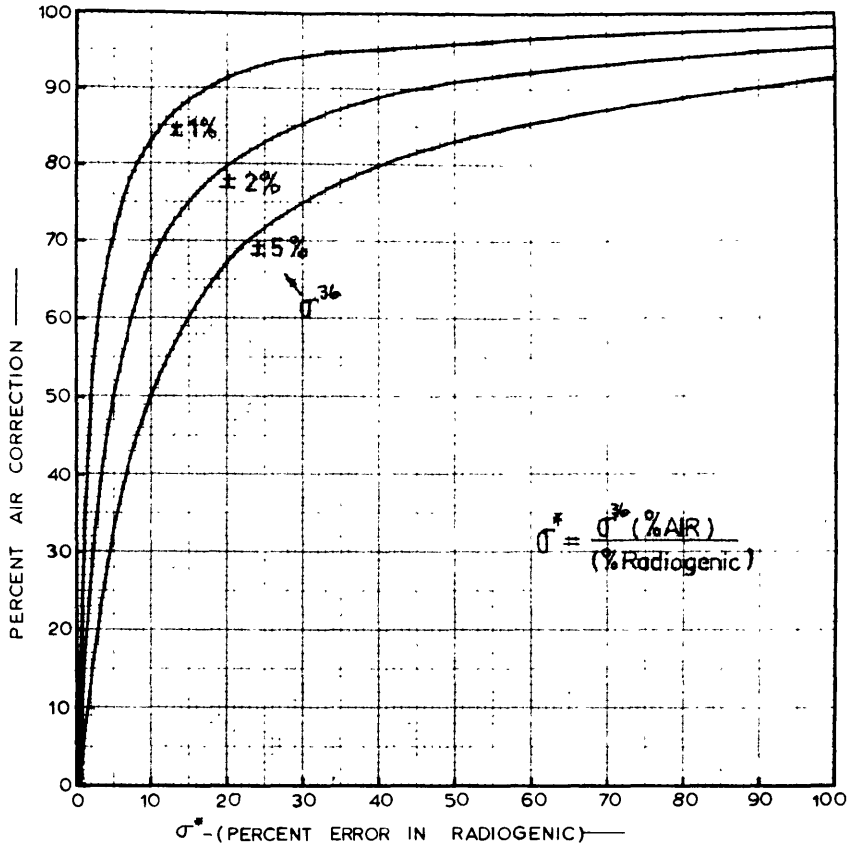

FIG 6 – DEPENDENCE OF ACCURACY ON AIR CORRECTION

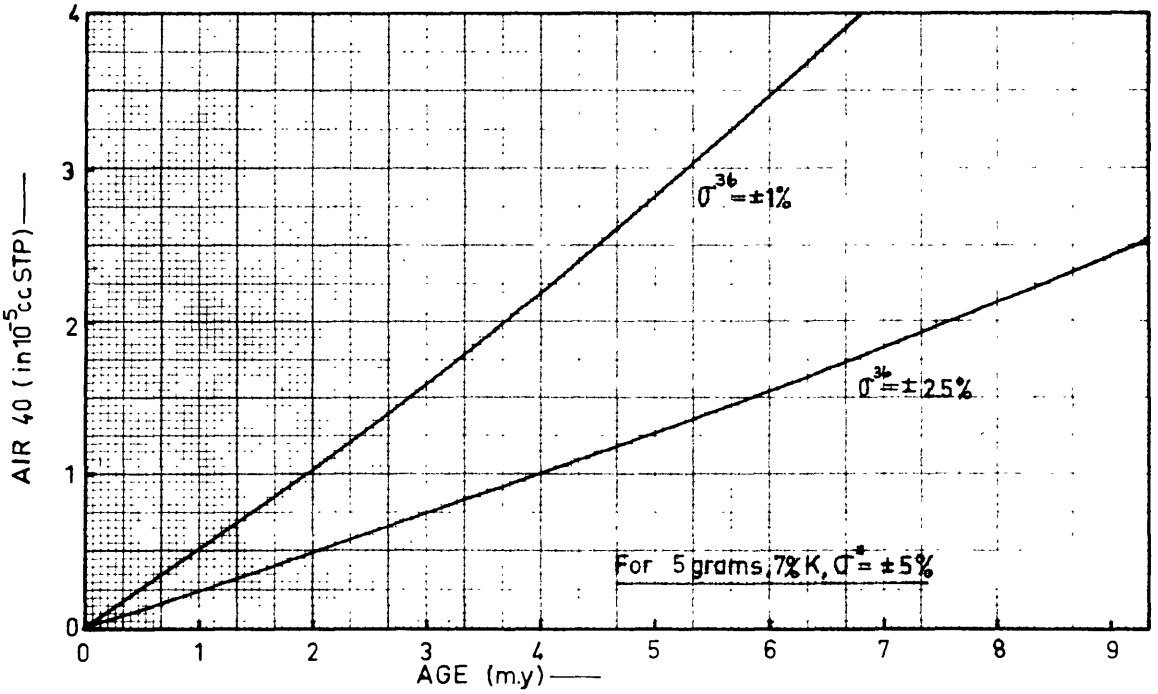

FIG 7 – MEASURABLE AGE LIMIT VS. AIR

Overall Argon Accuracy

Accuracy is affected by systematic errors in spike calibration, mass 36 background increases, scale change factors, etc. A test was made of overall accuracy by running a 0.274 gram sample of B 3203, the standard biotite. This duplicated the conditions of routine runs with respect to the argon 36 air correction. This run, with 43% air correction, gave a radiogenic argon value of 3.85×10^{-4} cc stp. This compares well with the average value, 3.88×10^{-4} cc stp, of other investigators.

2. Potassium Analyses

In the case of potassium measurements an estimate of precision is easily made, as all flame photometer analyses were made in duplicate. As stated in the section on techniques, duplicate photometric determinations were not generally made as these were always found to reproduce very closely (<.3%). The standard deviation error for a series of duplicate analyses may be determined from $\sigma = \sqrt{\frac{\Sigma \delta^2}{2n}}$, where n is the number of pairs of solutions analyzed. Sixteen duplicate analyses of biotites were made (K>5%), and eight duplicate analyses of hornblendes were made (5%<K<2%). For the biotite analyses σ = 1.0%, and for the hornblende analyses σ = 1.4%. This difference is considered real even though the number of duplicate analyses in each case is not statistically sufficient.

Estimates of accuracy are not so easily made. A limited number of isotope dilution analyses show no systematic differences with

the flame photometer results. Since both are calibrated against the same standard solution this does not necessarily represent a measure of accuracy. Professor Pinson has made a number of flame photometer analyses of standards (standard biotite, Haplo granite, G-1, W-1, N.B.S. #70, etc.) and the results indicate a possible positive bias of about one per cent. This may reflect mainly a basic difference between gravimetric and flame photometer analyses for potassium.

3. Rubidium Analyses

The best estimate of precision and accuracy in rubidium analyses is gained from work done jointly by the project staff on a shelf solution supplied to us by Dr. G. R. Tilton of the Geophysical Laboratory. This was a RbCl solution containing approximately 70 μgms/ml rubidium. Three aliquots were spiked in a ratio of 1:1, 1:2 and 1:3. Analytical data is given in Table 1 .

Table 1.

Analytical Data on Rb Shelf Solution

	Spike:Shelf	Measured 85/87	Standard Error of Measured Ratio	Calculated Shelf Solution Concentration
1	1:1	.6355	0.27%	69.92 μgm/ml
2	1:2	1.008	0.10%	69.22
3	1:3	1.263	0.41%	68.82
		1.254	0.17%	

The isotope ratios for the duplicate determination on solution #3 agree with each other at the 95% confidence level, and the usually quoted error in isotope ratios of 0.5% would seem to be realistic, although this is the only duplicate Rb done as part of this research. The precision of a single Rb analysis as calculated from the above triplicate is $\sigma = 0.8\%$. This can be considered a minimum value for precision since analyses of the shelf solution involved less chemical processing than a normal mineral analysis. Replicate Rb analyses done on the standard biotite by other members of the project staff (Annual Report #6, 1958) show the precision of a single measurement to be about 0.45%. Two recent analyses of the standard biotite give 463.5 ppm and 462 ppm, indicating precision of the same order. This precision is exceptional and may or may not be representative of Rb isotope dilution analyses in general.

The accuracy of rubidium analyses, as suggested by a comparison of our values and those of two other laboratories on the above shelf solution, is probably better than 1%.

Interlaboratory Results on Rb Shelf Solution

1.	M.I.T.	69.3±.6
2.	Carnegie Institution	67.5
3.	P. Gast, University of Minnesota	68.5

These values are in fact the same, within experimental error.

Some of the Rubidium runs were assigned larger errors (up to 5%) owing to underspiking. It is easily shown from a plot of normal to spike ratio (N/S) versus the Rb^{85}/Rb^{87} ratio that a given error in the isotope ratio results in a much larger error in (N/S) for values of N/S>1. This result may be written as:

$$\frac{\text{Error in } (N/S)}{\text{Error in } 85/87} \approx 1.7\,(N/S)$$

That is, if a 0.5% error is taken as being normal for the measurement of the 85/87 ratio, for a (N/S) ratio of 5 the error in the (N/S) ratio is about 4.2%. Magnification of error from improper spiking can be very serious. Gross overspiking of the order of (N/S) = .05 can also result in large errors because of the 1.7% of Rb^{85} in the spike.

4. Strontium Analyses

Measurement of isotope ratios: For whole rock samples only slightly enriched in radiogenic strontium, measurement of the Sr^{87}/Sr^{86} ratio is the determining factor in precision. To evaluate this, one unspiked whole rock sample was run in triplicate. Table 2 shows the analytical results.

The most striking observation here is that the standard error associated with the actual measurement of the ratios is considerably smaller than the actual spread of the triplicate determinations. This effect is probably due to fractionation which varies from run to run depending on matrix effects in the sample load, filament temperature, size of sample load, etc.

Table 2.

Results of Triplicate Strontium Isotope Ratio Measurements

Run	86/88	87/86	Normalized 87/86
1	.1187±.0004 (±0.34%)	.7959±.0010 (±0.125%)	.7936
2	.1198±.00027 (±0.23%)	.7906±.0011 (±0.134%)	.7920
3	.1191±.00014 (±0.12%)	.7938±.0004 (±0.05%)	.7929
Mean	.1192±.00032 (±0.27%)	.7934±.0016 (±0.20%)	.7928 ±.0005 (±.06%)
Standard deviation of a single analysis	(±0.48%)	(±0.34%)	(±.1%)

If it was just simple fractionation, one could normalize the ratios to a constant value of 86/88 and expect to improve the precision of the 87/86 ratios. In this particular triplicate, normalizing to an 86/88 ratio of .1194 resulted in a marked improvement (a factor of 3) in the standard deviation and standard error of the mean of the triplicate. The mean 87/86 ratio remained essentially unchanged by the normalizing procedure. The procedure assumes that mass fractionation is responsible for run-to-run variations in the ratios and this is no doubt partly true. In a series of four runs on a standard strontium carbonate done by project members, normalizing again improved the precision of the mean and of a single analysis, while not changing the mean itself. (.7119→.7122) Many more replicate analyses would have to be made to justify normalizing as a routine procedure.

STRONTIUM CARBONATE QUADRUPLICATE

	Standard	Normalized
Standard Error of the Mean	±0.12%	±0.05%
Standard Deviation	±0.24%	±0.10%

Another point demonstrated by this triplicate analysis is the better precision of the 87/86 ratio as compared to the 86/88 ratio. This is a function of the smaller step interval from 86 to 87 and is one reason why a Sr^{86} spike should be better than a Sr^{84} spike for isotope dilution analyses.

It may be concluded that a ±.5% error routinely attached to isotope ratio measurements is justified and conservative. This depends of course on the quality of the run. The above triplicate represented three average strontium ratio runs, whereas poorer runs occasionally have to be used.

The effect of this isotope ratio error on the calculated fraction of strontium 87 which is radiogenic can be shown simply as

$$\sigma^* = \sigma^{87/86} \left[\frac{100 - \%\ \text{RADIOGENIC}}{\%\ \text{RADIOGENIC}} \right]$$

For a sample 10% enriched in radiogenic strontium ($87/86 \simeq .79$) and assuming a 0.5% error in 87/86, σ^*, the error in the fraction of radiogenic, is 4.5%. If the sample is 100% radiogenic, there will be no error involved in correcting for common strontium contamination. The advantage of making a separate unspiked run to determine the radiogenic fraction, when this is small, is easily illustrated. An unspiked sample 10% enriched

in radiogenic strontium is only about 7.7% enriched when spiked in a 1:3 ratio (N/S=3). The error then becomes 6% as compared to 4.5% for the unspiked run. The actual difference between the radiogenic strontium determination in spiked and unspiked runs on three samples averaged 11%. These samples were all better than 10% radiogenic.

Measurement of Strontium Concentrations

Very few replicate determinations are available in recent project history to assess properly the accuracy of isotope dilution strontium runs. Four repeats on the standard biotite (Sixth Annual Report, 1958) gave a standard deviation of 6.0%. Some of this variability may be caused by a variable strontium blank, as the radiogenic strontium 87 analyses showed an error of only 2.8%. As a working estimate, an error of ±3% is assumed to be realistic.

It may be pointed out that the spiking of strontium analyses is also somewhat critical in regard to magnification of ratio measurement errors, in that the Sr^{84} spike used contains 28% Sr^{88}. In this case it is overspiking, not underspiking, which is serious. For example, if (N/S) = 0.35, the error in (N/S) due to an error in the isotope ratio is approximately doubled. No significant magnification results from underspiking, for (N/S)<10.

5. Summary of Errors in Determined Ages

The following are the error estimates applied to the concentration ratios Ar/K and Sr/Rb in normal runs.

	Precision	Accuracy & Precision	
Sr/Rb ($Sr^{87}*/Sr^{87}$=.1-.2)	±6%	±8%	(isotope dilution & separate isotope ratio)
Sr/Rb ($Sr^{87}*/Sr^{87}$ 7.5)	±2%	±4%	(isotope dilution only)
Ar/K (Biotites)	±2%	±3%	(K by flame photometer)
Ar/K (Hornblendes and pyroxenes)	±2%	±5%	(K by flame photometer)

E. Values of Constants Used

	Decay Constants	Isotopic Abundance
K^{40}	$\left\{ \begin{matrix} \lambda_e = 0.585 \times 10^{-10}\,yr^{-1} \\ \lambda = 5.30 \times 10^{-10}\,yr^{-1} \end{matrix} \right\}$	1.22×10^{-4} g/g K
Rb^{87}	$\lambda = 1.47 \times 10^{-11}\,yr^{-1}$	0.283 g/g Rb
U^{238}	$\lambda = 1.54 \times 10^{-10}\,yr^{-1}$	0.993 g/g U
U^{235}	$\lambda = 9.72 \times 10^{-10}\,yr^{-1}$	0.0071 g/g U
Th^{232}	$\lambda = 4.99 \times 10^{-11}\,yr^{-1}$	1 g/g Th

Common strontium 87 abundance = 0.0702

Air argon, 40-36 ratio = 296

Appendix II: Diffusion Effects in Isotope Age Dating

A. Theoretical Considerations

1. Introduction

It is the main premise of this thesis that discordant isotopic mineral ages can most often and most easily be explained by daughter product diffusion under the influence of thermal metamorphism. This not only offers the most plausible physical interpretation, but provides a direct quantitative path to understanding the almost complete combination of age discordances which have been found by different methods on various minerals.

2. Diffusion

It was first suggested by Einstein that the virtual force acting on a diffusing atom or ion in a binary solution is proportional to the negative gradient of the chemical potential. This may be expressed as

$$F_{ix} = -\frac{1}{N}\frac{\partial \mu_i}{\partial x} \qquad 1.$$

where F is the force on particle i in the x direction and N is Avogadro's nuber. Defining a "coefficient of mobility" B_i (the velocity of the particle per unit force) gives for the velocity of the particle

$$V_{ix} = -\frac{B_i}{N}\frac{\partial \mu_i}{\partial x} \qquad 2.$$

The diffusion flux then is

$$J_{ix} = -\frac{C_i B_i}{N}\frac{\partial \mu_i}{\partial x} \qquad 3.$$

where C_i is the nuber of moles of i per unit volume.

In the limiting case of ideal solutions where concentration is proportional to mole fraction

$$\frac{\partial \mu_i}{\partial x} = \frac{RT}{c_i}\frac{\partial c_i}{\partial x}$$

and

$$J_{ix} = -D_i \frac{\partial c_i}{\partial x} \qquad 4.$$

where D_i, the "diffusion coefficient" of i, is equal to

$$\left(\frac{RTB_i}{N}\right)$$

Equation 4. is equivalent to Fick's Law, a phenomenological law postulated by Adolf Fick in 1855. This law is the basis for most quantitative descriptions of diffusion phenomena. Fick's law has been shown experimentally to be valid for sufficiently low concentrations and concentration differences. In the form $\left(\frac{\partial c}{\partial t} = D\frac{\partial^2 c}{\partial x^2}\right)$ it is readily amenable to mathematical solution for a variety of geometric shapes and boundary conditions. To gain an understanding of the effects of nonideality on the diffusion coefficient, it may be evaluated in terms of thermodynamic properties. Comparison of equations 3. and 4. gives for Di

$$D_i = \frac{RTB_i}{N}\left(1 + X_i\frac{\partial \ln \gamma_i}{\partial x_i}\right) \qquad 5.$$

where B_i can be said only to be some function of composition at constant P and T; and X_i is the mole fraction. This reduces to the D_i of equation 4. for ideal solutions where $\gamma_i = 1$. Alternatively, γ_i can be very large and have little effect on D_i as long as X_i is small, as it is for most cases to be considered. However, most of the natural systems to

be considered are not binary, but multicomponent systems, and extrapolation of equation 3. to multicomponent systems cannot be justified a priori. For a component in a ternary system, for example, equation 3. should be written

$$J_1 = R_{11}\nabla\mu_1 + R_{12}\nabla\mu_2 + R_{13}\nabla\mu_3 \qquad 6.$$

There is no real justification for believing that only the coefficient R_{11} has a nonzero value. However, it will be assumed here that the diffusion flux of a given component is independent of the chemical potential gradients of other components.

Phase Equilibria

An understanding of thermodynamic equilibria is essential to the meaningful interpretation of "age discordancies". Consider an assemblage of phases in a closed chemical system. At equilibrium, for a given value of temperature and pressure, the compositions of the phases are determined uniquely regardless of the number of components. A change in P or T requires that either the composition or relative masses of the phases must change, if equilibrium is to be maintained. The distribution of K, Rb, Sr and Ar between phases in equilibrium, then, is a function of P and T (and initial bulk composition). A change in P or T will require some redistribution of these elements. It is this redistribution during metamorphism which is of interest in the interpretation of mineral age discordancies. Qualitatively, redistribution of the parent elements

K and Rb should be less than that of Ar and Sr. This is because the parent elements probably reached an equilibrium distribution initially, during formation of the assemblage. A small change of the K and Rb concentration in each phase will establish equilibrium again after a change in P or T, whereas gross changes in Sr and Ar are necessary to establish their equilibrium distribution. The criterion of distribution equilibrium is that the chemical potential of a component be equal in all possible phases. For ideal solutions this is equivalent to $K(P,T,X_j) = \frac{N_i^{\alpha}}{N_i^{\beta}}$ (Nernst distribution law, N_i the concentration or mole fraction of i in phases α and β.)

Argon

The equilibrium distribution for argon is one in which most of the argon occurs as a gas phase in grain boundaries and possibly in the structural holes of some minerals. If the system is open to argon most of it will eventually escape to the atmosphere, where its chemical potential is lowest.

Potassium

Potassium in minerals like hornblende and pyroxene might undergo marked changes, especially if the stability limit of a coexisting potassium-rich phase is exceeded. The potassium in feldspars and micas is nearly stoichiometric, so it would change only slightly. For example, in thirty pure biotites of varying composition analyzed by Phinney (1959) and Brownlow (1960), the potassium concentration varies over a total range of 20%.

Rubidium

The extent to which the distribution coefficient of rubidium varies with changes of P and T might be estimated by measuring this ratio for many rocks formed under varying P-T conditions. A tabulation of available measurements of the rubidium concentrations in coexisting minerals indicates the effect of P and T on this distribution coefficient to be relatively small.

	K_{Rb}	K_{Sr}	No. of Pairs
Biotite / Feldspar	3.2±.9	(.01-.8)	10
Biotite / Muscovite	1.7±.6	(.07-2.0)	7

(Standard deviation error shown)

Since this sampling represents rocks of different bulk composition, the above should represent the maximum variability of K_{Rb} in a rock of fixed composition. It seems likely then that the rubidium content of biotite, muscovite and feldspar will not change by more than 35% during metamorphism unless the system is open to rubidium.

Strontium

By virtue of the different geochemical affinities of rubidium and strontium, measurable radiogenic strontium usually is produced in those minerals in which its chemical potential

is high relative to that in coexisting phases. The distribution coefficient of common strontium indicated by the tabulation above is extremely variable. (This may be accounted for in part by impurities in the analyzed phases and possibly by non-ideal behavior of strontium in minerals like biotite.) Also, in the case of strontium, the criterion for equilibrium is the equality of the chemical potential of <u>each isotope</u> in all phases. In addition to concentration changes caused by the change of K_{Sr} with P and T, there will be the change in radiogenic strontium concentration needed to bring about isotopic equilibrium. For a case where K_{Sr} does not change, only diffusion of radiogenic Sr^{87} need be considered. If the radiogenic Sr^{87} occupies a different site in the mineral from the common strontium, there may also be a chemical potential gradient within the mineral itself.

Consider the case where only diffusion of the radiogenic component takes place. This must be treated mathematically as a two phase problem because the concentration at each phase surface is a function of the diffusion parameters of the coexisting phases, and of the distribution ratio of the strontium. If K is the equilibrium distribution ratio Sr^{β}/Sr^{α}, and D^{α} and D^{β} are the diffusion coefficients of phases α and β respectively, the concentration at any point x from a plane phase interface in an infinite cylinder may be written as (Jost, 1952)

$$C = C_0 \left\{ 1 - \frac{K\sqrt{D^\beta}}{K\sqrt{D^\beta} + \sqrt{D^\alpha}} \left[1 + \operatorname{erf} \frac{x}{2\sqrt{D^\alpha t}} \right] \right\} \quad \text{for phase } \alpha$$

$$C = C_0 \left\{ \frac{K\sqrt{D^\alpha}}{K\sqrt{D^\beta} + \sqrt{D^\alpha}} \left[1 - \operatorname{erf} \frac{x}{2\sqrt{D^\beta t}} \right] \right\} \quad \text{for phase } \beta$$

The overall rate of diffusion is controlled by D^α or D^β, whichever is smaller. The diffusion loss of strontium from biotite, then, may depend very much on the nature of the coexisting phases and it is not enough to merely specify the diffusion parameters of strontium in the biotite. Useful information concerning the relative values of D^α, $D^\beta \ldots D^n$ could be obtained by analyzing the strontium and rubidium in the phases of an assemblage which had not reached equilibrium during a period of metamorphism. Data is available in one such case (H. W. Fairbairn, personal communication) from the Sudbury, Ontario district. Several samples show evidence of having reached equilibrium during a metamorphic period at 1.2 billion years. The criterion for this equilibrium is a mutual intersection of biotite, feldspar and whole rock radiogenic growth lines at 1.2 b.y. One sample (3094) shows discordant mineral ages but no mutual intersection. The Sr 87/86 ratios of the whole rock, feldspar and biotite from this sample are all greater than 0.82 (at 1.2 b.y.). However, the 87/86 ratio in garnet is less than 0.72, suggesting that the diffusion coefficient of strontium in garnet is smaller than that in feldspar or biotite.

Effect of Compositional Changes

It is clear that the diffusion loss of argon and strontium from minerals will be influenced by compositional changes made in response to changing environmental conditions. Consider the assemblage biotite-magnetite-K feldspar. Very slight changes in the temperature or partial pressure of oxygen will require that an equilibrium biotite change composition (this itself being a diffusion process). Loss of strontium or argon then will be taking place in an unstable or changing structure, and under these circumstances their diffusion rates may be much higher. The mineral phases with the largest stability range would be least affected by metamorphism. As Wones (1960) pointed out, muscovite-feldspar assemblages are stable over large variations of T and P compared to biotite, and this may explain the fact that muscovites frequently show older ages than biotites. All iron-magnesium minerals would be especially sensitive to P-T changes in assemblages containing other iron or magnesium minerals.

B. Argon Diffusion Experiments

1. Calculation and Treatment of Data

Mathematical Description of Argon Diffusion

The concern here will be only with the presentation, solution and numerical evaluation of Fick's Law for those geometries and boundary conditions which best apply to the diffusion of argon under natural and experimental conditions. These solutions will be used in the next section to describe the results of laboratory diffusion experiments and, later, as an aid in interpreting the results of field age measurements.

For a homogeneous phase with uniform initial concentration of argon and uniform concentration of argon at the surface at all times (taken equal to zero), solutions of Fick's Law for a sphere, infinite cylinder, and infinite sheet are readily obtained. (Jost, 1952; Barrer, 1941; Crank, 1956). These have been converted into solutions in terms of F, the fraction of total argon released at any time t.

Sphere

$$F = 1 - \frac{6}{\pi^2} \sum_{1}^{\infty} \left[\frac{1}{n^2} \exp\left(\frac{-n^2 \pi^2 Dt}{a^2} \right) \right] \qquad 1.$$

where a is the radius of the sphere.

This series converges rapidly for large values of F, and one term is sufficient for $F > 0.85$. Three terms are sufficient for $0.4 < F < 0.60$. Below $F = .4$, convergence is very slow. Reichenberg (1953) obtained an approximation, accurate for $0 < F < 0.85$, by using a Fourier Integral transform which gives

$$F = \frac{6}{\pi^{3/2}}\sqrt{Bt} - \frac{3}{\pi^2}(Bt) \qquad 2.$$

(since $\frac{\pi^2 D}{a^2}$ always appears together, the substitution $B = \frac{\pi^2 D}{a^2}$ is generally made.) For values of F<.01, we need use only the first term of equation 2, or

$$Bt = .862 F^2 \qquad 3.$$

Infinite Cylinder (This refers either to a cylinder of infinite length, or a cylinder with sealed, impermeable ends.)

$$F = 1 - \sum_{1}^{\infty}\left[\frac{4}{\xi^2}\exp\left(\frac{\xi^2 Dt}{r^2}\right)\right] \qquad 4.$$

where r is the radius of the cylinder and ξ (Sum, n=1 to ∞) are the roots of the equation $J_0(x)=0$. $J_0(x)$ is the Bessel function of zero order (ξ = 2.405, 5.520, 8.654, 11.792, 14.931,...). For F>0.6, this series converges in one term; for values of F<0.02, the series can be approximated by

$$F \approx \frac{4}{\sqrt{\pi}}\sqrt{\frac{Dt}{r^2}} \qquad 5.$$

or

$$Bt = 1.945 F^2 \qquad 6.$$

Infinite Slab (or slab with impermeable edges)

$$F = 1 - \frac{8}{\pi^2}\sum_{n\ odd}\left[\frac{1}{n^2}\exp\left(\frac{-n^2 Bt}{4}\right)\right] \qquad 7.$$

where $B = \frac{\pi^2 D}{L^2}$ and L is the half-thickness of the slab. Here one term is sufficient for F>.36, and for F<.03 the series can be approximated by

$$F \approx \frac{2}{\sqrt{\pi}}\sqrt{\frac{Dt}{L^2}} \qquad 8.$$

or $Bt \approx 7.76 F^2$

Fig. 8 shows the numerical solution of these equations as values of F versus Bt. Tabulation of some of these values is found in Reichenberg (1953), Serin and Ellickson (1941), Andrews and Johnston (1924) and Darken and Gurry (1953).

Treatment of Experimental Data

Data received from diffusion measurements is usually in the form of the "fraction of argon released" at a given temperature for a given length of time. In general, measurements of the "fraction released", F, are made at four to eight time intervals, giving four to eight F versus t experimental points. Using the curves of Fig. 8, a value of Bt is read off for each value of F, using the appropriate geometric model. These values of Bt are then plotted on linear graph paper versus the time corresponding to the particular measurement of F. If the argon is diffusing at a constant value of the diffusion coefficient, the points will fall on a straight line intersecting the origin. The slope of this line, B, is related to the diffusion coefficient by $B=\pi^2\left(\frac{D}{a^2}\right)$. Conversion can then be made to determine D, taking care to express the time in seconds. In actual practice, since the effective radius for diffusion of argon in minerals is not known but can be shown to be often smaller than the actual physical size, the measurements here will be reported as values of (D/a^2). In this way, no artificial bias is introduced.

Consider the more general case where the argon in the mineral occupies several different structural positions, with

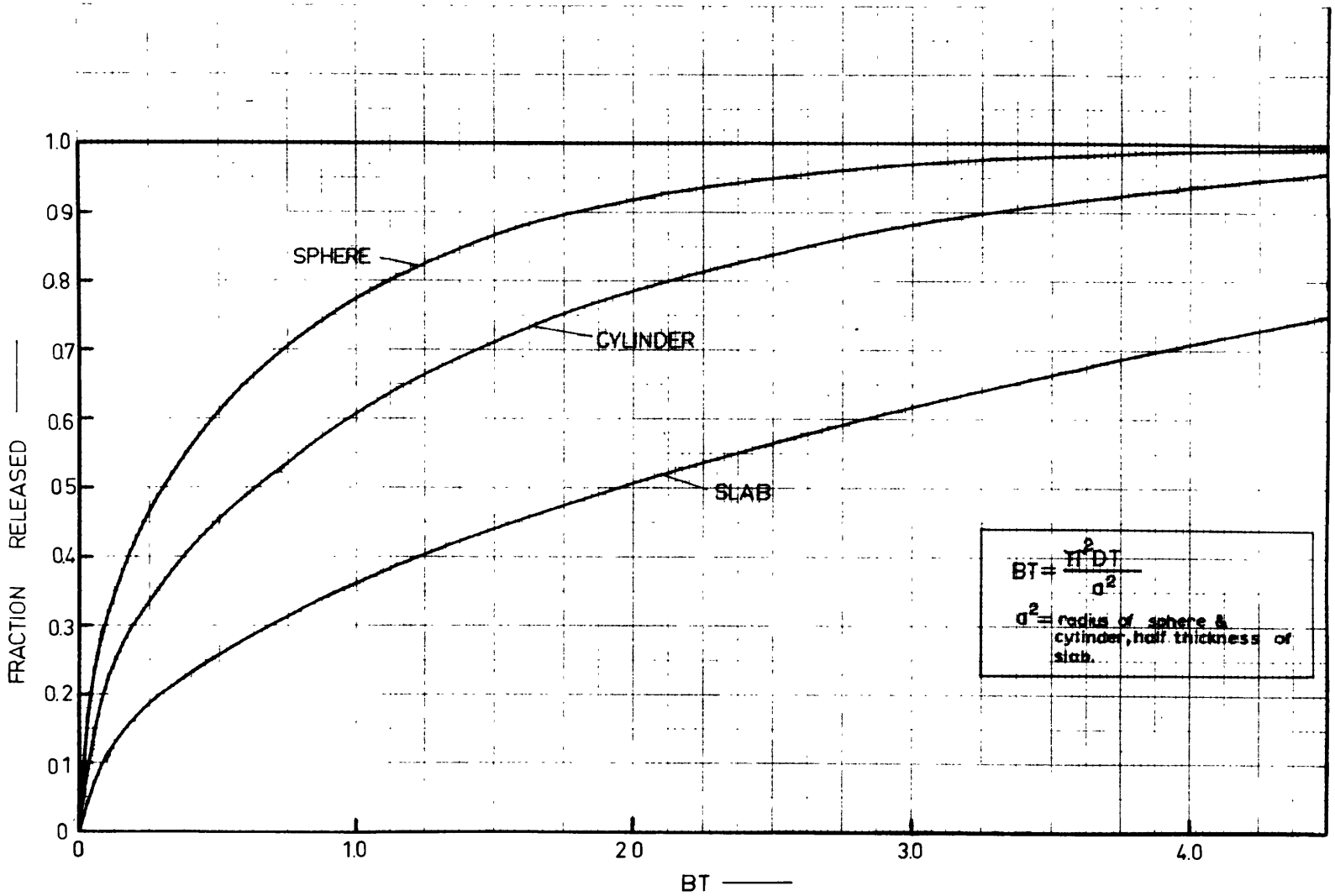

FIG. 8 — DIFFUSION CURVES FOR THE SPHERE, CYLINDER, AND SLAB.

a different activation energy associated with each position. As the mineral is heated isothermally, argon from successively higher activation sites is released, the least tightly held argon coming off first. On the graph of Bt versus t, the experimental points will fall on intersecting straight line segments of successively smaller slopes (values of D/a^2). If the slopes are less than a factor of ten different, there will be very little curvature in the intersection region. However, for large differences in slope, there may be an appreciable curved region between the segments. Since the argon being released at any time is a mixture of argon from several sites, a correction must be made for this when calculating D/a^2 for each segment. For a given segment this is done by extrapolating back the next segment and obtaining the difference. By such successive corrections it is also possible to tell the quantity of argon held in each position, except in those cases where the measurements were not extended far enough to pick up the next break in slope. When calculating the fraction of argon released from each position, it must be remembered that this is the fraction of the total argon in a particular site, not of the total argon in the sample.

It is usually possible to correlate the various line segments from one temperature to another by calculation of the quantity of argon represented by each segment. This then allows a calculation of the activation energy corresponding to argon diffusion from each site. It should be noted that

the calculations and treatment of data above assume that the argon in each structural site can be considered independent of that in other sites. The experimental curves are entirely consistent with this interpretation of non-coupled volume diffusion from different structural sites. The curves also may be consistent with a different interpretation.

In many cases the points do not define the slope of a given line segment. This is usually true of the initial segment. Lines have been drawn on the graphs to connect the points. These lines may not be unique.

In lieu of information concerning the actual diffusion symmetry of various minerals, all calculations are based on a spherical model. This would introduce less than a factor of two error should micas actually have cylindrical symmetry. Recalculation of the data to a cylindrical or sheet model is straightforward.

2. Radioactive Argon Counting Method

Introduction

Initially it was felt that the use of radioargon as a tracer in diffusion experiments provided the easiest and most sensitive approach for studying diffusion of argon in natural minerals. Argon has three radioactive isotopes, 35 day Ar^{37}, 260 year Ar^{39} and 1.8 hour Ar^{41}, all of which can be produced in usable quantities by irradiation in a nuclear pile. The following are possible production reactions:

$Ca^{40}(n,\alpha)\ Ar^{37}$
$K^{39}(n,\rho)\ Ar^{39}$
$Ar^{40}(n,\gamma)\ Ar^{41}$
$K^{41}(n,\rho)\ Ar^{41}$

Reynolds (1957) used Ar^{39} to measure the diffusion rates of argon in a K-Ca-Silica glass, and recently Fechtig used Ar^{37} (1960) to measure the diffusion coefficients of argon in fluorite, anorthite, augite, and margarite. The method used by Fechtig is sufficiently sensitive that he was able to measure the diffusion rate of argon at room temperature.

Preliminary results obtained on orthoclase and glauconite are reported in the following pages. The results obtained on orthoclase were quite satisfactory, but for several reasons further investigation was discontinued in favor of mass spectrometric analysis. First, gas purification was found to be necessary for the glauconite, nullifying one of the main advantages of the method. Most important, the basic question of how much geologic applicability the measurements allow could not be answered without considerable effort. That is, neutron irradiation produces damage to the mineral structure; the argon which is formed then is not only diffusing in an atypical structure, but may also be originating from atypical structural positions. Later mass spectrometric studies have shown that natural radiogenic argon occupies several types of structural sites with a characteristic activation energy

associated with each. Since the primary purpose of these diffusion studies is to provide quantitative data for understanding the loss of radiogenic argon from natural minerals under conditions of thermal metamorphism, it is imperative that natural conditions be approximated as closely as possible. A comparison of the preliminary results that were obtained by radioactive argon counting and by mass spectrometric analysis of radiogenic argon is of interest and is presented in a later section.

Apparatus for Counting Experiments

The initial experiments were carried out using argon 41 activity, with later conversion to argon 39 intended. A glass vacuum system was constructed consisting of an Inconel furnace, connected by tapered seal joint to a gas train consisting of a mercury manometer, pirani gauge, charcoal traps, cold finger, and glass counting volume. The counting volume was surrounded by two inches of lead brick and shielded from the furnace by six inches of lead. The background counting rate was about 50 cpm with an active sample in the furnace, using a lab monitor G-M tube in the counting volume. The total argon 41 activity in the sample at the start of a run ranged from 1500 to 10,000 cpm, depending on the irradiation time. The Inconel furnace was externally heated by a resistance heater wound with 20 feet of 40 mil Kanthal A wire and insulated with magnesium oxide and nickel shields. Temperatures of 1200° C could be obtained, and were continuously recorded on a Brown "Electronik" recorder using a platinum,

platinum-10% rhodium thermocouple inserted between heater and inconel tube. Temperatures could be read to $\pm 2^{\circ}$ C, and with no regulation on the heater, could be maintained to $\pm 10^{\circ}$ C for periods of several hours. The thermocouple was frequently replaced and calibrated at the melting point of pure copper. During heating up there was a time lag of several minutes between the temperature readings and the actual sample temperature.

Procedures for Counting Experiments

Eight to ten grams of sample were sealed in a plasticene tube and irradiated with fast neutrons in the M.I.T. cyclotron for times ranging from ten minutes to one hour. After a two hour activity cooling period, the sample was transferred to the Inconel furnace, then a grease seal joint was made, vacuum pulled, the system isolated, and the sample heated in about 15 minutes to the desired temperature. The counting rate of the released gas was determined periodically by taking minute interval averages of the activity registered on a counting rate meter. Background was checked frequently by pulling the gas out of the counting volume onto a charcoal trap at liquid nitrogen temperature. Measurements were continued until the decay rate was greater than the diffusion rate; then either a higher diffusion temperature was established or the sample was fused to release the remaining gas activity. After final fusion, the activity was followed for several hours to determine the half life and to demonstrate that the measured activity was due to argon 41.

Feldspar Results

Fig. 9 shows the measured activity (10 minute irradiation) during heating of an 11 gram sample of othoclase perthite from a syenite at Massey, Ontario (Sample No. F3802). The sample was sized at +200. The median grain size was about 200 microns. Fig. 10 shows the fraction of argon 41 released versus time for two temperatures, 795° C and 1040° C. The fraction released was obtained by extrapolating the final activity to time zero, correcting for background and making a ratio with the activity at a given time. Using the curve of the solution for the spherical diffusion equation (see previous section), values of Bt are calculated for each experimental point. These are plotted as a function of time in Fig. 11.

For volume diffusion from a stable isotropic sphere, the experimental points should fall on a straight line intersecting the origin. In actual practice, due to the "heating-up" time, the experimental curves do not intersect the origin. The portion of the curves labelled A is interpreted to represent loss of argon at a single value of the diffusion coefficient by true volume diffusion from a stable structure. The curve labelled B at 795° C can not be assigned to diffusion from a different structural position, as this could only take place with smaller values of the diffusion coefficient (i.e., line of lower slope). The segment B must be related to a change, or changing of structure, and may be due to mixing of the two phase feldspar. To test this possibility, samples were heated

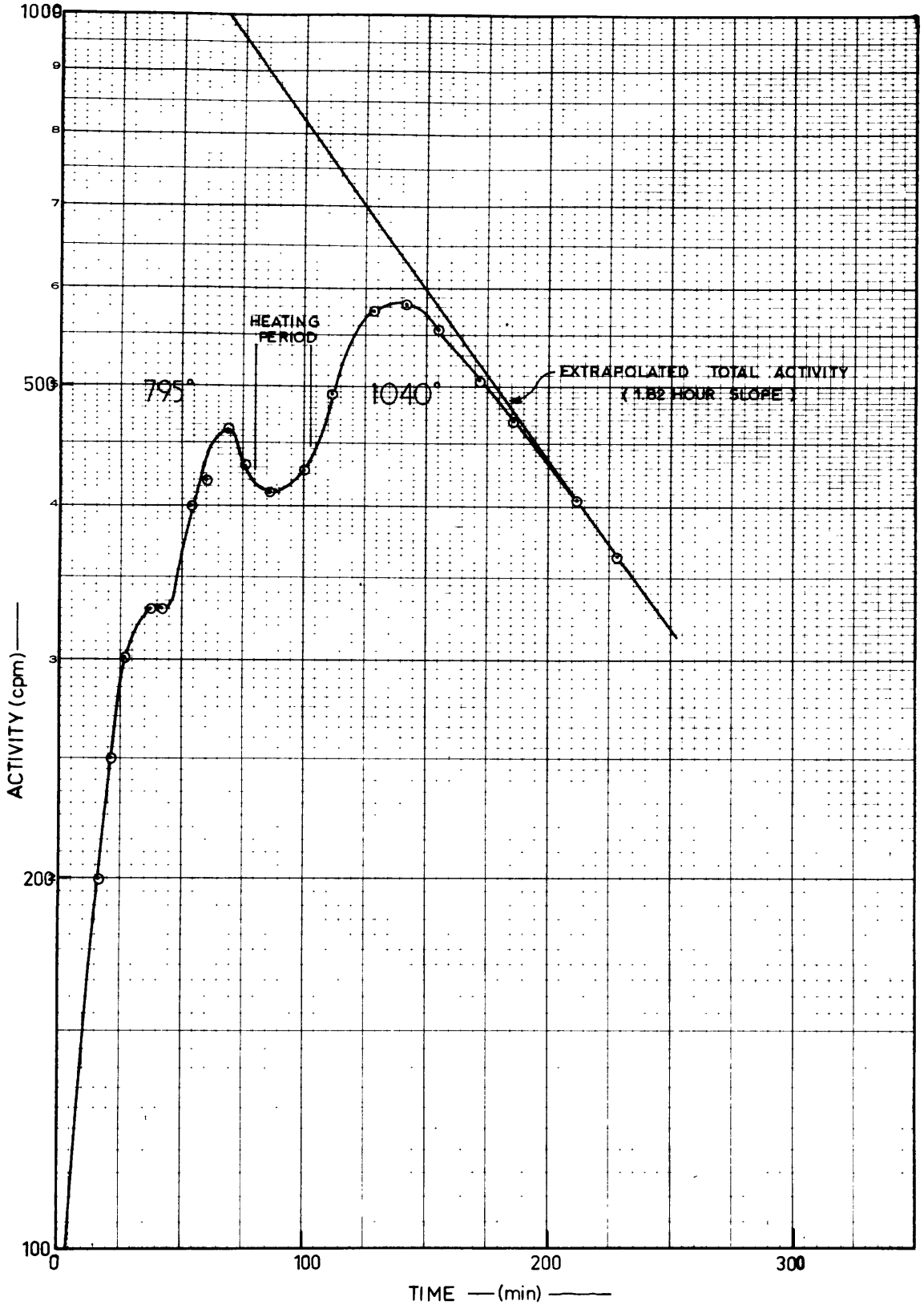

FIG. 9 — ARGON ACTIVITY FROM HEATED FELDSPAR

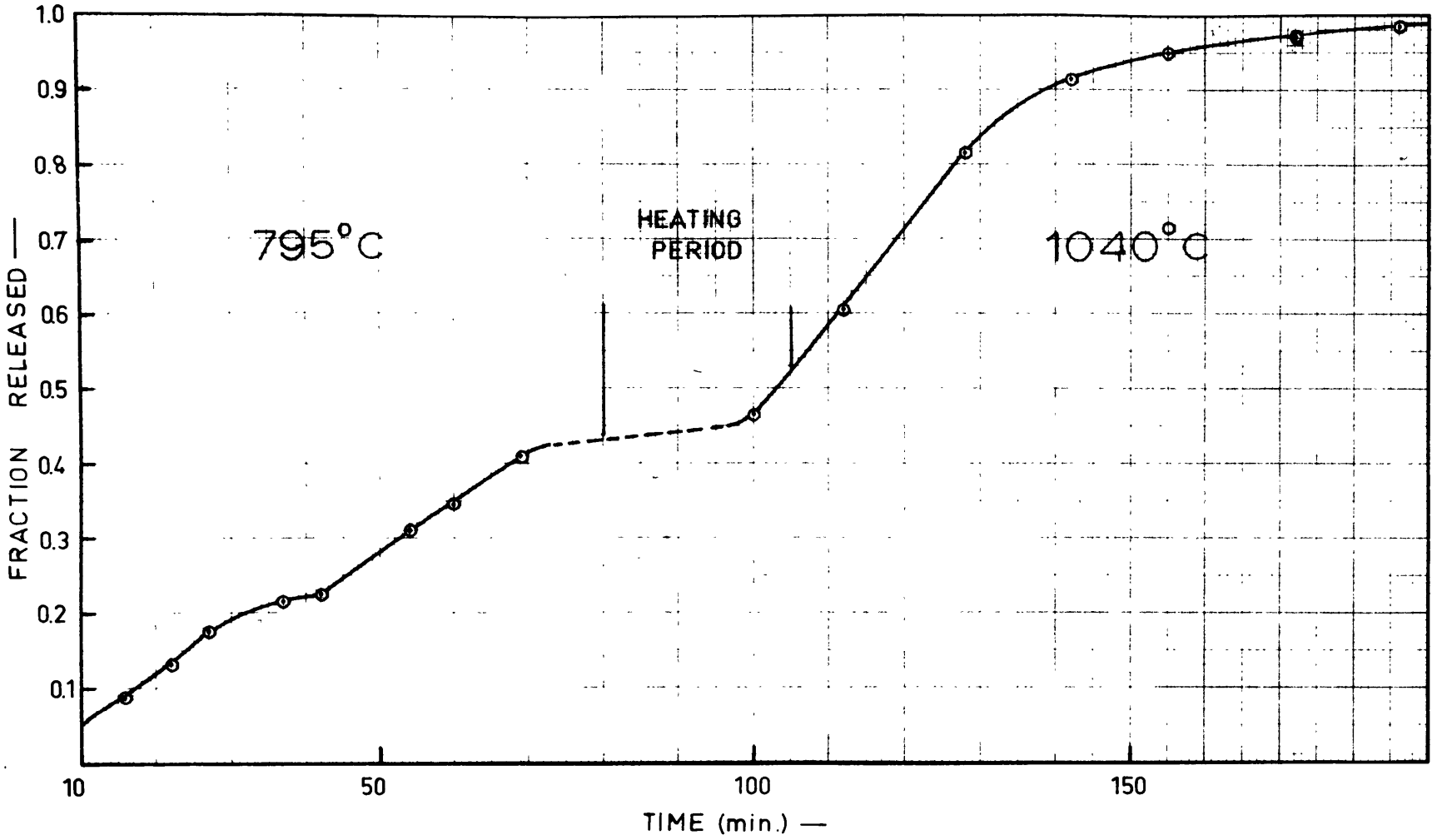

FIG.10 - RELEASE OF RADIOACTIVE ARGON FROM FELDSPAR

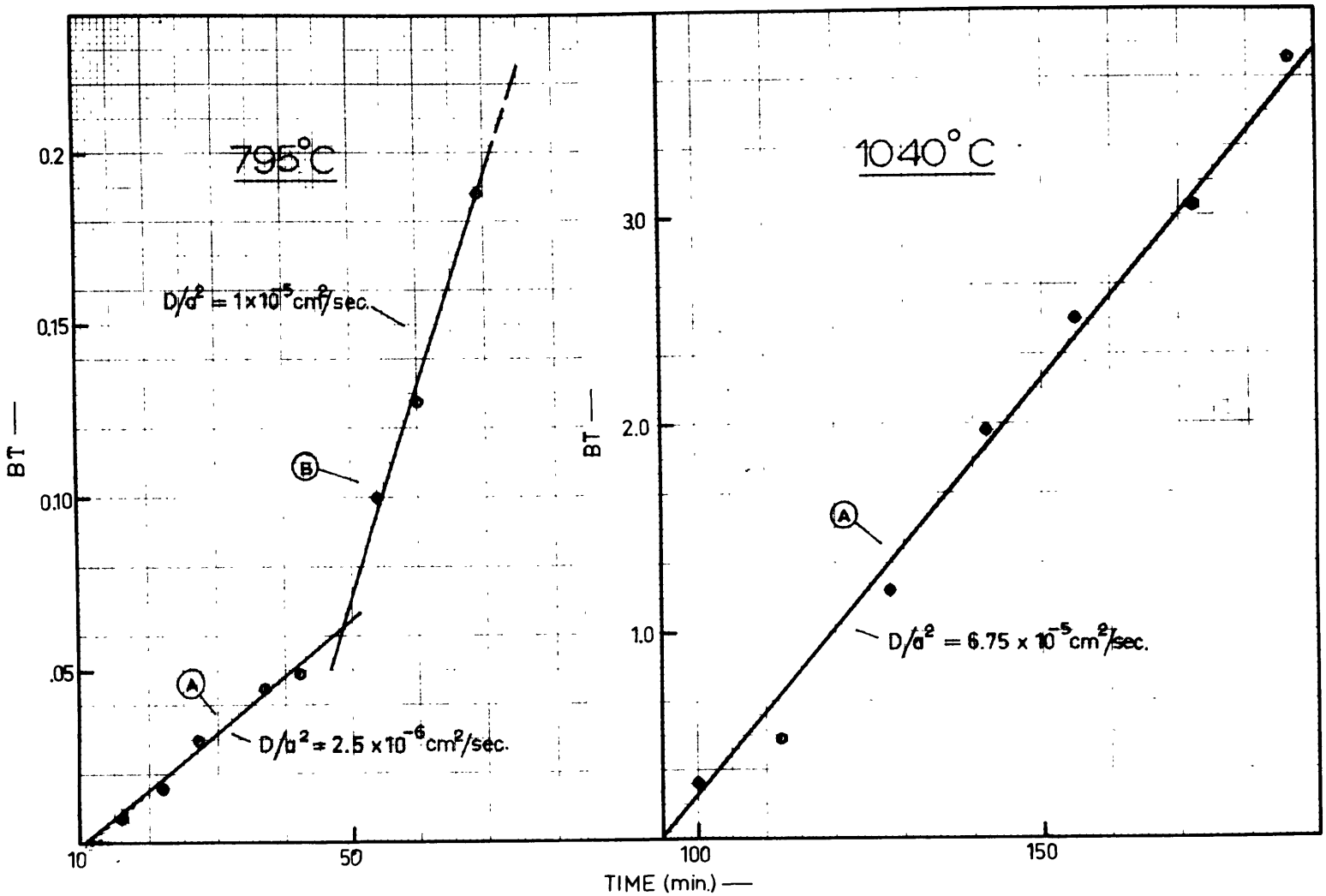

FIG. 11. - POINTS FROM DIFFUSION EQUATION SOLUTION

at 810°, 900° and 1050° for times up to 45 minutes. X-ray diffraction measurements were then made of the ($\bar{2}$01) reflections of albite and orthoclase. None of the heated samples showed any significant change in composition and the relative intensity of the orthoclase and albite peaks stayed the same. This indicates that mixing did not take place to a measurable extent. Tuttle and Bowen (p. 23, 1958) found that low temperature alkali feldspars could be homogenized in from 4 to 40 hours at 900° C, providing the feldspar was greater than 60% orthoclase component. It is possible then that slow mixing, in terms of days rather than hours, is responsible for the abrupt increase in the argon diffusion rate of segment B. This would mean that the curve A for 1040° C actually relates to an unstable structure, but one which is changing at a constant rate. It is noteworthy that no increase in diffusion rate similar to curve B was found for diffusion of natural radiogenic argon from the same feldspar (see next section). This suggests some other explanation for curve B, possibly relating to effects caused by the neutron irradiation.

It should be noted that there is no evidence for diffusion of argon from more than one activation site, as is the case for natural radiogenic argon. Also, it is clear that the diffusion coefficients, as determined at the two temperatures, cannot be used to calculate an activation energy, since the structure, and possibly the effective diffusion radius, is different at each temperature.

Glauconite Results

Fig. /2 shows the measured activity of gas released during heating at 590° C of 8 grams of glauconite from the Franconia formation (G3280). This sample was irradiated for one hour. Here the decay rate of the activity indicates the presence of a contaminating gas of shorter half life. Chlorine is the only gas with isotopes of a half life which would fit the observed activity. 37 minute Cl^{38} could be produced by a $K^{41}(n,\alpha)Cl^{38}$ reaction and it would have to be at least as abundant as Ar^{41} to produce the observed slope. This particular run was made without a charcoal trap or cold finger open to the gas. When the gas was later absorbed and released from a charcoal trap the activity immediately changed to a 1.8 hour decay slope, indicating retention of the contaminating gas on the charcoal. It is also evident from Fig. /2 that relatively more of the shorter-lived activity is released after heating to 850° C, suggesting that the diffusion rate of the argon 41 is higher than the diffusion rate of the other gas.

No calculation of a value for the diffusion coefficient of argon in glauconite was made because of the uncertainty introduced by the contaminating gas activity.

3. Radiogenic Argon Mass Spectrometric Method

Introduction

Diffusion measurements have been made on samples of hornblende, pyroxene, muscovite and orthoclase perthite. The

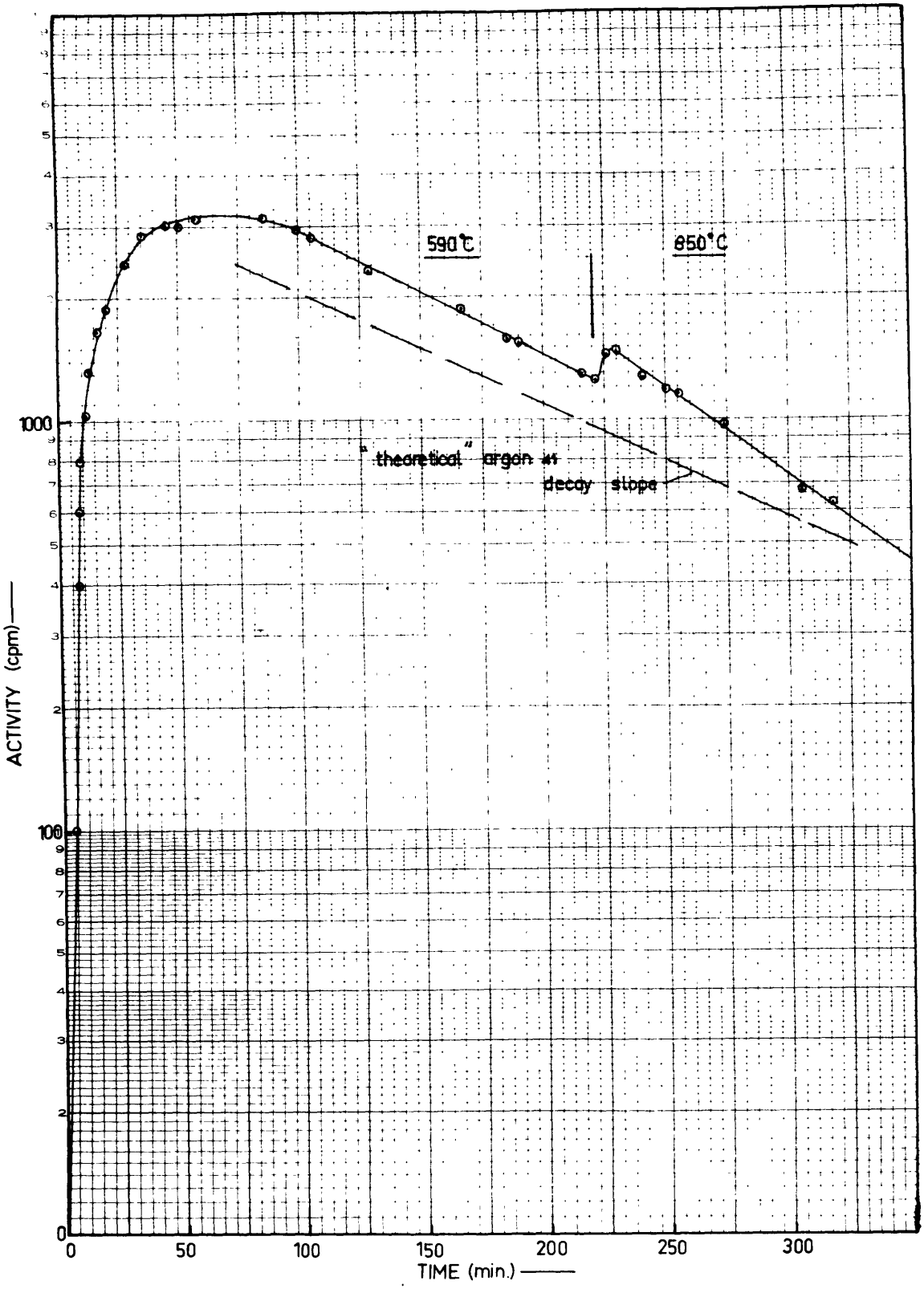

FIG. 12 – ARGON ACTIVITY FROM HEATED GLAUCONITE

measurements were made using the natural radiogenic argon contained in potassium minerals rather than artificially produced radioactive argon. This method is considerably less sensitive than the counting method. The counting method can measure $1x10^{-14}$ std cc radioactive argon 41 with the same accuracy that $1x10^{-7}$ std cc of radiogenic argon can be measured mass spectrometrically. For this reason the following experiments were carried out at relatively high temperatures where diffusion rates are high. Most measurements were made in the range 600^{o} c to 1000^{o} C. These temperatures are somewhat high with regard to geologic application, but important observations regarding mechanisms of diffusion and relative diffusion rates in different minerals can nevertheless be made. Extrapolation of this data to temperatures of geologic interest is justified in some cases.

The procedure involved isothermal heating of the samples in a vacuum. Under these conditions the hydrous minerals are unstable with respect to water loss. The effect of this on argon diffusion is unknown, though in one case it was shown to be small by heating a muscovite under high water pressure in a bomb.

Apparatus

The apparatus used for radiogenic argon diffusion experiments is the same as that used for argon age studies, though it was specifically designed for diffusion experiments. A general description can be found in Appendix I. Temperatures

were measured using two Pt, Pt-10% Rh thermocouples; one above the sample and one below it. The difference in the two readings, as measured on a Brown recorder, was usually less than 10° C. Larger differences usually indicated deterioration of the top thermocouple which was in very near proximity to the sample. Calibrations against the melting point of copper were made prior to each run. Temperatures were maintained to ±10° C over periods up to 48 hours, with no regulation on the furnace power.

Procedure

A sample charge of one to ten grams, contained in an alundum crucible, was placed in the furnace and pumped on overnight. It was outgassed for one to four hours at a temperature of 250° C to 350° C. The furnace system was then isolated from the pumps, the first spike added, and the temperature raised as quickly as possible to the desired level. As soon as the diffusion temperature was reached, the first cut of gas was taken as follows. The gas plus spike mixture in the furnace volume was expanded into the purification line whose volume is roughly equivalent to that of the furnace. After a few minutes equilibration, the stopcock to the purification line was closed, the time recorded, and gas purification procedures started. At the same time, the furnace volume was pumped for one or two minutes to remove the remainder of the "first cut" before collection of the second cut was started. There was never more than 2% loss of the second cut due to this pumping procedure. As soon as collection of the second

cut was started another spike was added. All succeeding cuts were taken in the same way. The minimum interval between them was set by the time needed to purify and analyze the previous cut on the mass spectrometer, bake the titanium, and pump out the purification train. Using this procedure it was possible to keep the sample heating continuously, with no cooling periods necessary. Occasionally the early cuts of gas were stored on charcoals to allow collection at shorter time intervals. The procedure is tedious and demands almost constant attention. For this reason most runs were limited to thirty to forty hours. For the final cut, a spike was added and the temperature increased to the fusion point, where any remaining argon was released.

Accuracy of the measurements varies widely, being $\pm 2\%$ at best and possibly $\pm 50\%$ at worst, depending primarily on the amount of air contamination. No significance can be attached to the amount of air argon measured since most of it does not come from the sample but from leakage into the furnace.

Diffusion in Feldspar

Diffusion measurements were carried out on Sample F3802 at temperatures of 815° C and 960° C. This is the same orthoclase perthite that was used for the radioactive argon measurements. Table 3 shows the analytical data for the two runs. Fig. 13 shows the data plotted as values of Bt versus t for each temperature.

Table 3

Analytical Data for Feldspar Diffusion Runs

Temp. °C.	Cut No.	Σt(min.)	Radiogenic Ar^{40} (cc stp/g)	ΣAr^{40r}	Fraction of Total	Bt (spherical)
300-810	1	35	1.40×10^{-4}	1.40×10^{-4}	0.293	0.088
815	2	82	0.360	1.76	0.368	0.147
815	3	238	0.210	1.98	0.413	0.191
815	4	378	0.0966	2.07	0.433	0.214
815	5	638	0.131	2.20	0.461	0.247
1110	Fusion	(30)	2.58	4.78	1.0	—
2 gram sample						
400-940	1	19	relative ratios measured		0.450	0.234
960	2	75	only - no absolute stan-		0.525	0.340
960	3	184	dard used.		0.620	0.522
960	4	330			0.720	0.798
960	5	584			0.837	1.32
960	6	1318			0.885	1.67
1120	Fusion	(30)			1.0	—
~10 gram sample						

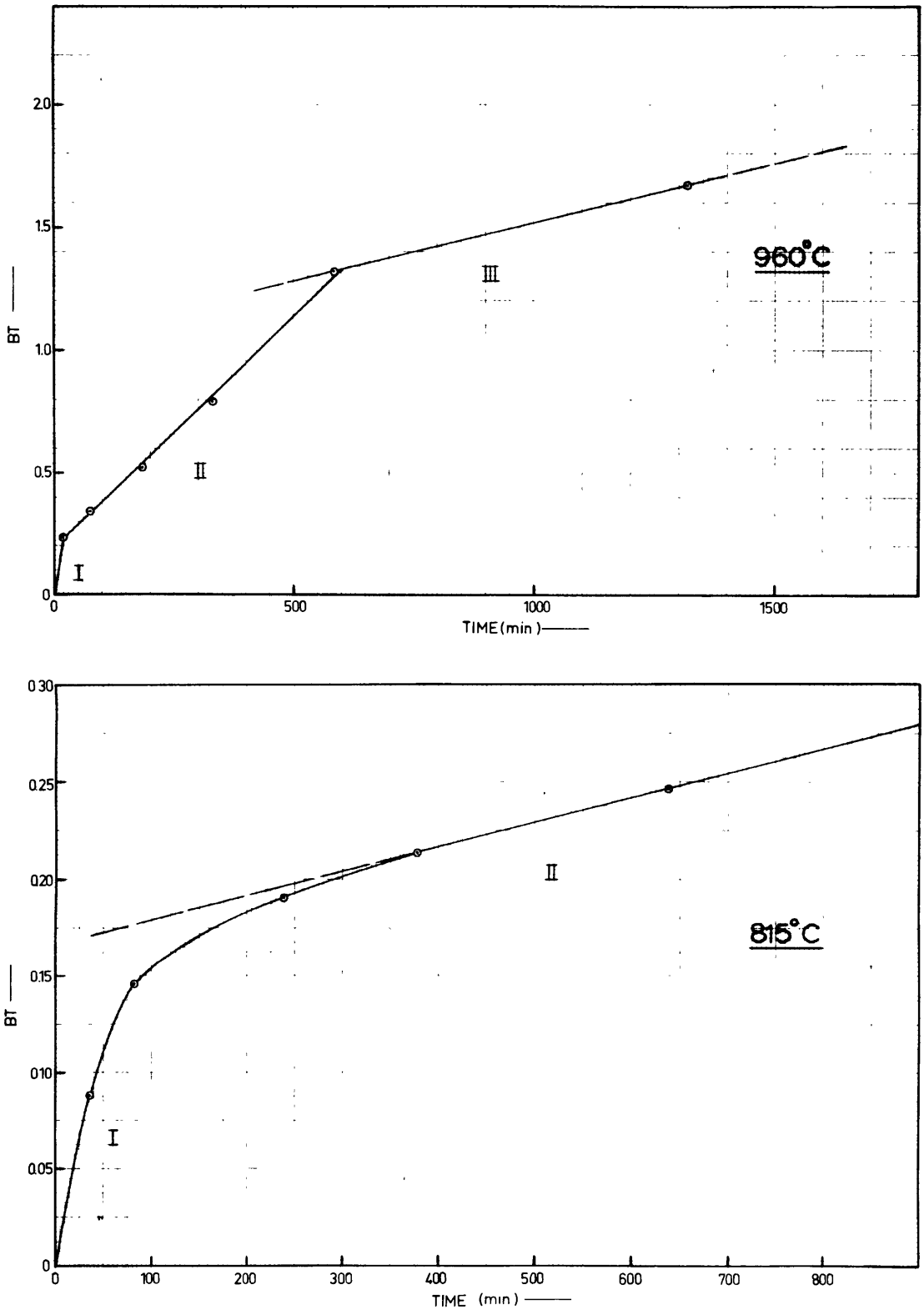

FIG 13 — FELDSPAR DIFFUSION CURVES, 815°C, 960°C.

815° C Results

At 815° C the points define a curve representing continuously decreasing values of (D/a^2). No significant straight line portions are evident except for the last two points, which seem to be approaching a straight line asymptote. After subtraction of the argon from phase II, the points on the curved portion show a reasonable fit to a volume diffusion law. It is interesting, however, that they also fit a relation of the type $\frac{dAr}{dt} = \alpha(Ar_0 - Ar)$ where Ar_0 is the initial argon content, Ar the amount discharging at time t, and α an arbitrary constant. This can be integrated to express it in terms of the fraction released $f = (1 - e^{-\alpha t})$. Fyfe (1958) found that hydration-dehydration reactions usually fit an expression of this type. He concluded that the rate controlling factor was one of surface or sorption phenomena. It is possible that the initial discharge of the 30% of argon from phase I is a desorption process rather than a volume diffusion process. This possibility remains to be tested.

In general, when argon is observed diffusing from more than one site, it will be designated as phase I, phase II, etc. in order of appearance.

In addition to the relatively rapid loss of the phase I argon, the curve approaches an asymptote which is believed to represent argon from a second phase. Calculations show that there is about 31% of the total sample argon in phase I and approximately 50% in phase II.

960° C Results

The points at this temperature define three straight line segments, with only a maximum slope assignable to segment III. The quantity of argon represented by the rapid loss at segment I was calculated to be 32%, and so can be correlated with phase I of the 815° C curve. Phase II contains 48% of the total argon and can be correlated with phase II of the 815° C curve. Only the first part of phase III was picked up so only a maximum can be assigned to its diffusion coefficient. The following table gives a summary of the calculated results, including a calculation of the activation energy* for phases I and II which were recognized at both temperatures. Inherent in this activation energy calculation is the assumption that no structural or phase changes occur between the two temperatures.

Feldspar Diffusion Results

	815° C		960° C		Activation Energy
Phase	Fraction	D/a^2	Fraction	(D/a^2)	(per mole)
I	31%	$5.6\times10^{-5}\,sec^{-1}$	32%	$>2.2\times10^{-5}\,sec^{-1}$	~15 Kcal
II	~50%	$2.5\times10^{-7}\,sec^{-1}$	48%	$3.2\times10^{-6}\,sec^{-1}$	46 Kcal
III	not observed		<20%	$<4.7\times10^{-7}\,sec^{-1}$	

The activation energy of phase I is approximately the same whether one assumes a diffusion law or a desorption law. The existence of such a large proportion of loosely held

* The term "activation energy" as used throughout this thesis is defined by the relation $D=D_0\exp(-Q/RT)$, where D_0 and R are constants and Q is the activation energy.

argon in feldspar suggests a correlation with the mica-feldspar age discrepancy. The same mechanism that caused 30% of the argon in this sample to be in a low activation site might also have caused as much again to be in a lower activation site, from which it has been subsequently lost at earth surface temperatures. Such a mechanism undoubtedly has something to do with the unmixing of the perthite. Sardarov (1957), in comparing the ages of coexisting micas and feldspars, found the feldspar age always lower and showed a definite correlation between the difference in age and the "extent of perthitization". The fact that sanidines seem to give reliable ages also suggests a mechanism relating to perthite formation. Since unmixing takes place relatively soon after crystallization, when very little argon has been formed, it is difficult to see how the actual unmixing process could be responsible for large losses. The formation of perthite would certainly result in a decrease in the effective grain size for diffusion but this in itself is not sufficiant to cause large losses.

The data on diffusion of radiogenic argon in feldspar is basically different from that obtained by the radioactive argon counting technique. First and most important, there is no loosely-held phase I apparent in the radioactive argon data; in fact, there is no suggestion of the presence of more than one phase. This would seem to eliminate the possibility that the appearance of three distinct phases in the radiogenic experiments was caused by the heating rate, structural changes during heating, or any experimental variable. When argon is

produced in a mineral by neutron irradiation most of it should remain in a single site, that of the parent nucleus (in this case potassium). It is not surprising than that only one phase was recognized in the radioactive argon experiments. By the same token, radiogenic argon should form initially in a single site and it must be redistributed by some later process.

Disregarding the loosely held phase I, it is also apparent that the radiogenic argon in phase II has a diffusion coefficient an order of magnitude smaller than that of the radioactive argon. This difference could be accounted for by the effects of the neutron irradiation on the mineral structure. Measurements of diffusion phenomena made with radioactive argon would seem to be of little direct application in the interpretation of geologic age problems.

Diffusion in Hornblende

The sample used for these measurements, H4067, is from one of the Colorado contact zone suites. It was shown to have remarkable argon retentivity by comparison with K-Ar and Rb-Sr ages on associated biotite. The sample is very pure hornblende and was crushed to a grain size ranging from 140 to 300 microns. A split from the same sample was then ground further to a size ranging from 44 to 53 microns. Diffusion measurements were made at 645° C, 855° C and 870° C. The analytical data is presented in Table 4. Figs 14 and 15 show the data plotted as Bt versus t values. The relatively low argon content of this hornblende, coupled with very small diffusion coefficients, resulted in low accuracy for the measurements.

Table4

Analytical Data for Hornblende Diffusion Runs

Temp. °C.	Cut No.	Σt(min.)	Radiogenic Ar^{40} (cc stp/g)	ΣAr^{40r}	Fraction of Total	Bt (spherical)
300-650	1	60	1.05×10^{-6}	1.05×10^{-6}	0.0158	0.000215
645	2	326	0.116	1.17	0.01753	0.000265
645	3	1261	0.295	1.46	0.0220	0.000417
645	4	1603	< 0.180	< 1.64	< 0.0246	< 0.000522
845	5	1723	0.258	1.90	0.0388	0.00133
1150	Fusion	(20)	62.9	64.8	1.0	—
8 gram sample						
200-855	1	30	2.70×10^{-6}	2.70×10^{-6}	0.0439	0.00171
870	2	152	0.257	2.96	0.0481	0.00204
870	3	309	0.492	3.45	0.0561	0.00281
870	4	384	0.120	3.57	0.0580	0.00300
870	5	586	0.697	4.27	0.0694	0.00433
870	6	1466	1.00	5.27	0.0855	0.00660
1140	Fusion	(16)	56.5	61.5	1.0	—
6 gram sample						
300-840	1	50	2.19×10^{-6}	2.19×10^{-6}	0.0360	0.00115
855	2	140	0.292	2.482	0.0408	0.00147
855	3	244	0.356	2.838	0.0467	0.00193
855	4	354	0.0372	2.875	0.0472	0.00197
855	5	697	0.830	3.705	0.0610	0.00332
1130	Fusion	(14)	57.1	60.8	1.0	—
4 gram sample						

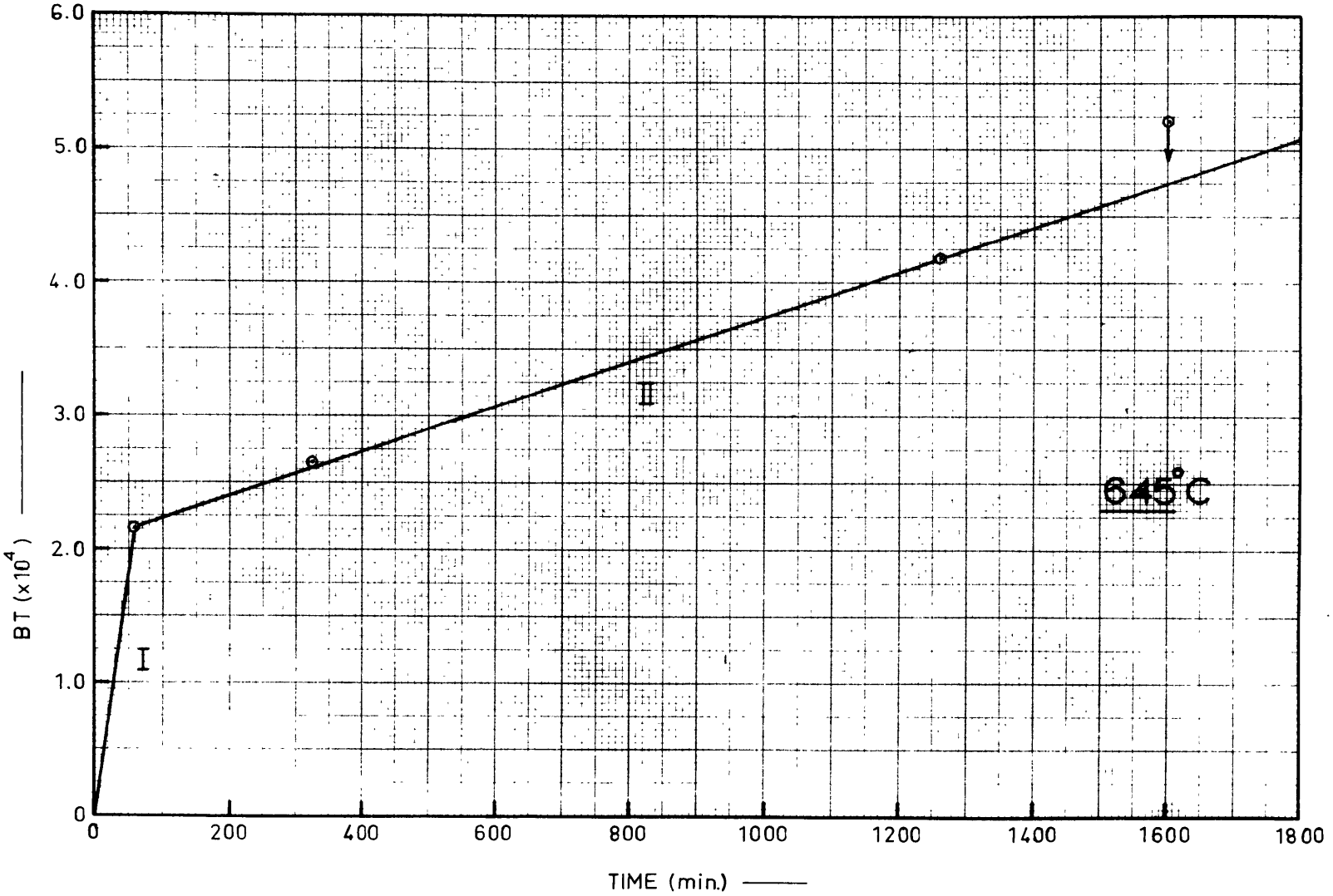

FIG.14 — HORNBLENDE DIFFUSION CURVE

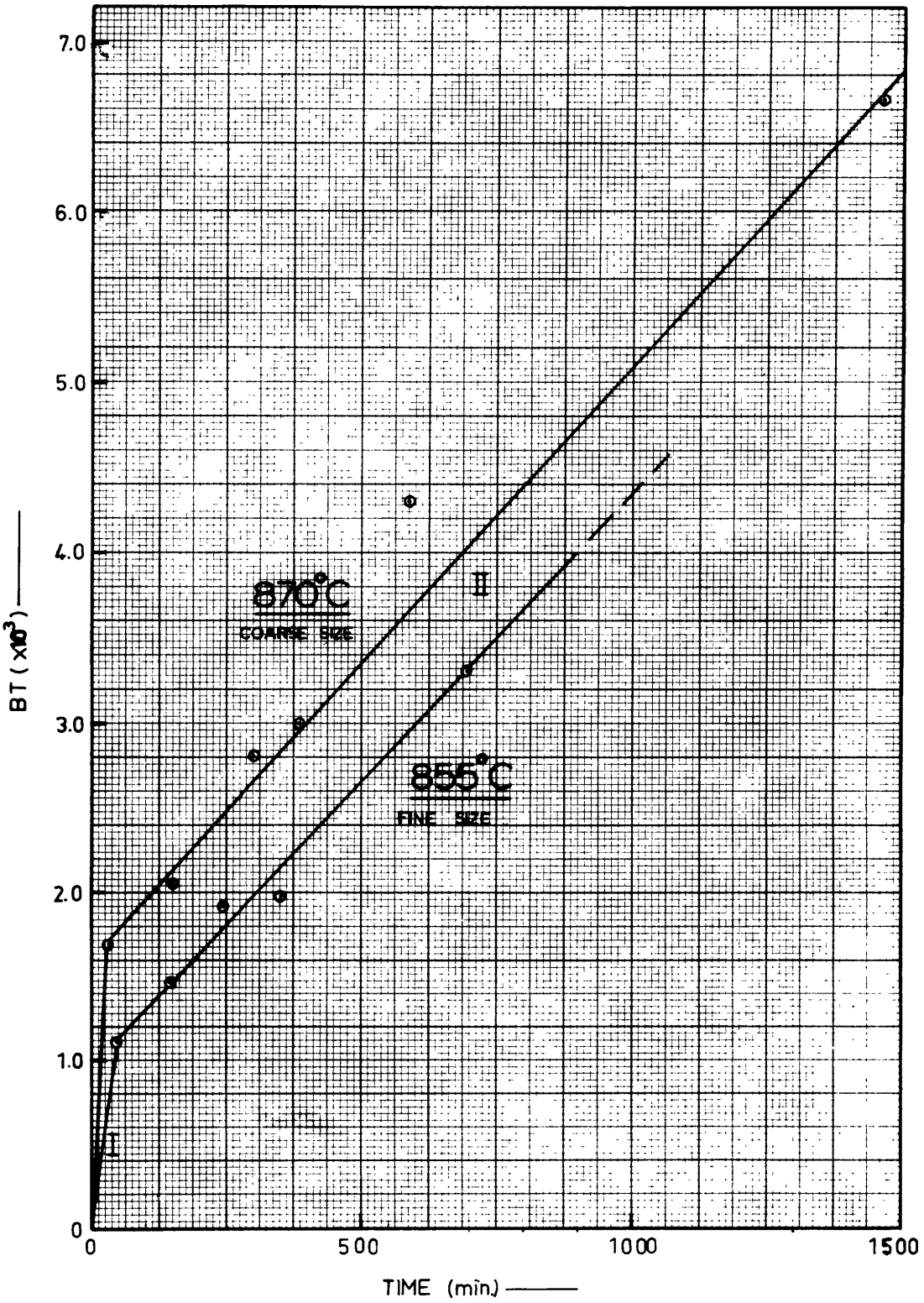

FIG.15 - HORNBLENDE DIFFUSION CURVES

645° C Results - Coarse Fraction

Within the limits of error the points define two linear segments. Phase I corresponds to a rapid loss of about 1.4% of the total argon. Phase II represents an unknown portion of the total sample argon and shows a very small value for the diffusion coefficient.

870° C Results - Coarse Fraction

At this temperature the points also define two linear segments. It should be noted in all these cases that the slope of phase I can be assigned a minimum limit only. On account of the very rapid loss, measurements could not be made at small enough intervals to define the slpe. The proportion of argon in phase I was 3.3% at this temperature. Whether phase II constituted the remainder of the argon or not cannot be determined since only a total of 6% was released. A run at a much higher temperature would be needed to establish the proportion of argon in phase II.

To establish a limit for the effective diffusion radius of this hornblende, the finely crushed sample was run at nearly the same temperature, 855° C. From Fig. *15* it is apparent that the value of D/a^2 for the two runs is very similar. However, in this run there was less loss from phase I (2.3%), as opposed to 3.3% in the 870° coarse fraction run. This could be interpreted as partial loss of phase I during the grinding. However, since phase I was only 1.4% at 645°, this interpretation is questionable. These two size fractions differed by a factor of 20 in their physical (a^2) value but gave

values of (D/a^2) which were almost the same. (Actually the fine size D/a^2 was 50% larger). This is considered conclusive proof that the effective radius for diffusion in this hornblende is less than 30 microns. The average physical radius of the hornblende, as measured in thin section, is about 500 microns.

Hornblende Diffusion Results

	645° C	870°C (coarse)	855°C (fine)
fraction in phase I	1.4%	3.3%	2.3%
D/a^2 phase I	$>4.8\times10^{-9}$ sec^{-1}	$>2.6\times10^{-8}$ sec^{-1}	$>2.6\times10^{-8}$ sec^{-1}
D/a^2 phaseII	7.4×10^{-11} sec^{-1}	2.8×10^{-9} sec^{-1}	3.6×10^{-9} sec^{-1}

Activation Energy, phase I, ~15 Kcal/mole

Activation Energy, phase II, 34 Kcal/mole

There is no evidence for the existence of more than two argon phases in this hornblende; however, the data do not rule out the possibility.

Diffusion in Muscovite

Diffusion measurements were made at temperatures of 615° C and 750° C on a sample of muscovite from Clarendon, Vermont (M4052A). This was the 74-140 micron size fraction of the suite tested for age variation with grain size (see Appendix IIC) and contained about 10% calcite and chlorite impurities.

The data is presented in Table 5 and plotted in Fig. 16-17as values of Bt versus t. The measurements in this case are considered quite accurate as relatively large amounts of argon were liberated.

615° C Results

The data for 615° C suggests three segments, with the slope of the third given only a maximum limit. Unlike the feldspar and hornblende curves, there is no rapid initial loss of argon from this muscovite. The phase I segment intersects the t axis at 82 minutes, which was exactly the time at which the sample reached final temperature. The fact that there was no loss during the heating up period suggests a high activation energy for all phases. The amounts of argon in phase I and II are 9% and 3% respectively.

750° C

Here the points define two straight line segments, again with no rapid initial loss observed. The quantity of argon in the steepest segment, 17%, suggests that it may be a combination of both phases I and II. These may not have been resolved on account of the masking effect of argon from phase III. Calculation shows phase III to consist of about 70% of the total argon, which indicates that there may also be a fourth phase. No explanation was found for the discrepant 781 minute point. It is definitely outside experimental error.

Table 5

Analytical Data for Muscovite & Pyroxene Diffusion Runs

Temp. °C.	Cut No.	Σt(min.)	Radiogenic Ar^{40}(cc stp/g)	ΣAr^{40r}	Fraction of Total	Bt (spherical)
0-270	1	(40)	$<5\times10^{-8}$	—	<0.0005	—
270-600	2	142	3.27×10^{-6}	3.27×10^{-6}	0.0319	0.00087
615	3	524	5.40	8.67	0.0846	0.0064
615	4	1329	2.98	11.65	0.114	0.0118
615	5	1995	1.81	13.46	0.131	0.0159
615	6	2865	0.84	14.30	0.139	0.0180
1190	Fusion	(30)	86.7	101.0	1.0	—
2 gram sample - muscovite						
230-755	1	65	1.52×10^{-5}	1.52×10^{-5}	0.140	0.0183
750	2	145	1.00	2.52	0.231	0.0525
750	3	265	0.779	3.30	0.303	0.0949
750	4	509	0.677	3.97	0.365	0.144
750	5	781	0.715	4.69	0.432	0.212
750	6	1381	0.848	5.54	0.510	0.316
1200	Fusion	(30)	5.33	10.8	1.0	—
2 gram sample - muscovite						
250-890	1	36	1.52×10^{-6}	1.52×10^{-6}	0.165	0.0257
905	2	249	4.30	5.82	0.630	0.545
910	3	581	(.145-.78)	(6.0-6.6)	(0.65-.715)	(0.594-0.78)
1190	Fusion	(10)	2.32	9.23*	1.0	—
4 gram sample - pyroxene						

* value obtained in a previous run used because of uncertainty introduced by large air correction on Cut No. 3.

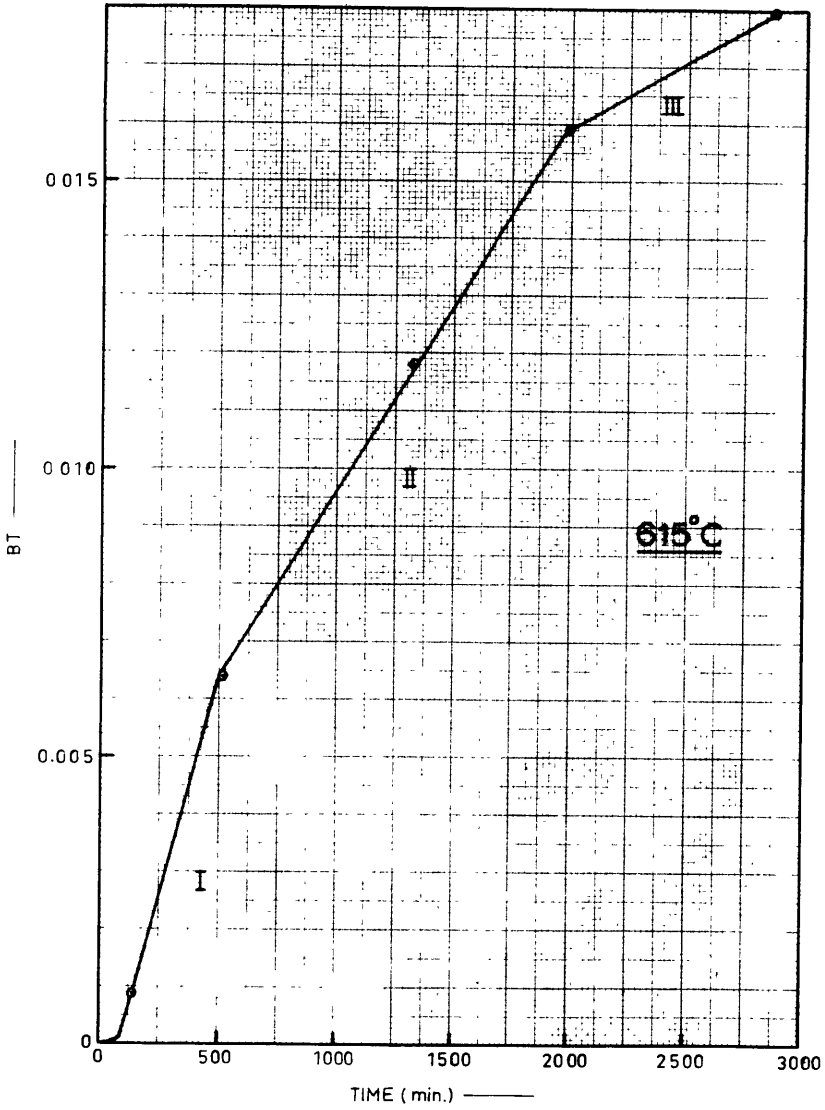

FIG.16 - MUSCOVITE DIFFUSION CURVE

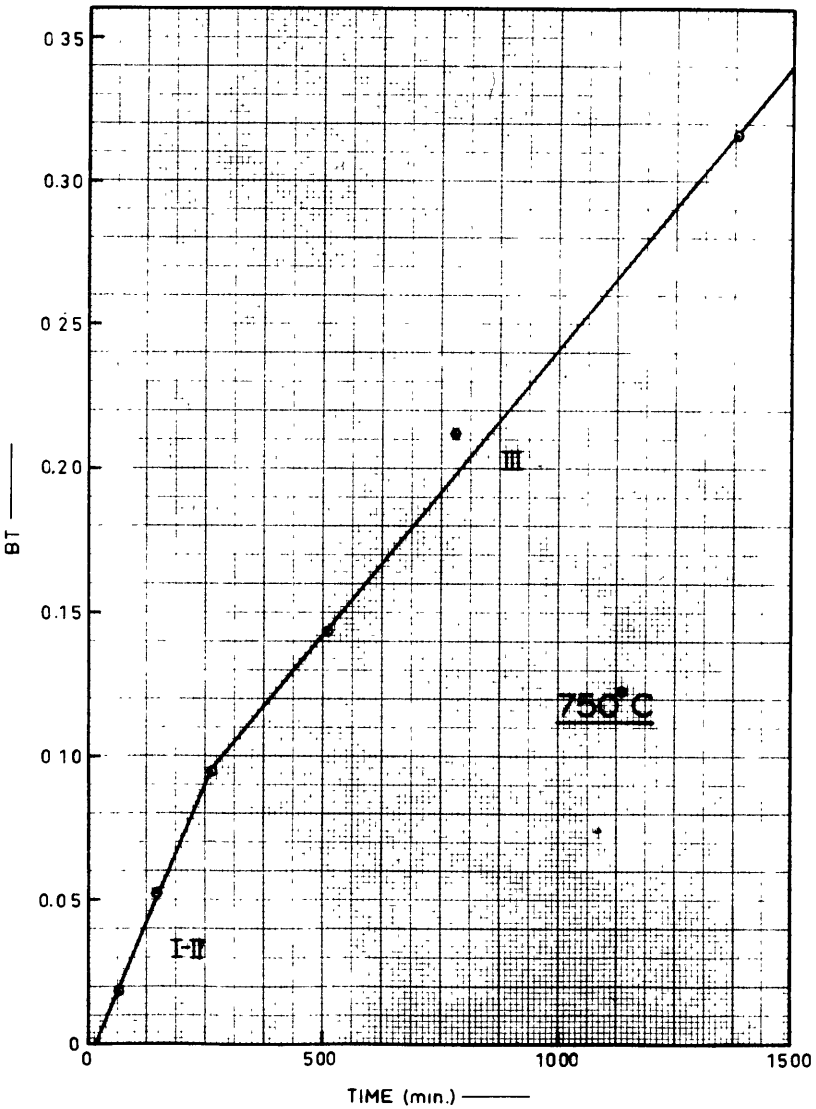

FIG.17 - MUSCOVITE DIFFUSION CURVE

Muscovite Diffusion Results

Phase	615° C Fraction	615° C D/a^2	750° C Fraction	750° C D/a^2	Activation Energy (per mole)
I	9%	$2.4 \times 10^{-8} sec^{-1}$	17%	$6.4 \times 10^{-7} sec^{-1}$	47 Kcal
II	3%	$1.0 \times 10^{-8} sec^{-1}$			
III	—	$< 3.1 \times 10^{-9} sec^{-1}$	~70%	$3.4 \times 10^{-7} sec^{-1}$	>63 Kcal

Earlier it was mentioned that the loss of hydroxl water from hydrous minerals heated in vacuum may affect the diffusion loss of argon. To evaluate this possibility, a two gram charge of the same muscovite was placed in a stellite "Tuttle-type" cold seal bomb, put under 1000 bars pressure and heated at 710° C for 72 hours. The sample was removed from the bomb and the remaining argon was extracted and measured by normal techniques. The sample was found to have lost 32.3% of its argon during this treatment. This gives a value of 4.3×10^{-8} sec^{-1} for D/a^2. Extrapolating the above diffusion data to this temperature allows a comparison to be made.

	$\frac{710° C}{D/a^2}$
Phase I & II	$= 3.5 \times 10^{-7} sec^{-1}$
Phase III	$D/a^2 < 1.4 \times 10^{-7} sec^{-1}$
Bomb sample	$D/a^2 = 4.3 \times 10^{-8} sec^{-1}$

For the same time-temperature conditions, a sample heated in vacuo would have lost 53% of its argon. The temperature extrapolation involves very little uncertainty, so the difference is real and in the direction to be expected. That is, the muscovite sample heated under high water pressure lost about 40% less argon than the same sample heated in vacuo.

The difference is surprisingly small, however, considering the difference in conditions. It does demonstrate that diffusion measurements made on samples heated in vacuo, or even in air, should be considered as maximum limits only. It may be argued that conditions in nature are frequently "dry", in which case the measurements above can be considered to bracket the extremes of possible environmental variations.

Diffusion in Pyroxenes

Pyroxenes were considered as possible "highly retentive" minerals for argon because of their proven retentivity for helium. To check this, a sample of pyroxene from the Sudbury gabbro (P3426) was heated at 905° C for ten hours. This pyroxene was extremely pure with a grain size range of 140-300 microns. The data is presented in Table 5 and plotted in Fig. 18 . There is no rapid initial loss and the argon seems to be in at least two positions. The first phase accounts for 45% of the argon.

Phase I 45%, $(D/a^2) = 4 \times 10^{-6} sec^{-1}$

Phase II , $(D/a^2) = 2 \times 10^{-6} - 2 \times 10^{-7} sec^{-1}$

The measured diffusion coeffident does not indicate exceptional retentivity at the given temperature; it is about the same as the muscovite values and three orders of magnitude larger than the hornblende values.

Discussion of Results

The results of all the diffusion measurements are plotted in Fig. 19 as values of $\log(D/a^2)$ versus $\frac{1000}{T}$ o K. The values are connected for graphical clarity where correlation

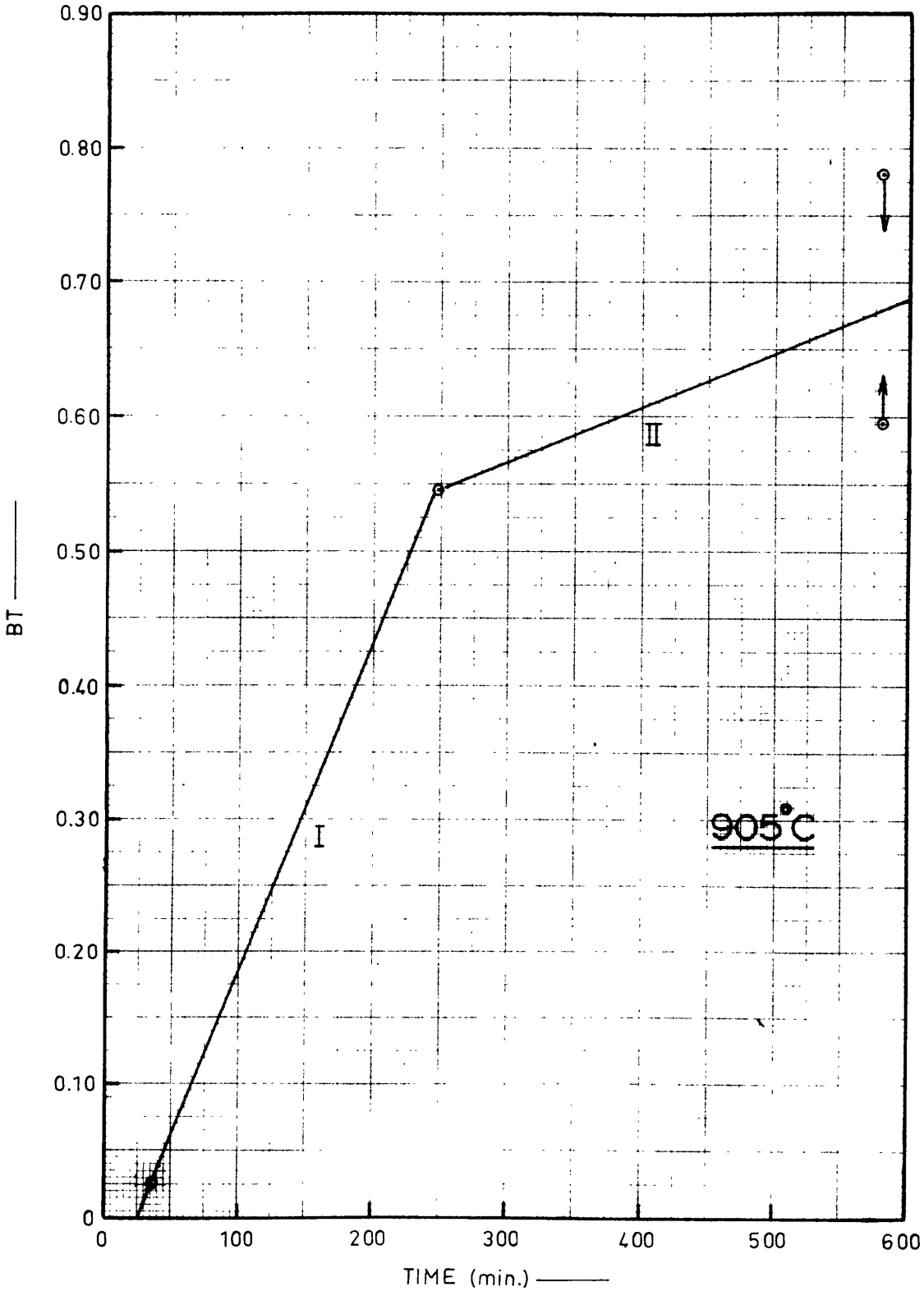

FIG. 18 – PYROXENE DIFFUSION CURVE

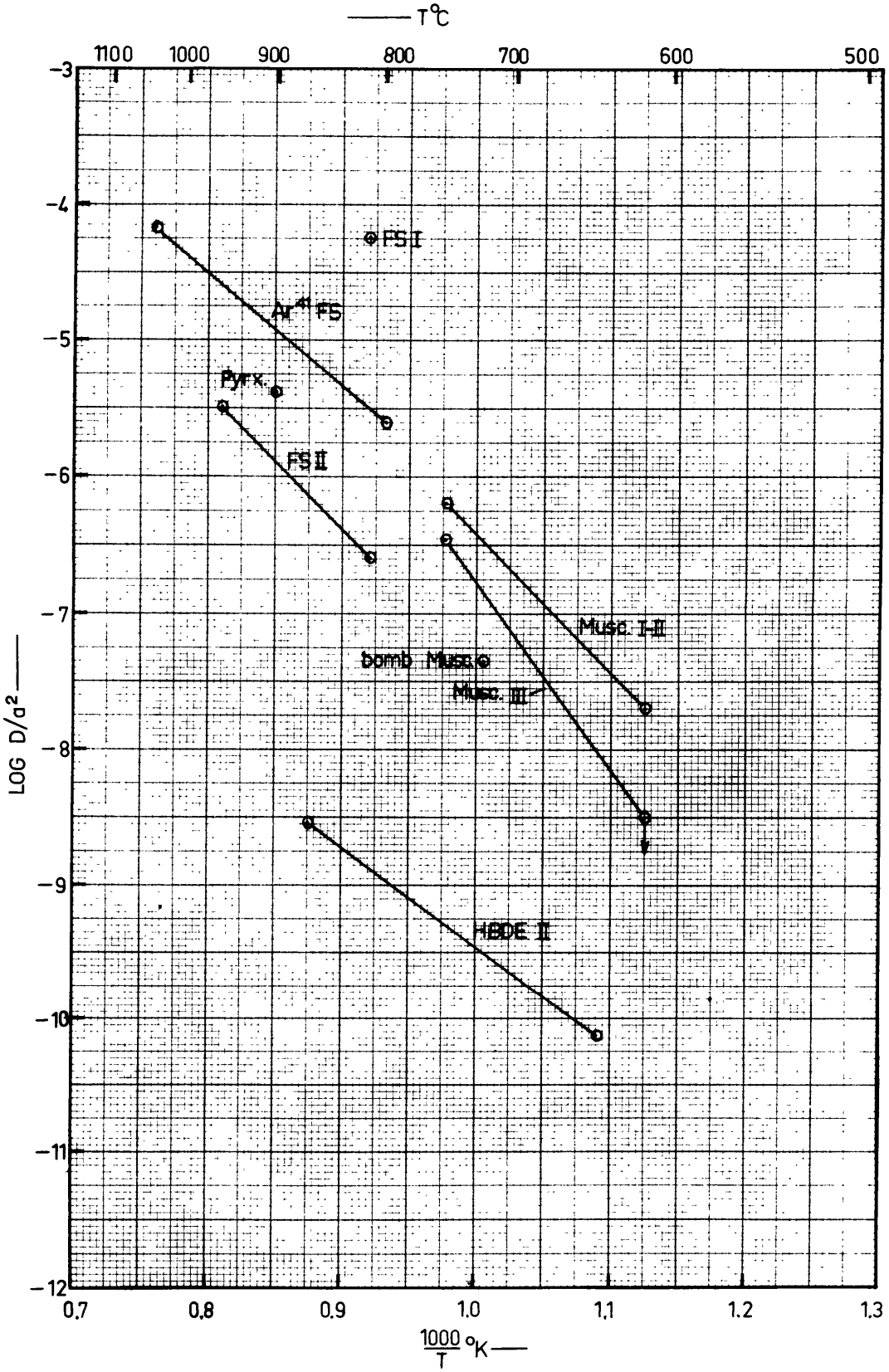

FIG. 19 — DIFFUSION COEFFICIENTS VS. TEMPERATURE

of the argon phases indicates this to be reasonable. Linear extrapolation between points is assumed although there is no proof that the join is not curved or even discontinuous. The slope of these joins is proportional to the activation energy of the corresponding argon phase.

In the 700° to 900° C temperature region, hornblende is considerably more retentive than all the other minerals. Owing to its relatively low activation energy, however, there would be very little difference between it and muscovite at 400° to 500° C. It is possible that most of the argon in hornblende is in a third undetected phase. This would have a higher activation energy and have lower (D/a^2) values at all temperatures. It is interesting to note that Amirkhanov (1959a) measured a (D/a^2) value of 3×10^{-6} cm^2/sec at 500° C on a pegmatitic hornblende. The difference between this value and those reported above is about 6 orders of magnitude! This brings up the general question of how much variation would be expected between different samples of the same mineral. Since a number of different investigators have made argon diffusion measurements on similar minerals, some correlation should be possible.

Gerling (1957, 1958) made very detailed measurements of the discharge of argon from muscovite, phlogopite, biotite, and microcline-perthite. However, he used a different mathematical model for his calculations and, as a result, his data are not comparable. Recalculation of his data is also difficult

since it is presented on small scale graphs and not tabulated in tables. He did find that the argon in micas was held in three types of sites: a few percent in the first, 60 to 70% in the second and the remainder in the third. For microcline-perthite he observed five different sites in which the argon was held ; the first three phases accounted for 20% of the argon and had an activation energy of about 20 Kcal, the fifth contained the bulk of the argon, 65%, and the activation energy for that phase was 130 Kcal. These results are in general agreement with those of this thesis. The differences in the number of argon phases and quantity of argon in each are considered to be real and probably reflect variations in the environmental history of the different samples.

Evernden et al (1960) made argon diffusion measurements on glauconite, microcline, sanidine, leucite, and phlogopite. Their experimental method was such as to obscure the possible observation of argon from different structural positions. They measured only one fraction of argon at each temperature, then heated the same sample up to a higher temperature and measured another fraction. For a mineral with argon in several positions the low temperature measurements would represent the loosely-held argon. The high temperature measurements would be weighted in favor of the high activation phases. They state that "Irregularities of the diffusion curve are manifestations of dynamic lattice change. They are not to be considered as indications of argon atoms in successive lattice positions."

It is, in fact, impossible to demonstrate this from any of their data. The only case where they made measurements isothermally as a function of time was on a glauconite. Of this experiment they say, "The glauconite results prove that all argon can be lost from a mica-type lattice at a single activation energy." When their data is replotted on a Bt versus t plot the points do not fall on a single line. They define almost a continual curve which suggests either three argon positions or a steady decrease in (D/a^2) due to structural changes.

By determining the argon loss from a number of samples of feldspar of different grain size Evernden et al. were able to show that the effective diffusion radius in the feldspar was less than 35 microns. This is similar to the results obtained in this thesis on hornblende and emphasizes the need for reporting diffusion data as (D/a^2) values.

In order to determine whether diffusion of argon from mica takes place in a direction parallel to or perpendicular to the cleavage, Evernden et al. measured the argon loss from two samples of phlogopite. One sample was flakes 15 x 15,000 microns, the other was the same phlogopite cut to flakes 15 x 2000 microns in size. By comparison of the results on the two sizes they concluded that the diffusion direction was perpendicular to the cleavage. This is not the direction one would intuitively favor, since the largest channelways are parallel to the cleavage. However, in order for the above

tests to be valid, it must be proven that the effective radius for diffusion in the sample is greater than 2000 microns. This was not done.

Amirkhanov (1958a, b, 1959a, b, c, d, 1960) has made many argon diffusion measurements on various potassium minerals. He observed only one argon phase in a phlogopite and he observed three phases in each of two samples of feldspar. These corresponded to argon fractions of 38%, 56%, 4.8% and 22%, 71%, 7.2%, for phases I, II and III respectively; these proportions are very similar to those found in the feldspar used in this thesis. The diffusion coefficients (reconverted to D/a^2 values) for the minerals measured by Amirkhanov are plotted in Fig. 20 to allow comparison with the values from this thesis. Except for hornblende the general agreement suggests that the variation of diffusion parameters from sample to sample might be small. The fact that Amirkhanov's four feldspar points fall nearly on a straight line is also an indication of the degree to which extrapolation between and beyond points is valid. If pyroxenes indeed have the high activation energy reported by Amirkhanov they will become a very useful mineral for age studies in metamorphic areas.

The values obtained from these various diffusion measurements will be used in later sections to interpret the time-temperature histories of two types of geologic environments: a contact metamorphic zone, and a regional metamorphic zone.

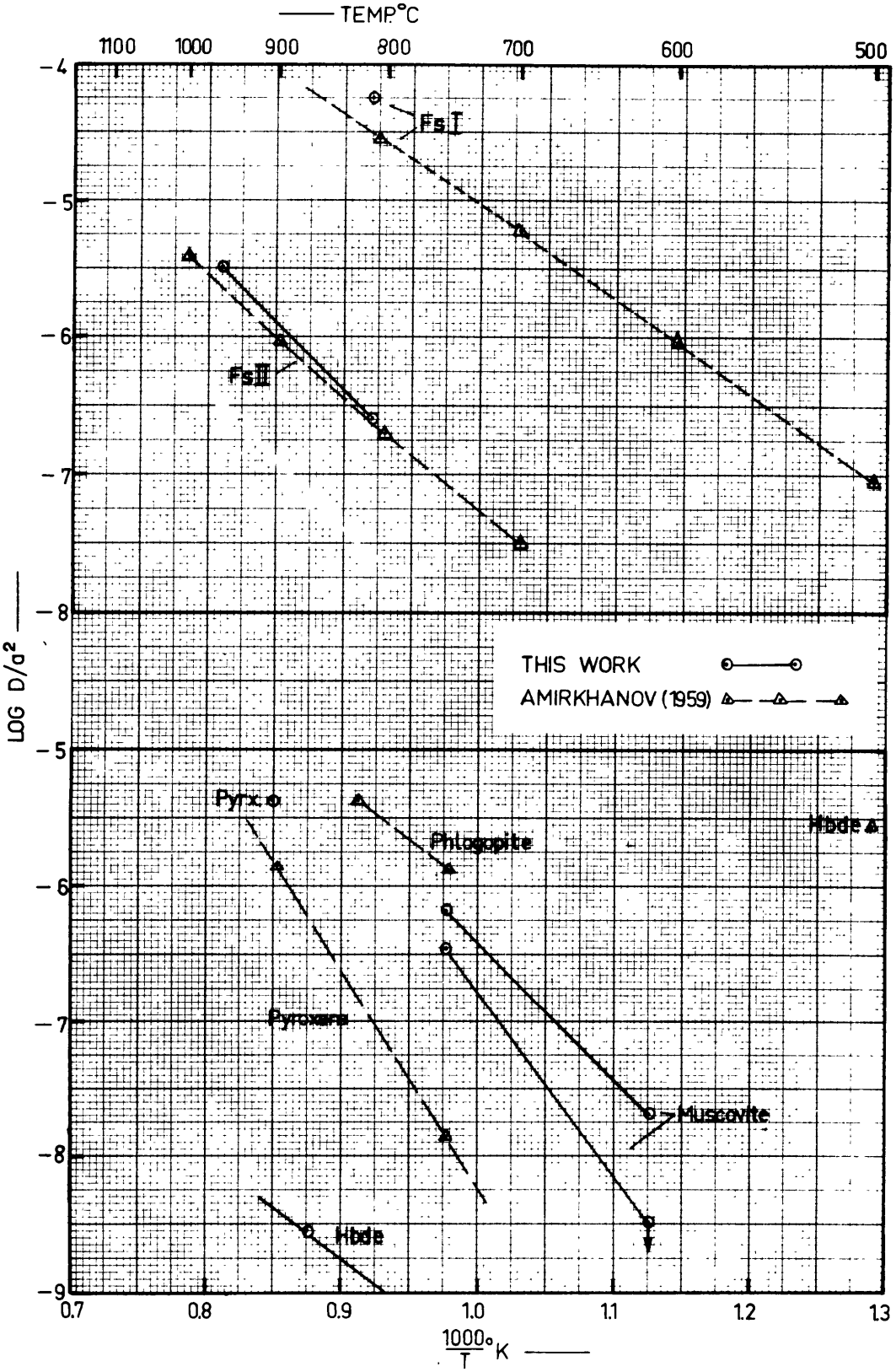

FIG. 20 —COMPARISON OF DIFFUSION RESULTS

As a summary of the data, the following table lists the temperatures at which each of the minerals discussed above would lose 50% of their radiogenic argon if heated for 1.0 million years.

Pyroxene	425° C
Muscovite	350° C
Hornblende	300° C
Perthitic Feldspar	240° C
Phlogopite	200° C

Calculations such as these involve the assumption that there is no knee in the curves of D/a^2 versus $\frac{1000}{T}$ caused by a change in the mechanism of diffusion at temperatures below the experimental temperatures. There very likely is a knee in the curves below 500 to 600° C, so the above temperatures may be regarded as minimum values.

C. Variation of Apparent Age with Grain Size

Wasserburg (1954) suggested that if radiogenic argon was lost by diffusion "the amount lost would be critically dependent on the grain size and structure of the potassium minerals." Nicolaysen (1957) advised performing age analyses on several mineral samples from the same locality "possessing a hundredfold variation in grain size", to test the feasibility of daughter-isotope diffusion in radioactive minerals. The basis for these suggestions is the (D/a^2) term in the diffusion equations. The mineral radius, occurring as the square, will be a strong factor in governing the loss of daughter products.

As shown in the previous section, it is the effective diffusion radius and not necessarily the physical grain size which is the important parameter. In some cases these two sizes may be identical. They are not identical for feldspar or hornblende. To carry out an "age variation versus grain size" study it is necessary first to find a mineral whose physical grain size is equivalent to or smaller than its effective diffusion size. The metamorphic history must be such that complete loss of the daughter element has not occurred. The grain size itself must be variable, and finally, the grains must be liberated from the sample without changing their size. This poses a rather restrictive set of conditions. A sample of muscovite-bearing marble was found which meets the requirements reasonably well. This sample was collected by Professor W. H. Pinson at Clarendon, Vermont (Stop #1, Field

Trip #H, New England Intercollegiate Geological Conference, 51st Annual Meeting). This marble is part of the Precambrian Mount Holly series and is in a region which was affected by metamorphism during the early Paleozoic. The rock is composed dominantly of calcite, with abundant muscovite and quartz, and minor amounts of an epidote, chlorite, and slightly sericitized potash feldspar. The muscovite occurs in all sizes from fine felted aggregated up to large bent and strained plates. The calcite and quartz are also strained and show undulatory extinction.

The sample was reduced in a jaw crusher and ground once lightly. Sieving showed 60% of the sample to be +50 mesh size. A coarse sample of flakes about 4 mm to 10 mm in size was handpicked. The remainder was sieved in 10, 20, 28, 40, 50, 100 and 200 mesh screens and purified by magnetic, heavy liquid, jigging and fine grinding methods. Even after this, some of the size fractions contained considerable impurity. Sample splits for Rb-Sr analysis were washed in cold 6N HCl for 30 minutes. The analytical data is given in Table 6 .

Table 6: Analytical Data for Muscovite Grain Size Analyses

Sample Number	Grain Size	K%	$*Ar^{40}$ (in 10^{-4} cc stp/g)	$\frac{*Ar^{40}}{\text{Total } Ar^{40}}$	Rb (ppm by wt)	$*Sr^{87}$ (ppm by wt)	$\frac{*Sr^{87}}{\text{Total } Sr^{87}}$
—	4mm-10mm	8.26	2.67	0.96			
C	-10+20	8.93	2.25	0.94			
D	-28+40	7.81	1.56	0.85			
B	-50+100	5.29	0.816	0.92	274	0.489	0.156
A	-100+200	6.26	1.02	0.82	282	0.485	0.140

* Radiogenic

The calculated ages and the median grain radii are given in Table 7 .

Table 7 : Calculated Muscovite Ages and Grain Radii

Sample Number	Approx. Median Radius (microns)	Radius Squared (cm^2)	K-Ar Age (m.y.)	Rb-Sr Age (m.y.)
—	3500	1.4×10^{-1}	675 ± 25	
C	690	4.8×10^{-3}	545 ± 20	
D	250	6.2×10^{-4}	440 ± 15	
B	110	1.2×10^{-4}	350 ± 10	430 ± 30
A	55	3.0×10^{-5}	360 ± 10	410 ± 30

Discussion

The K-Ar ages show a consistent trend of decreasing age with decreasing grain size. The two smallest sizes A and B may be interpreted as having undergone complete loss of argon at the time of metamorphism, about 355 m.y. The largest size was also affected and shows an age in between that representing complete loss and complete retention. It is assumed that the true age is 1000 to 1100 m.y. (Grenville). The Rb-Sr ages would seem to indicate that the two smallest sizes also lost all their strontium during the metamorphism, but in this case the time of metamorphism seems to be around 420 m.y. The argon and strontium ages of these two samples do not overlap within experimental error. An alternative explan-

ation would be that the Rb-Sr ages of A and B both indicate some retention of strontium, the variation of this with size being masked by experimental error.

The argon ages do not fit a (D/a^2) law exactly. It is likely that the finer samples all contain appreciable amounts of the coarse "high age" material which was reduced during the grinding. It was hoped that this effect would be small because of the relative softness of the calcite matrix. For the observed ages to fit a D/a^2 diffusion law, most of samples C and D would have to be ground-down coarse material. There is unquestionnably a variation in the age of the samples; the problem is in determining over what range of grain size this variation takes place. Theoretically a factor of four difference in grain radius should be sufficient to produce the total variation from 675 m.y. (54% lost) to 350 m.y. (100% lost). The actual variation in this case takes place instead over a grain size range of a factor of 35. In addition to the spreading effect caused by ground down coarse material, it is possible that the effective radius for diffusion is smaller than the coarsest material, in which case the actual variation in (a^2) would be smaller than that inferred from the physical size variation. A minimum limit of 0.7 mm can be placed on the effective diffusion radius, however.

A completely different interpretation can also be made from the age data on this muscovite. It is possible that prior to metamorphism the muscovite was all in textural equilibrium and existed as large flakes only. The metamorphism, while

causing argon loss from the large flakes, also caused the new growth of a series of finer sizes. The observed ages then would represent a mixture of muscovite formed at the time of metamorphism and ground-down original muscovite.

Regardless of the interpretation, it is clear that an age obtained on a single size fraction would be meaningless by itself. By analyzing a series of size fractions at least the time of metamorphism can be determined.

Using linear extrapolations of the argon diffusion data on this muscovite (Appendix II-B), it is possible to estimate the time-temperature history of the metamorphism. The age of the coarse size fraction corresponds to 54% argon loss from a 1000 m.y. sample heated at 355 m.y. If the initial age was actually 900 m.y. it would only cause a 10° C difference in the final answer, so the temperature estimate is relatively insensitive to the choice of initial age. The major uncertainty comes in estimating the effective diffusion radius of the coarse sample. It is clearly between .7 mm and 3.5 mm. The actual choice will make a considerable difference. The following table shows the results of calculations of the temperature-time history for two values of the coarse fraction radius.

t (m.y.)	Temp $^{\circ}$C (a=1 mm)	Temp $^{\circ}$C (a=3.8 mm)
0.1	490	540
1.0	450	500
5.0	420	470
10.0	410	450
50.0	390	430

The temperatures are relatively insensitive to the time estimates because of the high activation energy of argon in muscovite. Also an error in placement of the muscovite "D/a^2 versus $1000/T$" diffusion curve of a factor of two only causes a 10° to 15° change in these temperatures. For these reasons, a study such as this could in principle be developed into a very sensitive geothermometer. Pyroxene would be even more sensitive because of its larger activation energy, and could cover the higher ranges of temperature. In spite of the diffusion grain size uncertainties, the present study shows that the temperature of Paleozoic metamorphism in the Clarendon, Vermont area was almost certainly higher than 400°C and probably less than 500° C. This is not in conflict with estimates based on geological considerations (J. B. Thompson, personal communication).

The above study demonstrates that "apparent age" may be a function of grain size. Several cases have been reported in the literature (Gerling, 1957a; Hurley et al., 1958; Wasserburg et al., 1959), where muscovite from a pegmatite shows an older age than muscovite in the country rock cut by the pegmatite. These may be most easily explained by reference to the larger grain size of the pegmatite muscovite. A post-crystallization metamorphism would cause relatively more loss of argon and strontium from the finer grained country rock muscovite.

Appendix III

Mineral Ages in a Contact Metamorphic Zone

1. Introduction

Almost a complete range of mineral age discordancies has been observed in certain "mixed-age" or "noisy" areas. Ages by the same method on different minerals and by different methods on the same mineral may all be discordant. The discordancies may even vary in sign from area to area. Most of the "mixed-age" areas which have been previously studied are the result of regional metamorphism. In these areas it is generally impossible to relate age discordancies to any specific environmental factors. At the point where reliable indicators of metamorphic grade have developed, all but the most resistant minerals will have lost all evidence of any pre-metamorphic age.

A contact metamorphic zone would seem to offer the best possibility of correlating mineral age discordancies with at least one variable, the temperature. Knowledge of the relative temperature distribution about an intrusive can be obtained from heat flow theory with no need for relying on paragenetic analysis. A contact zone provides, in effect, a furnace for long-time diffusion experiments. This should be especially useful for diffusion studies of elements in low-activation states, such as lead in zircon.

It is not common to find intrusives cutting country rock which is markedly older than the intrusives, and yet unaffected by orogenic effects contemporaneous with the intrusives. The Montregian intrusives of Quebec are singular in being free from accompanying orogenic effects but the poorly exposed, fine-grained and low grade contact rock is far from ideal. The Paleozoic-aged Cuttingsville stock, cutting the Precambrian of the Green Mountains, Vermont, may have more ideal contact rocks but it was not learned about in time for this study. Future study is planned for it. The Laramide intrusives in the Precambrian of the Front Range, Colorado are ideal in many respects. The country rock is much older than the intrusives, allowing easy differentiation of age discordancies without straining the limits of the analytical methods. The country rocks are granite, gneisses and high-grade schists which are stable in the given contact zone; gross metamorphic recrystallization then will not obscure simple thermal diffusion effects. The coarse-grained and salic nature of the contact rock permits ready separation of at least two potassium-rich minerals. The effect of grain size variations on diffusion loss can be studied in the schist, which contains biotite of widely varying sizes. The contact rocks are well exposed, permitting continuous traverses for hundreds of feet. The extensive hydrothermal mineralization in the Front Range represents the main disadvantage of the area. Study of the area was pursued with this in mind.

2. Regional Geology

Most of the following is taken from the detailed description of the geology and ore deposits of the Front Range compiled by Lovering and Goddard, 1950.

The crystalline core of the Front Range is essentially Precambrian granite, schist and gneiss; it is nearly everywhere bordered by steeply tilted Paleozoic rocks. Many stocks and dikes were intruded into the central part of the range during the Laramide revolution but are uncommon elsewhere.

The oldest rocks in the Front Range are the schists and gneisses of the Idaho Springs formation. These are highly metamorphosed sedimentary rocks consisting chiefly of quartz-biotite and quartz-biotite-sillimanite schists. Although these rocks have been closely folded their original bedding planes are in most places parallel to the foliation. The Idaho Springs formation is overlain by the Swandyke hornblende gneiss, and both formations are cut by an extensive series of Precambrian granitic intrusives. The oldest of these intrusives are small stocks and masses of quartz monzonite gneiss and granite gneiss which show a concordant habit in the metamorphics. The younger Boulder Creek granite forms stocks and small batholiths which are satellitic to the larger batholiths of the even younger Pikes Peak granite. The Silver Plume granite, found in stocks and small batholiths, is the youngest of the major Precambrian rocks in the Front Range.

Cutting the Precambrian of the Front Range is a series of about ten major stocks, Paleocene or Eocene in age. These stocks, ranging in size from two square miles to fifteen square miles, occupy a narrow belt about five miles wide extending southwestward across the Front Range from Boulder to Breckenridge. Many smaller irregular bodies and dikes and most of the early Tertiary ore deposits of the Front Range occur in a strip ranging in width from two to ten miles, just southeast of the line of stocks. The linear structure within most of the stocks indicates that they have been intruded upward at a steep angle and some of the stocks undoubtedly occupy old volcanic throats. The composition of the stocks ranges from diorite to quartz monzonite.

Orogenic activity during the Laramide revolution consisted chiefly of broad folding or arching, faulting, and intrusion of the stocks in the porphyry belt. There is no evidence of any regional thermal metamorphism since Precambrian time.

3. Sample Location and Geology

In August, 1959, five days were spent in the Front Range investigating contact zones and collecting samples. Portions of the contact zones of six of the Laramide stocks were examined. The contacts of the stocks at Jamestown, Empire and Montezuma could be narrowed down only to within a hundred foot zone. Two sections of the contact of the Eldora

stock could be defined to within ten feet. The contact of the Caribou stock and the Audubon-Albion stock were exposed and knife sharp. Sample suites were collected from the Audubon-Albion and Eldora contact zones.

Audubon-Albion Area (see sample map, Fig. 21)

This stock occupies an area of about seven square miles in the northwestern part of the Front Range. It lies four miles west of Ward, Colorado, and about one mile east of the continental divide. It is most easily reached from the Brainard Lake N.F.S. Campground. The eastern contact, which is not well exposed, is about one mile by trail from the campground. The western contact is three trail miles from the campgroupd and well exposed in rugged terrain. Most of the western contact zone lies above 11,000 feet elevation. The contact plane at one point just north of Lake Isabelle dips 70° east. The general topographic trend of the whole western contact indicates a dip of the same nature, while the eastern contact tends to be nearly vertical.

Just north of Lake Isabelle there is a contact between the Silver Plume granite and the Idaho Springs formation which runs approximately perpendicular to the contact of these Precambrian rocks with the monzonite stock. This allowed a suite of contact samples of both granite and schist to be collected within 500 feet of each other. Thirteen samples of Idaho Springs formation were collected over a horizontal dis-

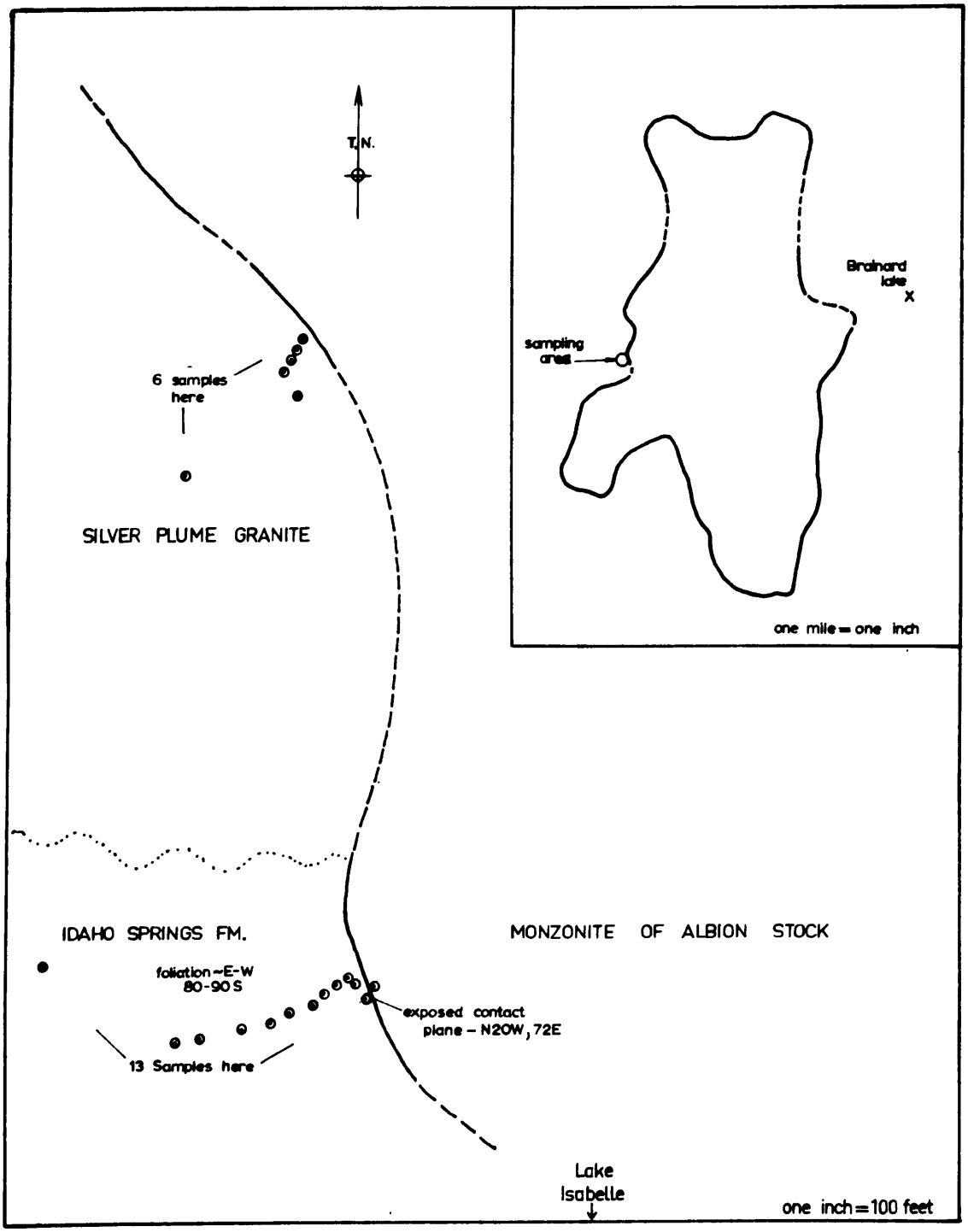

FIG. 21 —SAMPLE MAP, AUDUBON-ALBION AREA, FRONT RANGE, COLORADO.

tance of about 300 feet. Locations were determined by tape and compass measurement from the contact. The contact plane at this point forms a small cliff face which is near the crest of the ridge overlooking, and about 100 yards north of, Lake Isabelle. The Idaho Sppings formation here is a biotite-sillimanite-quartz schist with numerous pegmatitic lenses and stringers, and occasional massive granitic layers. The general east-west foliation is not noticeably affected by the intrusive. In fact, the only macroscopic aspect related to the intrusive is an absence of sillimanite in a fifty-foot zone near the contact. The sample furthest from the contact was gneissic granite, suggesting near proximity to the gradational Silver Plume-Idaho Springs contact. No effort was made to obtain representative samples. Most of the samples were from the biotite-rich layers in the schist.

Five hundred feet further north a suite of six samples was collected from the Silver Plume granite. The granite here does not show the parallelism of lathlike feldspar crystals which is typical of most Silver Plume granite. It is finer grained, with less abundant and less homogeneously distributed mafics. The samples which were taken were large enough to be representative. There was no macroscopic change in appearance of the samples as the contact was approached.

In all, a total of nineteen samples, 150 pounds, was collected from the western contact of the Audubon-Albion stock.

Eldora Area (See sample map, Fig. 22)

The Eldora stock is much more irregular in outline than the Audubon stock and of about the same size. The northern contact is directly accessible from the road between Eldora and Hessie. The section sampled is one mile west of Eldora and 50 to 100 yards north of the road, on the side of Mineral Mountain. The contact between the quartz monzonite stock and the Idaho Springs formation is gradational over a ten-foot zone. Many xenoliths and ghost structures of schist are present in the quartz monzonite up to distances of fifty feet from the contact. Across a fifty-foot zone in the Idaho Springs formation the foliation is vague and distorted, and pegmatitic lenses and quartz veins seem to be especially numerous. This contact zone is markedly different from the one at the Audubon-Albion stock. The difference may be accounted for by the more salic and fluid-rich nature of the intrusive at Eldora, by its earlier emplacement in the orogenic cycle, or by its higher intrusive temperatures.

Nine samples were collected over a horizontal distance of about 250 feet. The extreme variability of the Idaho Springs formation here allowed several types of samples to be collected at each location. Usually a sample of coarse biotite-feldspar pegmatite was taken, along with either a fine-grained biotite-quartz-feldspar schist sample or a plagioclase-hornblende amphibolite sample.

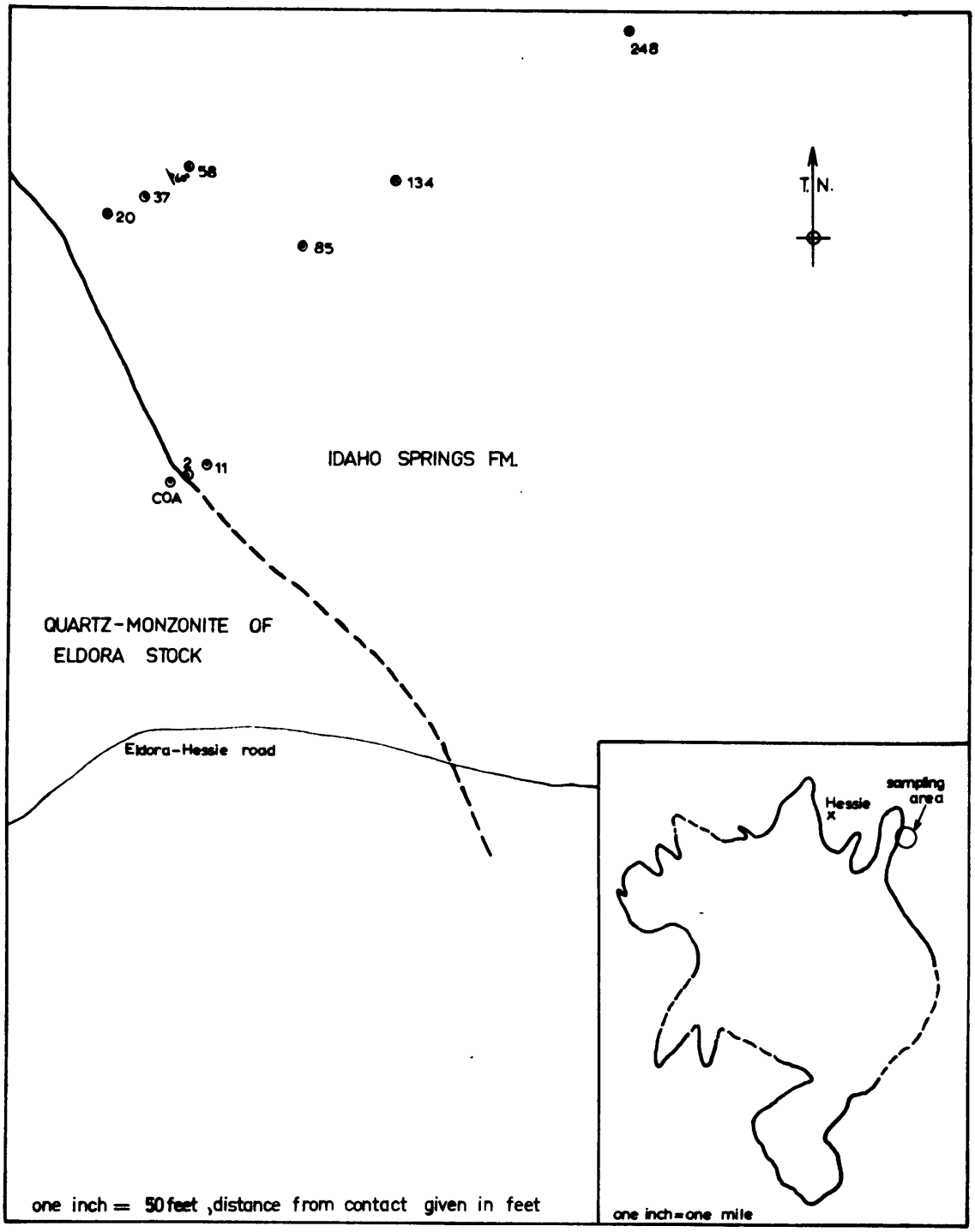

FIG. 22—SAMPLE MAP, ELDORA AREA, FRONT RANGE, COLORADO

4. Sample Description and Petrography

The samples were labelled A or C according to locality, Audubon or Caribou (Eldora), followed by a number representing the distance from the contact in feet. They were also assigned an M.I.T. project number. Following is a brief macroscopic and microscopic description of each sample.

Audubon Samples

A0A (4069) Biotite-bearing monzonite intrusive, fine-grained, equigranular. Thin sections shows zoned oligoclase, orthoclase, quartz, hornblende, biotite, magnetite, and sphene, in order of decreasing abundance. Biotite and hornblende intimately intergrown.

A6A (4070) Fine-grained biotitc schist, also some fine-grained granitic material. Thin section shows large porphyroblasts of altered orthoclase, non-undulatory quartz, albite, strained biotite with abundant pleochroic haloes, magnetite, and skeletal garnet associated with the biotite and magnetite.

A12A(4071) Medium-grained biotite-rich schlieren in schist. Thin section shows non-oriented random-size biotite with few pleochroic haloes, quartz, slightly altered orthoclase, subhedral garnet occasionally anisotropic, magnetite, and albite.

A18A (4072) Similar to A12A

A23A (4073) Fine-grained biotite gneiss. Thin section shows quartz, ironstained biotite, albite, orthoclase, magnetite and relict garnet altering to chlorite and chloritoid.

A38A (4074) Medium-grained quartz-biotite schist. Thin section shows quartz, orthoclase, albite, biotite with rare pleochroic haloes, skeletal magnetite, and small partially developed garnet.

A51A (4075) Fine-grained biotite schist, also a sample of medium-grained granitic segregation. Thin section shows quartz, albite, biotite, orthoclase, magnetite, small euhedral garnet, and hematite alteration of magnetite.

A74 (4076) Medium-grained biotite-sillimanite schist. Thin section shows felted aggregates of medium-grained sillimanite, quartz, orthoclase, biotite, albite, magnetite and yellow chlorite, serving as matrix for much of the sillimanite. No garnet observed.

A88A (4077) Medium-grained biotite-quartz-sillimanite schist. Thin section shows quartz, sillimanite, biotite, albite, orthoclase and magnetite, minor amounts of yellow chlorite.

A122A (4078) Medium-grained biotite-quartz-sillimanite schist. Thin section shows quartz, highly sericitized orthoclase, sillimanite, biotite with pleochroic haloes around large monazite grains, magnetite, and well crystallized green chlorite. No albite observed, may be completely altered.

A152A (4079) Medium-grained quartz-biotite-sillimanite schist. Thin section shows quartz, partially sericitized orthoclase, sillimanite, biotite with abundant pleochroic haloes, albite, magnetite, and green chlorite alteration of some of the biotite.

A169A (4080) Medium-grained quartz-biotite-sillimanite schist. Thin section shows albite, quartz, orthoclase, biotite with pleochroic haloes (around very abundant grains of rounded monazite and some subhedral zircon), magnetite and sillimanite.

A300A (4081) Medium-grained granitic facies, some foliation. Thin section shows orthoclase, quartz, albite, biotite with pleochroic haloes, magnetite, subhedral garnet occasionally anisotropic, muscovite interlayered in the biotite and as skeletal patches in orthoclase, and some sillimanite which is not euhedral as in other sections.

Discussion of Mineral Assemblages in Audubon Contact Zone

All the samples contain the assemblage quartz, orthoclase, albite, biotite and magnetite. In addition the rocks up to 74 feet from the contact have garnet and no sillimanite, whereas the rocks 74 feet and further from the contact contain sillimanite and no garnet. The 300 feet sample contains sillimanite, garnet and muscovite. However, the sillimanite occurs at one end of the section and is not associated with garnet or muscovite. This indicates a reaction relatianship and suggests

that the assemblage including sillimanite-garnet-muscovite is not a stable assemblage. The appearance of garnet in samples near the contact seems to be related to the contact and not to bulk compositional differences. It is probably a retrograde reaction of the form biotite + quartz + magnetite + sillimanite $\longrightarrow$ garnet. The assemblage at 300 feet suggests the same reaction, but with muscovite forming from a KFS + sillimanite reaction. The 300 feet sample essentially marks the retrograde garnet isograd, and suggests the presence of a thermal source some distance beyond and unrelated to the exposed contact of the Audubon stock. The presence of such a heat source is borne out by the age determinations on the Audubon contact samples.

Eldora Samples (Thin sections were cut only from hornblende-bearing samples.)

C0A (4060) Medium-grained equigranular quartz monzonite, containing biotite and hornblende. Thin section shows strongly zoned oligoclase, quartz, large partially sericitized orthoclase phenocrysts, hornblende, biotite with few pleochroic haloes, epidote, sphene and magnetite.

C2A (4061) Coarse-grained biotite-feldspar pegmatite, and medium-grained hornblende-plagioclase amphibolite. Thin section (amphibolite) shows twinned oligoclase with untwinned overgrowths, ragged green-brown hornblende, epidote, magnetite,

sphene, biotite intergrown in the hornblende, quartz, and orthoclase.

C11A (4062) Medium-grained quartz-feldspar pegmatite and amphibolite. Thin section (amphibolite) shows large clean green-blue hornblende and twinned unzoned oligoclase, minor magnetite. A few traces of biotite alteration on hornblende are present.

C20A (4063) Coarse-grained biotite-feldspar pegmatite pod.

C37A (4064) Coarse-grained biotite-feldspar pegmatite pod.

C58A (4065) C85A (4066) Coarse-grained biotite-feldspar pegmatite pod and fine-grained biotite-feldspar granitic segregation.

C134A (4057) Feldspar-biotite pegmatite, and amphibolite. Thin section shows brown hornblende, unzoned twinned oligoclase, diopside altering to hornblende, magnetite and quartz, no traces of biotite.

C248A (4068) Coarse-grained biotite-feldspar pegmatite stringer and amphibolite. Thin section (amphibolite) shows large clean brown-green hornblende altered in places to blue-green hornblende, unzoned twinned andesine, diopside occasionally altering to blue-green hornblende, magnetite, epidote and trace quartz. No biotite.

Discussion of Eldora Mineral Assemblages

The abundance of rimmed plagioclase, sphene, and alteration biotite in C2A is an indication of the gradational nature of the contact. Samples further from the contact show

no evidence for metasomatism. The lack of pyroxene in samples near the contact suggests a retrograde reaction due to the thermal contact metamorphism. Sample C134A contains pyroxene in various stages of alteration to hornblende. This may or may not be the first sign of the retrograde reaction.

Idaho Springs Sample

To serve as a standard, a sample of Idaho Springs formation was collected at a location away from the influence of any contact metamorphism. The sample was collected from a fresh blasted road cut at the junction of routes 6 and 40, five miles east of Idaho Springs, Colorado. The sample is a coarse-grained biotite-quartz schist with abundant feldspar-quartz pegmatite stringers in it.

5. Procedures

Samples were fragmented and mineral separates obtained by the procedures outlined in Appendix IA. The analytical procedures used are discussed in Appendix I B and C.

6. Results, Audubon-Albion Contact Zone (Samples AOA to A300A)

The biotite argon ages presented in Table 8 are summarized below for clarity.

Distance from Contact	Biotite K-Ar Age, m.y.
0	70
38	66
74	65
88	110
122	87
152	69
169	63
300	65

With the exception of biotites A88A and A122A, the average of the other five is 66.3 m.y. with a standard deviation of 4%, and a standard error of 1.7%. This is about the spread which would be expected from experimental error in this age range. These five biotites apparently lost all their argon at the time of intrusion and serve to date the stock as being 66.3±1.1 million years old. Samples A88A and A122A have retained some argon, but are in between samples which show complete loss. This can be explained by the existence of an unseen heat source at some greater distance from the contact. The appearance of retrograde garnet in sample A300A also points to a second heat source. The asymmetry of samples A88A and A122A with respect to the two garnet isograds suggests that the temperature gradient on the side toward the secondary source is flatter.

Orthoclase feldspar from sample A88A gave an argon age 40% lower than the age of the intrusive. This probably

represents the usual mica-feldspar discrepancy and should not be taken as an indication of a thermal event at 40 m.y. or younger.

A biotite at 300 feet gave a rubidium-strontium age of 89 m.y. using a normal strontium 87 abundance of .0702. Using the intersection of the whole rock-biotite growth lines gives an age of 78 m.y. The experimental error on this may or may not overlap the K-Ar age of the intrusive. The error was larger than normal due to a very poor spiking ratio in the rubidium. run. In any event the biotite shows very little retention of radiogenic strontium.

The three whole rock Rb-Sr ages are widely scattered and imply that the chemical system represented by samples of the size collected was not a closed system. In a sense these samples are analogous to mineral phases in a rock. The radiogenic strontium should move from schist layers with a high Rb/Sr ratio to layers with a lower Rb/Sr ratio. The layer with the highest Rb/Sr ratio should give a valid minimum age. The other layers may give ages older than their true age. In general, the most biotite-rich samples available were collected. If the content of biotite is an adequate measure of the Rb/Sr ratio, then these samples should give meaningful minimum ages. The measured Rb/Sr ratios of the three samples were high: 1.7 for A88A, 5.0 for A152A, and 1.5 for A300A. The variability, however, shows that this ratio is not solely dependent on the biotite content in these three samples. It

is probaly more dependent on the minor amounts of strontium-rich phases. The three whole rock ages are not necessarily meaningful ages, then. However, they do serve to illustrate that radiogenic strontium can have considerable mobility during metamorphism.

Table 9 shows analytical and age data for the U-Pb analysis of a monazite separated from sample A169A. A -200+270 mesh sample fraction was put through bromoform and methylene iodide. After refinement on the Frantz the sample was 60% pure, xenotine being the principal impurity. Fifty milligrams of pure monazite was obtained by rolling on paper and hand-picking. The rounded pellet-like appearance suggests detrital origin. The chemical analyses and mass spectrometry were done during a week's visit to the Department of Terrestrial Magnetism and the Geophysical Laboratory, Washington, D.C. The author is especially grateful to Dr. G. R. Tilton of the Geophysical Laboratory who unselfishly devoted a week's time to instruction and supervision in the necessary techniques. The general analytical procedures are described in Appendix I C. The monazite was washed for 15 minutes in cold 6N H Cl before fusion. The lead 204 found, 0.4 micrograms, was attributed to laboratory contamination and is not reported in Table 9 . (The observed Pb^{206}/Pb^{204} ratio was 2700.)

These ages, while clearly discordant, show that monazite is resistant to thermal events in the same way as zircon. This monazite shows an age pattern which is the same as that

Table 9

Analytical Data for Monazite

Concentration in wt. %				Atom percent Abundance			
U	Th	Pb	Pb^{206}	Pb^{204}	Pb^{206}	Pb^{207}	Pb^{208}
0.580	5.46	0.396	0.1070	0	0.272	0.0252	0.703

	U^{238}/Pb^{206}	U^{235}/Pb^{207}	Pb^{207}/Pb^{206}	Th^{232}/Pb^{208}
Age, million years	1260	1360	1500	1100

usually observed for discordant zircons, i.e., 207/206 age > 235/207 age > 238/206 age > 232/208 age. Discordant monazites usually show either this pattern, or a 238/206 > 235/207 > 207/206 > 232/209 pattern (Tilton et al., 1957; Nicolaysen et al., 1958). Previous monazite determinations have usually been made on large single crystals from pegmatitic deposits. Since this monazite is undoubtedly of detrital origin, the age pattern could be the effect of three different metamorphisms (1600 m.y., 1350 m.y., 65 m.y.) and a detailed interpretation is pointless. Some restrictions can be applied, however, by using the "Concordia" plot of Wetherill (1956). If the monzaite has lost lead only at the time of contact metamorphism, the true age would be about 1550 m.y. In any event, regardless of the number or age of metamorphic episodes, if each episode results only in a net loss of lead or a net gain of uranium the true age must be greater than 1500 m.y.

Composition of Audubon Contact Zone Biotites

It was stated before that the relative temperature distribution about an intrusive can be calculated from heat flow theory. For the Audubon stock this is obviously not so, due to the secondary heat source inferred. Compositional changes in biotites can be used as an independent measure of the P-T contact conditions, to supplement heat flow calculations. This is true as long as the biotite is in an assemblage containing enough phases to eliminate bulk composition as a variable. The assemblages biotite-magnetite-feldspar-quartz-albite-sillimanite, and biotite-magnetite-feldspar-quartz-albite-garnet are both sufficient in this regard. For these assemblages the composition of the biotite is a function only of temperature, total water pressure and partial pressure of oxygen. If the activity of water and oxygen are controlled externally and everywhere the same, the composition of the biotite is a function of temperature only.

The iron-magnesium ratios of six of the biotites from the Audubon-Albion stock were determined on the optical spectrograph. Two chemically analyzed biotites were run as standards. The biotites were ground to -200+400 mesh size, repurified, mixed one part biotite to three parts carbon powder and loaded in 1/8" graphite electrodes. They were arced at 6 amps to completion. In most cases, triplicate analyses were made. The data is given in Table 10 . The lines used were Mg 2783 and Fe 2912. The two standard

samples Sp33 and Sp35 were biotites which had been analyzed by "rapid silicate" techniques by W. C. Phinney (1959). His values for the ratio, total Fe/Mg were used to normalize the relative intensity ratios of the other samples.

Table 10

Optical Spectrographic Data on Fe/Mg Ratios in Biotites

Sample Number	Rel. Intensity Ratio Fe/Mg	$\frac{FeO+Fe_2O_3}{MGO}$ (Average)	Standard Error of Replicate
Sp33	2.52, 2.66	2.66 (Standard)	2.7%
Sp35	1.57, 1.55, 1.66	1.62 (Standard)	2.2%
AOA	1.14, 1.21, 1.39	1.25	6 %
A38A	1.26, 1.19, 1.25	1.23	2.5%
A74A	1.78, 1.70, 1.95	1.81	5 %
A88A	1.78, 1.89, 1.75	1.85	2.4%
A152A	1.59, 1.59, 1.62	1.63	0.6%
A300A	1.85, 2.00, 2.11	2.03	3.8%

Phinney's chemical determinations are listed below.

	% FeO	% MGO	% Fe_2O_3	$\frac{\text{Total FeO}}{\text{MGO}}$
Sp33	19.21	8.62	3.62	2.66
Sp35	15.23	11.52	3.53	1.62

The biotites used for standards were not the identical samples analyzed by Phinney, but were separated from the same biotite concentrate. The use of standards is not necessary to establish

differences in the Fe/Mg ratio of biotites. For comparison with the literature, however, it was thought desirable to have the Fe/Mg ratio in absolute units. Also the standards served as a check on the accuracy of the spectrographic method. For example, for the standards the ratio $\frac{\text{Sp33 Fe/Mg}}{\text{Sp35 Fe/Mg}}$ was determined chemically to be 1.63, whereas the ratio determined on the optical spectrograph was 1.64. The average precision error of the replicates, about 3%, is considered quite sufficient for these purposes. Only total iron is determined on the optical spectrograph, and lumping FeO and Fe_2O_3 together for relative comparisons is strictly valid only if all the assemblages are at the same activity of oxygen. This is probably a reasonable assumption for a contact metamorphic zone.

The data are plotted in Fig. 23 to indicate the spatial relationships of the Fe/Mg ratios in the contact biotites. Wones (1959) has determined the direction of compositional changes in biotite-magnetite-sanidine assemblages for changes of Po_2 and T. The ratio Fe/Mg in these biotites decreases with increasing temperature and with increasing partial pressure of oxygen. Biotite compositions in the garnet assemblages are not strictly comparable with those in sillimanite bearing assemblages. Qualitatively, the biotite in the garnet assemblage should have a larger Fe/Mg ratio. With this in mind, the first four biotites in Fig. 23 show a compositional change consistent with decreasing temperature. The fifth

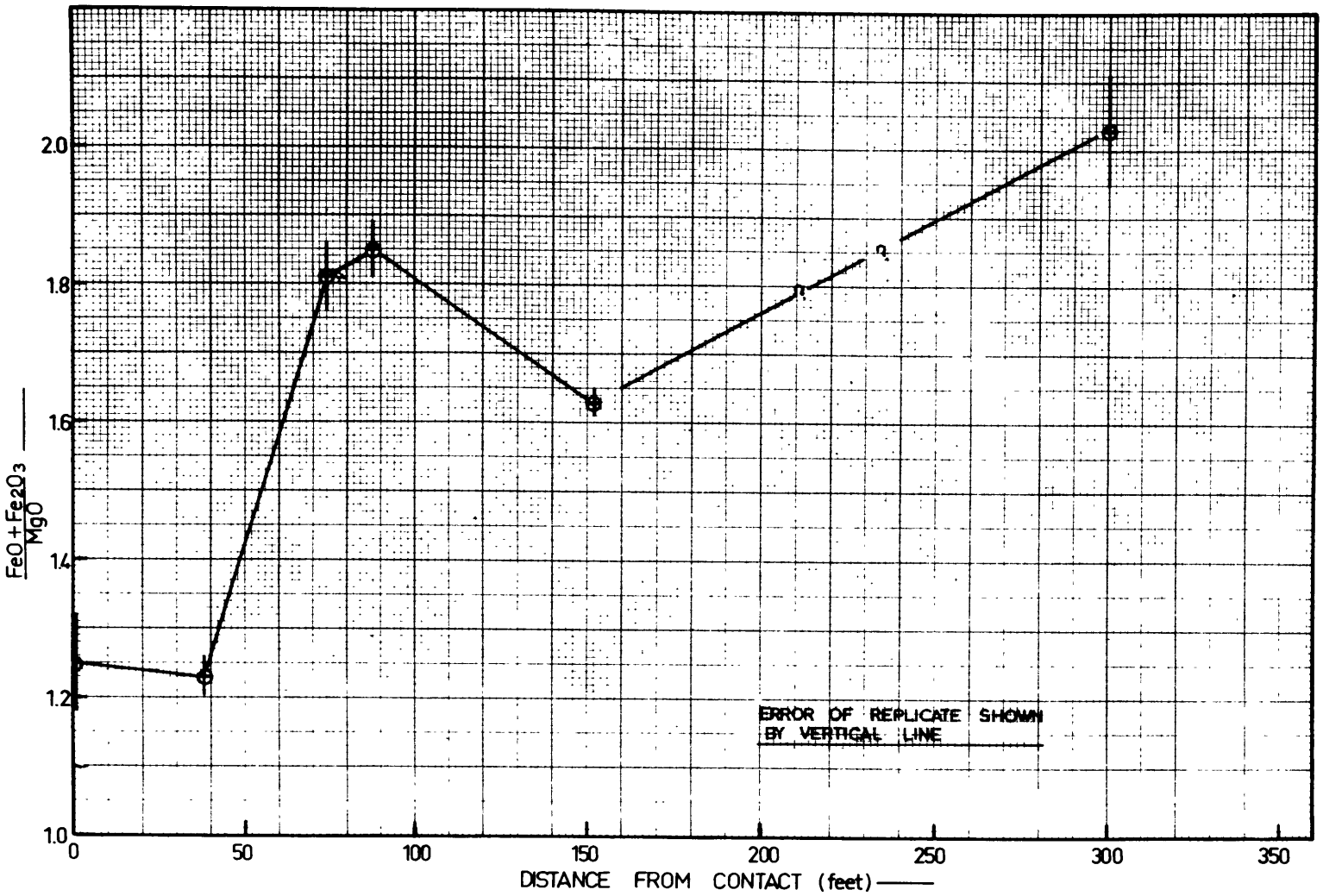

FIG 23—IRON-MAGNESIUM RATIOS IN CONTACT BIOTITES

biotite (A152A) indicates a reversal of the temperature gradient, as was inferred previously from several other lines of evidence. The biotite at 300 feet shows the highest Fe/Mg ratio of all and should represent the lowest temperature of all, given the assumptions above. Either the temperature really was lowest there, or the activity of oxygen and water there is different because of lack of communication with the other samples. A choice cannot be made from the limited data obtained so far.

7. Results, Eldora Contact Zone (Samples C0A to C248A)

The ages determined on minerals from the Eldora contact zone are presented in Table 8 and illustrated graphically in Fig. 24 . The ages on samples from this contact zone do not indicate any heat sources other than the intrusive itself. The hornblendes show a striking retentivity for argon relative to the retention of either strontium or argon in the biotites. The age of 1160 m.y. on the hornblendes at 134 feet and 248 feet is believed to represent the general age level of the Precambrian in this district. That is, these two samples show complete retentivity. The biotite argon age of 68 m.y. at 58 feet probably represents complete loss of argon. The age of the Eldora stock is essentially identical with the age of the Audubon stock.

It may be noted that the biotites from Audubon show relatively more retention of argon than biotites from a similar

Table 8

Analytical Data for Colorado Contact Suites

Sample Number	Grain Size	Mineral	K %	$*Ar^{40}$ (10^{-5} cc stp/g)	$\frac{*Ar^{40}}{\text{Total } Ar^{40}}$	Rb (ppm wt.)	$*Sr^{87}$ (ppm wt)	$\frac{*Sr^{87}}{\text{Total } Sr^{87}}$	K-Ar Age (m.y.)	Rb-Sr Age (m.y.)
A0A	-50+100	Biotite	4.84, 5.15	1.42	0.69				70±2	
A38A	+50	Biotite	7.52	2.04	0.77				66±3	
A74A	-50+100	Biotite	7.49, 7.59	2.02	0.47				65±2	
A88A	-50+100	Biotite 1	5.68, 5.85	2.70	0.73				114±4	
	-50+100	Biotite 2	5.59, 5.78	2.48	0.71				106±4	
	-100+200	Feldspar	9.77, 10.22	1.90	0.86				40±1	
	-50	Whole Rock				342	2.25(I.R.) 2.18(I.D.)	0.138(I.R.)		1650±120
A122A	-50+100	Biotite	6.55, 6.58	2.34	0.56				87±2	
A152A	-28+40	Biotite	5.82, 5.83	1.64	0.72				69±2	
	-50	Whole Rock				392	1.45(I.R.) 1.14(I.D.)	0.208(I.R.)		940±75
A169A	-100+200	Biotite	7.25, 7.24, 7.31	1.88	0.41				63±2	
A300A	-50+100	Biotite	6.83, 6.92	1.82	0.68	1240	0.457(I.D.)	0.174(I.D.)	65±3	89±7
	-50	Whole Rock				284	1.51(I.R.) 1.65(I.D.)	0.101(I.R.)		1340±60
C2A	-100+200	Hornblende	1.18	0.553	0.60				114 (unfused)	
				0.598	0.40				123±5	
C11A	-50+100	Hornblende	0.77, 0.79	3.84	0.91				950±35	
C58A	2-10 m.m.	Biotite	7.34, 7.48	2.06	0.83	907	1.15(I.D.)	0.31(I.D.)	68±2	305±15
C134A	-50+100	Hornblende	1.02, 1.07	6.65	0.94				1160±40	
C248A	5-10 m.m.	Biotite	7.34, 7.46	2.43	0.69	888	1.52(I.D.)	0.37(I.D.)	80±2	410±20
	-50+100	Hornblende	1.01, 1.06	6.56	0.85				1150±40	
4088	+50	Biotite	7.39, 7.61	38.3	0.98				970±30	

* Radiogenic

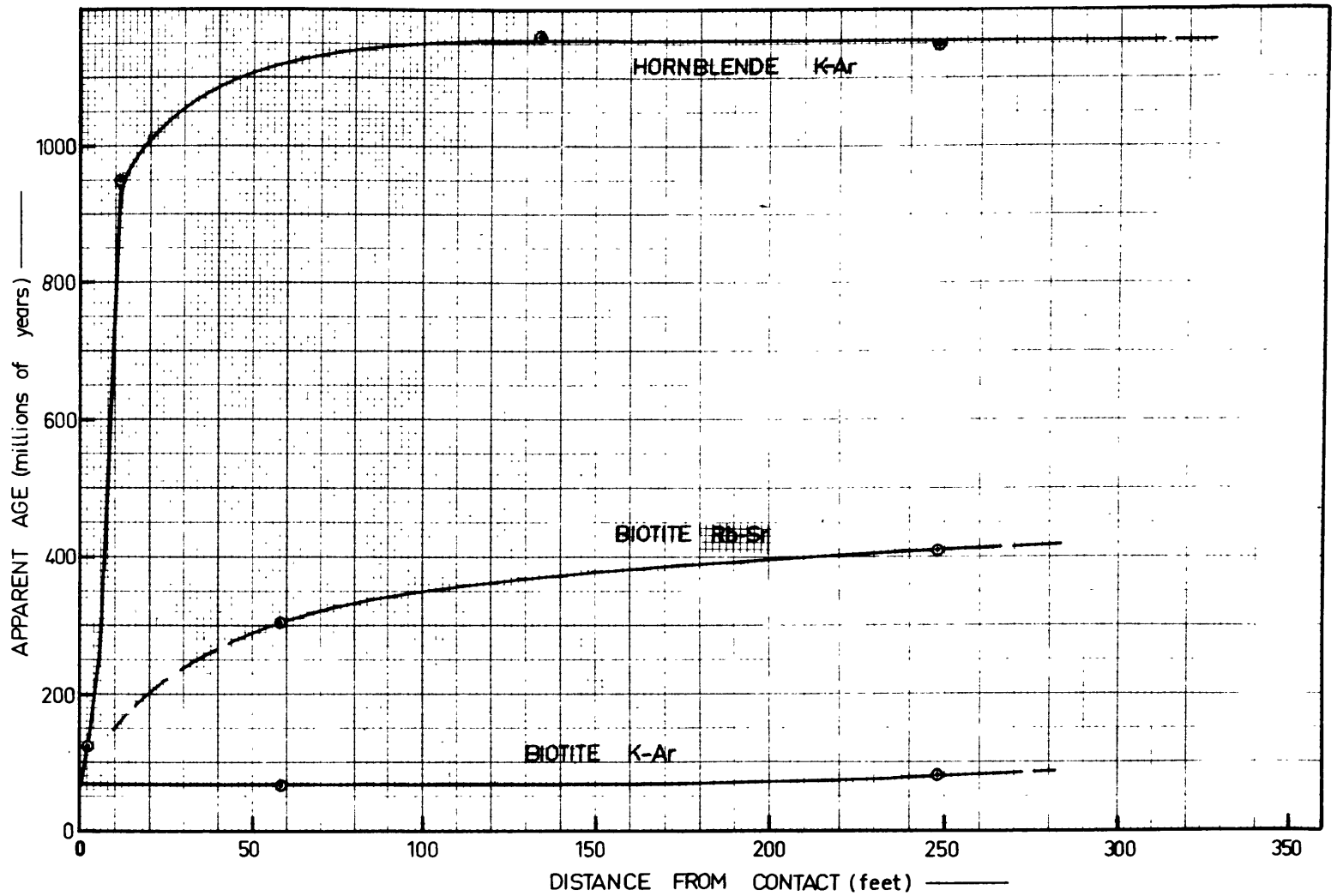

FIG. 24 — CONTACT ZONE AGES, ELDORA STOCK, FRONT RANGE, COLORADO

contact distance at Eldora. The reverse would be expected on the basis of the relative shapes of the intrusives near the sampling locations. A higher initial intrusive temperature for the Eldora stock could be one possible explanation. It is also possible that the Eldora intrusion was accompanied by larger amounts of circulating fluids which served to increase the wall rock conductivity and flatten the temperature gradient. The gradational contact, distorted foliation and abundance of quartz and pegmatite veins near the contact of the Eldora stock offer support for this hypothesis.

Qualitatively, the relative retentivities of argon and strontium in the minerals of the Eldora contact are obvious from Fig. 24 . However, the shape and displacement of these curves is also quantitatively significant with regard to the diffusion parameters of these minerals. The following model will help to illustrate the relationship which exists in a contact zone between the various diffusion and heat flow parameters.

Consider the heat flow from an intrusive stock such as that at Audubon. Geometrically, this stock may be represented by a rectangular parallelopiped, with X and Y dimensions of 2.4 km and 7.3 km. This X-Y cross section has the same area and perimeter as the surface exposure of the Audubon stock; the general expression for three dimensional heat flow in an infinite medium, as given by Lovering (1935), is

$$T_{(x,y,z,t)} = T_w + \frac{T_i - T_w}{8}\left[\mathrm{erf}(a) + \mathrm{erf}(b)\right]\left[\mathrm{erf}(c) + \mathrm{erf}(d)\right]\left[\mathrm{erf}(e) + \mathrm{erf}(f)\right] \quad 1.$$

T is the temperature at any point X, Y, Z at any time t, T_w is the initial wall rock temperature and T_1 is the initial temperature of the intrusive. erf(a) is the error function

$$\frac{2}{\sqrt{\pi}} \int_0^a e^{-\alpha^2} d\alpha$$

where $a = \frac{x_1 + x}{2h\sqrt{t}}$, x_1 being the semidiameter along the X axis, and h^2 the diffusivity. Similarly for erf(b), erf(c), etc., where

$$b = \frac{x_1 - x}{2h\sqrt{t}} \quad , c = \frac{y_1 + y}{2h\sqrt{t}} \quad , \ldots .$$

Expression 1 can be simplified by assuming the stock to be infinite in the Z direction. Then $[\text{erf}(e) + \text{erf}(f)] = 2$. This assumption can be justified a posteriori by noting that $[\text{erf}(e) + \text{erf}(d)]$ is less than two only for times greater than 10^5 years and that diffusion is negligible in this time region. The diffusivity of the wall rock and intrusive will be assumed to be the same and equal to 0.0081. Other necessary assumptions are: the intrusion occurs instantaneously, the intrusive and wall rock are initially at uniform temperatures, the latent heat of fusion is neglected, convection processes are not considered, and the wall rock is isotropic with respect to heat flow. If the Audubon stock represents a volcanic conduit, the first assumption is clearly violated. The latent heat and convection processes also are finite. The deviation due to these effects can qualitatively be considered as a stretching of the time scale.

Calculations were made for three contact distances: 11 feet, 88 feet, and 300 feet. The wall rock temperature was taken as 100° C and the intrusive temperature as 800° C.

The curves are shown plotted in Fig. 25 as values of the temperature at a given distance versus the time. The curves can be quickly converted to the case of zero wall rock temperature and 700° C intrusive temperature by subtracting 100° C from the temperature axis. It will be noted that the curves are equivalent for times greater than 10^5 years.

To evaluate the diffusion loss from a mineral which has been heated according to the time schedule of Fig. 25 it is necessary to know the values of the diffusion coefficient as a function of temperature. On a log D versus 1/T plot these are usually straight lines whose slope is proportional to the activation energy. Two curves are considered here, both passing through a D/a^2 value of 1×10^{-14} at 350° C. One has an activation energy of 34 Kcal, which is equivalent to a linear extrapolation of the hornblende diffusion curve determined experimentally in Appendix II. The other has a slope of 65 Kcal and is an approximate extrapolation of Gerling's phlogopite curve (Gerling, 1957). Diffusion loss from these two "hypothetical" minerals was calculated by graphical integration of the heat flow curves of Fig. 25 . The heat flow curves were divided into 1000 to 20,000 $\frac{\text{year}}{\Delta}$ intervals, depending on the slope of the curve. The theoretical loss was determined at the average temperature of each interval, using a spherical diffusion model. This loss was summed over all intervals to give the total loss. The loss for each interval followed a curve similar to the temperature curve itself, i.e., maximum loss occurred at the maximum temperature. Appreciable loss

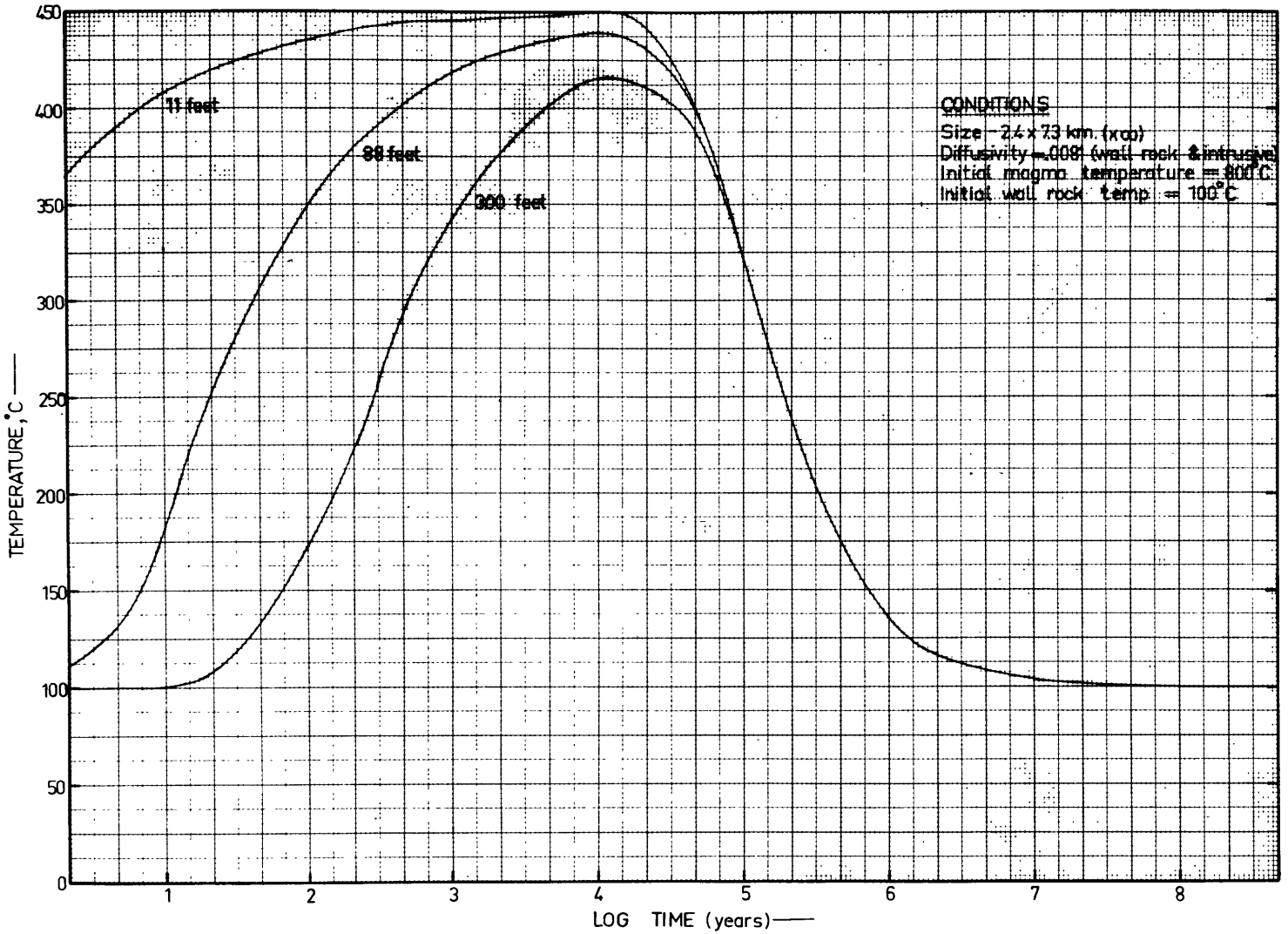

FIG. 25—HEAT FLOW CURVES FOR PARALLELOPIPED

was confined to the time interval between 10^3 years and 10^5 years. The results of this integrated diffusion loss calculation are shown in Fig. 26 . It should be mentioned that initial temperatures of 700° C for the intrusive and 0° C for the wall rock were used for these calculations. The higher 800° C temperature resulted in complete diffusion loss for all distances.

These curves show that the relative distance interval over which diffusion loss occurs is inversely proportional to the activation energy for diffusion. Consider the Eldora results, Fig. 24 , as an example. The loss of argon from hornblende takes place over a very short distance, about 100 feet, whereas the loss of strontium from biotite occurs over a distance at least five times that. This suggests a very low activation energy for strontium in biotite. It also suggests that the hornblende diffusion data of Appendix II is in error. The activation energy measured there, 34 Kcal, is certainly much lower than that suggested by the Eldora contact curves. This indicates that the bulk of the argon in hornblende is in a third position which was not detected in the experiments, a position of much higher activation energy. In addition to the shape of the diffusion loss curves, which are a measure of relative activation energies, their vertical displacement is a relative measure of the diffusion coefficients. An increase in D/a^2 of about 10,000 will change the diffusion loss from essentially zero to essentially 100%. An increase of a factor of 20 will increase the loss from 25% to 95%.

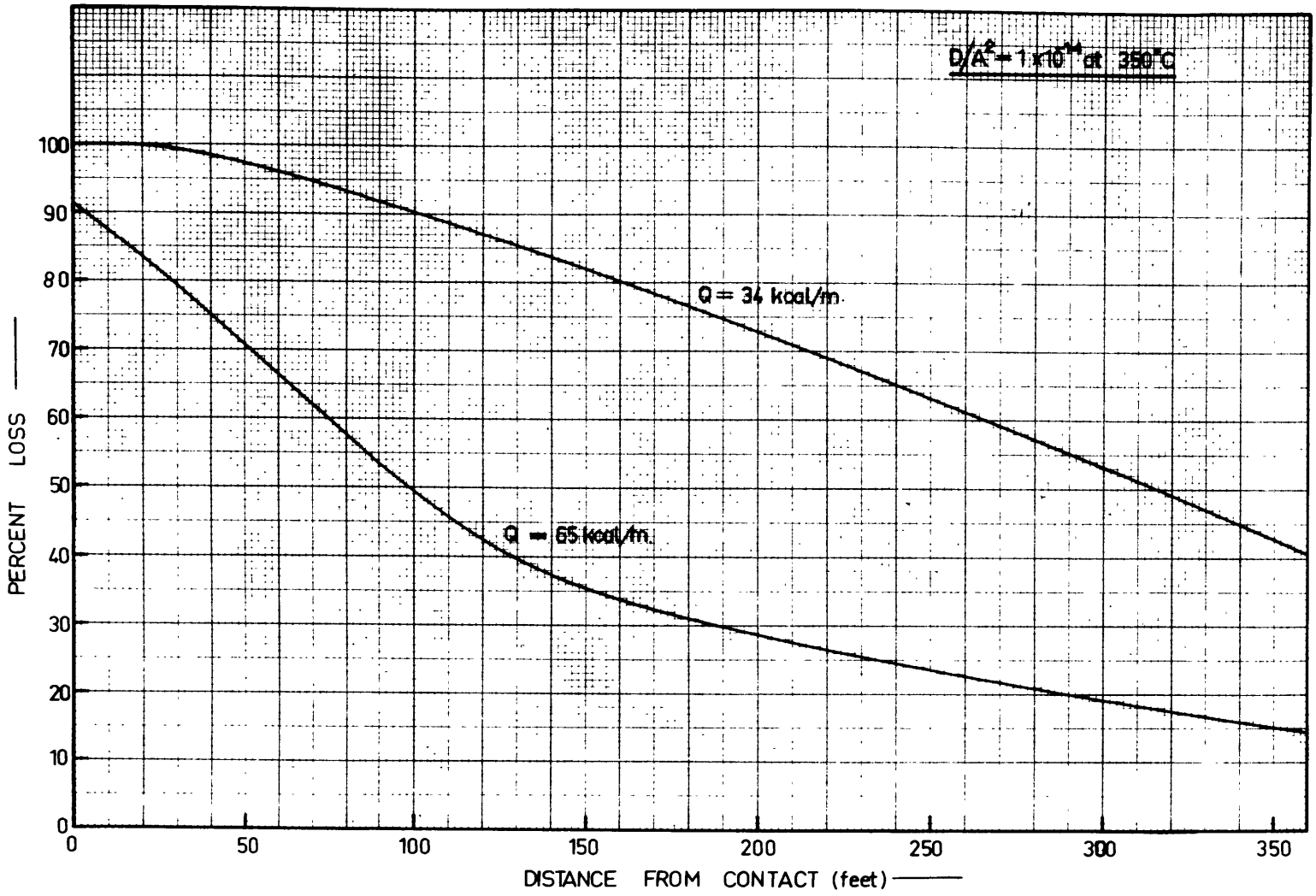

FIG. 26 — THEORETICAL DIFFUSION LOSS IN A CONTACT ZONE

8. Discordant-Age Theory

Consideration of the results from this contact study, especially the indication of a low activation energy for strontium in biotite, has led to the formulation of a discordant-age model. It is believed that this model can explain in a general way the relationships between many of the discordant age patterns which have been reported in the literature.

The model is illustrated schematically in Fig. 27. The lines represent the change of the diffusion parameter D/a^2 of the various daughter products with temperature. For minerals exposed to the same time-temperature history, the relative daughter product diffusion losses will be proportional to the relative values of D/a^2. The lines shown in Fig. 27 were positioned empirically according to the discordant age patterns observed from three types of geologic environments. The temperature scale is arbitrary.

Consider first the oldest stable shield areas which have been maintained at some low temperature T, for long periods of time (3×10^9 yrs). K-Ar and Rb-Sr ages of biotites and hornblendes from these areas frequently show no loss of argon or strontium. The zircon lead ages on the other hand are frequently discordant and have been observed to lie on a 500 m.y. to 2600 m.y. chord on a "Concordia" plot (Wetherill, 1956b). Tilton and Davis, 1960, have shown that episodic loss due to a 500 m.y. event is not a unique interpretation for this pattern. They suggest the more reasonable explanation of continuous diffusion loss of lead over the entire history of the sample. Tilton recognized that this must infer a very low activation energy for lead in zircon. For this first case, assuming a time of 3×10^9 yrs., a zero loss of argon and strontium, and a 50% loss of

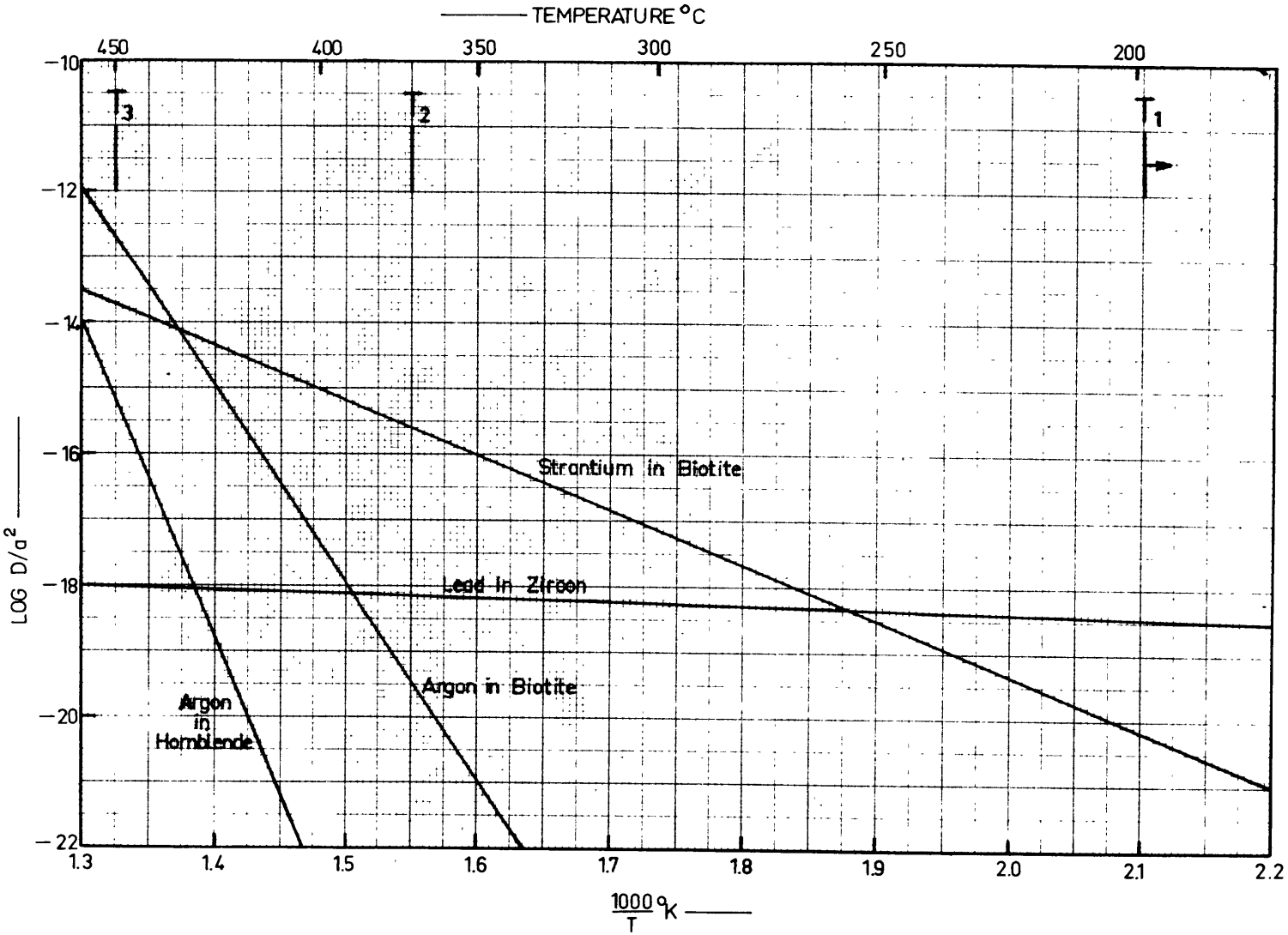

FIG. 27— GENERALIZED MODEL FOR DISCORDANT AGE THEORY

lead from zircon, the diffusion equation solutions of Fig. 8 can be used to calculate values of D/a^2 for strontium and argon in biotite, and lead in zircon at a temperature T_1.

The discordant age pattern exhibited by the contact samples discussed earlier was used to calculate D/a^2 values for the contact metamorphic environment, T_3. For this case, a time of 10^5 yrs. was assumed. The contact ages indicated little loss of argon from hornblende, complete loss of argon from biotite, about 60% loss of strontium from biotite, and little loss of lead from zircon (by analogy with monazite).

An intermediate case T_2, corresponding to moderate regional metamorphic temperatures, aided in positioning the empirical curves of Fig. 27. For this case the discordant age pattern observed at Sudbury, Ontario (Fairbairn, 1960) and at Devault, Pa., (Tilton, personal communication) was used. In these places the biotites show essentially complete loss of strontium and little loss of argon during the metamorphic event. The hornblendes also show little loss of argon. A heating time of 10^7 yrs. was used for this case. In other regional metamorphic terrains such as at Baltimore, Md. (Tilton, 1958b), the biotites show complete loss of argon and strontium while the zircons show only slight (<10%) loss of lead. It is of interest to note that the curves estimated from the above considerations are not in conflict with the diffusion results of Appendix II, with the exception of the hornblende discrepancy, as discussed on page 198.

While an empirical approach of this kind allows considerable latitude in the positioning of the various lines in Fig. 27, it is felt that this type of model provides a means for unifying many seemingly unrelated discordant age patterns. It is obvious that many deviations will occur, and a discordant age pattern will not always fit the proposed model. The relationships shown in Fig. 27

are unique only so long as the (a^2) values of the minerals remain in the given proportions. If, for example, the a^2 value for hornblende decreases, all others constant, hornblende might show partial or complete loss in case 3 (contact zones), etc. Since argon and strontium in biotite presumably have the same a^2 value, the ratio of the strontium age to the biotite age is a function of temperature only. If this function could be quantitatively determined it would provide a geologic thermometer which was independent of heating time estimates. This model also suggests that there is no such thing as a "best" mineral for dating purposes. It would be of interest to fit other minerals to this model, e.g., strontium in muscovite, feldspar and hornblende, argon in muscovite and pyroxene, lead in monazite, etc. Quantitative determinations of the scale of the temperature axis would lead to a much better understanding of gneral metamorphic processes.

9. Geologic Age Patterns in Colorado

The K-Ar age of 66±2 m.y. for the time of emplacement of the Laramide stocks in the Front Range is believed to be the first reliable measurement of this event. Nine pitchblendes from Laramide mineralization in the Front Range gave an average age of 59±5, as dated by Eckelmann and Kulp (1957). This would suggest that the mineralization in the Front Range followed the porphyry belt intrusions by some few millions of yeare. In an area such as this where the analytical errors are small in terms of absolute time, a careful study could yeild much useful information relating to the time sequence

of the intrusions, relationships of mineralization to the intrusion cycle, and the presumed eastward progression of activity during the Laramide.

Regarding the absolute time scale, andesitic pebbles believed to have come from lavas erupted from the volcanic throat of the Audubon stock are found at the base of the Upper Cretaceous-Paleocene Denver Formation (Lovering et al., 1950). A time of 66 m.y. then would fall somewhere in the Upper Cretaceous or Paleocene. Evernden's time scale (Evernden, 1959) puts the base of the Tertiary at 60 m.y.; Kulp's, and Holmes' time scales put it at 70 m.y. (Holmes, 1960). The date of 66 m.y. then is not inconsistent with either time scale, though it favors Evernden's.

About forty reliable analyses are reported in the literature which relate to the Precambrian history of Colorado. There is one grouping of ages at 1350 m.y., and another grouping at 1050 m.y. The 1050 m.y. event seems to be restricted to an area around Pikes Peak, and does not represent any major batholithic emplacements. Many of the granites around Pikes Peak which show ages of 1000 to 1100 m.y. are correlated by Lovering and Goddard (1950) as being older than the Silver Plume granite. The Silver Plume granite shows an age of 1350 m.y. to the north of Pikes Peak, indicating the 1000 m.y. ages around Pikes Peak to be metamorphic ages only. The 1350 m.y. event may represent the true age of the extensive granitic batholiths or it may also indicate only a metamorphic age.

Gast (1960) measured a whole rock Rb-Sr age of 1500 m.y. on the Quartz Creek granite, Gunnison, Colorado. Zircon from the Quartz Creek granite gave a discordant Pb^{207}-Pb^{206} age of 1700 m.y. (Aldrich et al., 1956a). Apatite from a granite at Uncompahgre, Colorado gave a discordant Pb^{207}-Pb^{206} age of 1810 m.y. (ALdrich et al., 1955). There is then some evidence which indicates that the true age of the Precambrian granites may be 1600 to 1700 m.y. The biotite argon age of 970 m.y. determined here on sample 4088, Idaho Springs formation, is certainly a metamorphic age, as is the 1160 m.y. hornblende argon age on samples C134A and C248A, Idaho Springs formation.

Acknowledgments

The author is indebted to all those who helped in the completion of this research.

Professor W. M. Pinson offered much help and instruction in the chemical procedures. Discussions with Prof. H. W. Fairbairn concerning analytical techniques, errors, and mineral separations proved very helpful. Prof. J. W. Winchester was instrumental in carrying out the neutron activation procedures. T..S. Lovering provided a helpful orientation to the geology of the Front Range during the author's visit to Denver, Colorado.

L. T. Aldrich made a week's visit to the Department of Terrestrial Magnetism possible. The author is very grateful to G. R. Tilton for his supervision in the monazite analysis during the week's visit and for many stimulating discussions regarding discordant age problems. G. R. Tilton and G. L. Davis supplied the author with an excellent suite of hornblendes from well-dated localities. Several muscovite samples and some age data from Vermont were furnished by Henry Faul.

Many fellow graduate students are thanked for their assistance and helpful discussions, especially D. G. Brookins, G. Faure, H. W. Krueger, and J. M. Moore.

The assistance rendered by the instrument makers K. Harper, F. Crowley and J. Annese is acknowledged, especially the willingness of John Annese to help at any and all times. Special thanks are due Miss Anne Farlow for her untiring efforts in typing the manuscript on a tight schedule.

Professor P. M. Hurley, through his patience, ready encouragement, stimulation and clear outlook, is largely responsible for the accomplishments of this research.

Successful completion of this research was insured by the unlimited confidence of the author's wife, Joanna.

Bibliography

AIP, 1941 and 195 , "Temperature - its Measurement and Control in Science and Industry", Symposium sponsored by American Inst. of Physics, Reinhold Publishing Co., vol. I and II.

Alberman, 1950, "Small High-Temperature Vacuum Furnace", J. Sci. Inst. 27, #10, p. 280.

Aldrich, L. T., J. B. DOak, G. L. Davis, 1953, "The Useof Ion Exchange Columns in Mineral Analysis for Age Determination, Am. J. Sci., vol. 251, pp. 377-387.

Aldirch, L. T., G. R. Tilton, G. L. Davis, L. O. Nicblaysen, C. C. Patterson, 1955, "Comparison of U-Pb, Pb-Pb, and Rb-Sr Ages of Precambrian Minerals", Proceedings of the Geological Association of Canada, Vol. 7, Part II.

G. L. Davis, G. R. Tilton, G. W. Wetherill, 1956a, "Radioactive Ages of Minerals from the Brown Derby Mine and the Quartz Greek Granite near Gunnison, Colorado, J. Geophys. Research, vol. 61, No. 2.

G. W. Wetherill, G. L. Davis, 1956b., "Determinations of Radiogenic Sr^{87} and Rb^{87} of an Interlaboratory Series of Lepidolites", Geochemical Note from Geochim. et Cosmochim. Acta, vol. 10, pp. 238-240.

G. W. Wetherill, G. R. Tilton, G. L. Davis, 1956, "Half-life of Rb^{87}", the Physical Review, vol. 103, No. 4, pp. 1045-1047.

G. W. Wetherill, 1958a, "Geochronology by Radioactive Decay", reprinted from Ann. Rev. Nuclear Sci., vol. 8, pp. 257-298.

G. W. Wetherill, G. L. Davis, G. R. Tilton, 1958, "Radioactive Ages of Micas from Granitic Rocks by Rb-Sr and K-Ar Methods", Trans. A.G.U., vol. 39, pp. 1124-1134.

G. W. Wetherill, 1960, "Rb-Sr and K-Ar Ages of Rocks in Ontario and Northern Minnesota", J. Gepphys. Research, vol. 65, No. 1, pp. 337-340.

Amirkhanov, K. I., "Rapid Method of Determining the Absolute Age of Geologic Formations by the Radioactive Decay of K^{40} to A^{40}", Bull. 3rd Session Comm. on the Det. of the Abs. Age of Geol. Formations, 1954.

V. S. Gurvich, SS. Sardorov, "Mass Spectrometric Method of Determining the Absolute Age of Geologic Formations by the Radioactive Decay of K^{40} to A^{40}", Trans, Ac. Sci. USSR, Ser. Geol. No. 4, 1955.

K. S. Magataev, and S. B. Brandt, 1957, "Determination of the Absolute Age of Sedimentary Minerals by Radioactive Methods", Doklady Ac. Sci. USSR, 117, #4, Geol. Series.

S. B. Brandt and E. N. Bartnitskii, 1958, "About the Question of Diffusion of Radiogenic Argon in Micas", in "Preservation of Radiogenic Argon in Rocks", Report of the Dagestan Branch, Ac. Sci. USSR, Makhachkala,

S. B. Brandt, E. N. Bartnitskii, 1958, "About Some Problems of the Theory of the Argon Method of Determining the Absolute Age of Rocks", in "Preservation of Radiogenic Argon in Rocks", report of the Dagestan Branch of Ac. Sci. USSR, Makhachkala.

S. B. Brandt, E. N. Bartnitskii, Gurvich, Gasanov and Ivanov, "The Thermal Stability of Radiogenic Argon in Dispersed Micas", in "The Preservation of Radiogenic Argon in Rocks", report of the Dagestan Branch, Ac. Sci. USSR, Makhachkala.

S. B. Brandt, and E. N. Bartnitskii, "The Determination of Absolute Age of K-Fs by the Argon Method", Ac. Sci. USSR, Geol. Ser. #11, p. 10, 1958.

S. B. Brandt, E. N. Bartnitskii, V. S. Gurvich and S. A. Gasanov, "On the Question of the Retention of Radiogenic Argon in Glauconite", Doklay. Ac. Sci. USSR, T. 118, p. 328, 1958.

E. N. Bartnitskii, S. B. Brandt and G. V. Bpitkevich, 1959, "On the Migration of Argon and Helium in Several Rocks and Minerals", Doklady Ac. Sci. USSR, 126, #1, Geochem. Ser.

S. B. Brandt, E. N. Bartnitskii, S. A. Gassanov and V. S. Gurvich, "On the Mechanism of Losses of Radiogenic Argon in Micas", Ac. Sci. USSR, #3, 1959, p. 104.

Amirkhanov, K. I., S. B. Brandt, E. N. Bartnitskii, 1959, "Diffusion of Radiogenic Argon in Feldspars", Doklady Ac. Sci. USSR, 125, #6, Geochem. ser.

S. B. Brandt, E. N. Bartnitdkii and S. N. Voronovski, 1959, "On the Diffusion of Radiogenic Argon in Sylvites", Geokhimiia, #6.

S. B. Brandt and E. N. Bartnitdkii, 1960, "Radiogenic Argon in Minerals and Rocks", AMSSSR, Makhachkala.

Baker, 1953, "Temperature Measurement in Engineering", Wiley and Sons, N.Y.

Bergh, P. S., 1948, "High Temperature Micro-Hardness Tester", Tech Report M-5, Kellex Corp. (Vitro Corp), Silver Springs Lab.

Brownlow, A. H., 1960, "Serpentine and Associated Rocks and Contact Minerals near Westfield, Mass.", Ph.D. Thesis, M.I.T.

Burke and Seybolt, 1953, "Procedures in Experimental Metallurgy", Wiley and Sons, N.Y.

Campbell, 1956, "High Temperature Technology", Wiley and Sons, 526 p.

Carr, D. R. and J. L. Kulp, 1955, "Use of A^{37} to Determine Argon Behaviour in Vacuum Systems", Rev. Sci. Instruments, Vol. 26, p. 379.

1957, "K-Ar Method of Geochronometry", Bull. G.S.A., vol. 68, p. 763.

Carslaw, H. S., J. C. Jaeger, 1947, "Conduction of Heat in Solids", Oxford University Press, London.

Compston, W. and P. M. Jeffery, 1959, "Anomalous 'Common Strontium' in Granite", Nature, vol. 184.

Curtis, G. N., J. F. Evernden, J. Lipson, 1958, "Age Determination of Some Granitic Rocks in California by the Potassium-Argon Method", Calif. Division of Mines, Report 54, San Francisco.

Damon, P. E., 1957, "Helium and Argon in the Lithosphere and Atmosphere", Ph.D. Thesis , Columbia University.

Darken, L. S., R. W. Gurry, 1953, "Physical Chemistry of Metals", Metallurgy and Metallurgical Engineering Series, McGraw-Hill Book Co. Inc.

Eckelmann, W. R., and J. L. Kulp, 1957, "Uranium-Lead Method of Age Detemination; Part II, North American Localities", Bull. G.S.A., 68, 1117.

Evernden, J. F., G. H. Curtis, R. Kistler, 1957, "Potassium-Argon Dating of Pleistocene Volcanics", "Quaternaria", IV, Rome.

and J. Obradovich, 1960, "Argon Diffusion in Glauconite, Microcline, Sanidine, Leucite and Phlogopite", in press.

Fairbairn, H. W., P. M. Hurley, and W. H. Pinson, 1960, "Mineral and Rock Ages at Sudbury-Blind River, Ontario", in press.

Fechtig, H. W. Gentner, and J. Zahringer, 1960, "Argon Determinations on Potassium Minerals, VII, Diffusion of Argon in Minerals and Its Effect on the Potassium-Argon Age Determinations", Geochim. et Cosmochim. Acta, vol. 19, p. 70.

Flynn, K. F., and L. E. Glendenin, 1959, "Half-life and Spectrum of Rb^{87}", Phys. Rev. 116, p. 744.

Folinsbee, Lipson and Reynolds, 1956, "Potassium Argon Dating", Geochem. Acta 10, p. 60.

Frenkel, J., 1955, "Kinetic Theory of Liquids", Dover Publications Inc. New York;

Fyfe, W. S., F. J. Turner, J. Verhoogen, 1958, "Metamorphic Reactions and Metamorphic Facies", G.S.A. Memoir 73.

Gast, P., 1955, "Abundance of Sr^{87} during Geologic Time", Bull. G.S.A., vol. 66, p. 1449.

1956, "Isotope Abundance of Sr^{87} in Igneous Rocks", Abstract, Bull. G.S.A., vol. 67, p. 1698.

1957, "Absolute Age Determinations from Early Precambrian Rocks", Ph.D. Thesis, Columbia University.

1960, "Limitations on the Composition of the Upper Mantle", J. Geoph. Research, vol. 65, #4.

Geiss, J. and D. C. Hess, 1958, "Argon-Potassium Ages and the Isotopic Compositon of Argon from Meteorites", Astrophysical J. 127, No. 1.

Gentner, W., R. Prag and F. Smits, 1953, "Age Determinations by the K.A. Method with Allowance for Diffusion of the Argon", Zeitschrift fur Naturforschung, vol. 8a, p. 216.

1953, "Argon Determination on K-Minerals II - the Age of a Potash Layer in the Lower Oligocene", vol. 4, P. 11, Geochim. et Cosmochim. Acta.

K. Goebel and R. Prag, 1954, "Age Determination on K Minerals, III - Comparison of Measurements by the K-A and U-He Methods", G.C.A, vol. 5, p. 124-133.

F. Jensen and K. R. Mehnert, 1954, "On Geological Age Determination on K-FS by the K-A Method", Zeitschrift fur Naturforschung, vol. 9a, 176.

E. Trendelenburg, "A Mass Spectrometric Method for the Determination of Diffusion Constants of Gases in Solid Bodies", Zeitschrift fur Naturforschung, vol. 9a, p. 802, 1954.

W. Kley, 1955, "On Geologic Age Determination by the K-A Method", Zeitschrift fur Naturforschung, vol. 10a, p. 822.

J. Zahringer, 1955, "Argon and Helium Determinations on Iron Meteorites", Zeitschrift fur Naturforschung, vol. 10a, p. 498.

W. Kley, 1957, "Argon Determination on K Minerals IV - The Question of Argon Loss in K FS and micas", G.C.A., vol. 12, p. 323-329.

1958, "Argon Determination on K Minerals, V - Age Determination by the K-A Method on Minerals and Rocks of the Black Forest", G.C.A, vol. 14, p. 98.

Gerling, E. K., M. E. Titov and G. M. Ermolin, 1949, "Determination of the Constant of the K-Capture Disintegration of K^{40}", Doklad. Ac. Sci. USSR, 68, p. 553.

M. C. Iaschendo, G. M. Ermolin and V. G. Barkan, 1955, "Argon Age Determinations - Methods and Applications", Trans. 3rd Session of Comm. on Absolute Age of Geologic Formations.

Gerling, E. K., 1956, "The Argon Method of Age Determination and its use for Disjunction of Precambrian Formations of the Baltic and Ukrainian Shields", Geokhimiia #5.

M. L. Iashchenko and G. M. Ermolin, 1956, "The Argon Method of Determining Age and its Applications", Bull. Comm. on Determinations of Absolute Ages of Geologic Formations (USSRAc. of Sci.) Moscow, #2.

I. M. Morozova, 1957, "Determination of the Activation Energy of Argon Isolation form micas", Geokhimmia #4.

1958, "Study of the Kinetics of Argon Isolation from Microdine-Perthite", Geokhimiia, #7.

A. A. Polkanov, 1958, "The Problem of the Absolute Age of the Precambrian of the Baltic Shield", Geokhimiia #8.

M. L. Iashchenko and L. K. Levsky and G. V. Ovchinikova, 1958, "Age Determination of Some Micas according to the Rubidium-Strontium Method", Geokhimiia, #6.

Giffin, C. E., and J. L. Kulp, 1960, "Potassium-Argon Ages in the Precambrian Basement of Colorado", Bull. G.S.A., vol. 71, pp. 219-222.

Goles, Fish and Anders, 1959, "The Record in Meteorites, part I: The Former Environment of Stone Meteorites as Deduced from K^{40}-Ar^{40} Ages", in press.

Hart, S. R., "Mineral Ages and Metamorphism", Proceedings of Conference on "Geochronology of Rock Systems, Annals of the New York Ac. Sci., in press.

Hayden, R. J., and J. P. Wehrenberg, 1960, "A^{40}-K^{40} Dating of Igneous and Metamorphic Rocks in Western Montana", J. Geol., vol. 68, No. 1.

Holmes, A., 1960, "A Revised Geological Time-Sclae", Trans, Edin. Geol. Soc. vol. 17, part 3, p. 183.

Hurley etal., 1958, M.I.T. Fifth Annual Progress Report, U. S. Atomic Energy Commission, NYO-3938.

Jaeger, J. C., 1957, "The Temperature in the Neighborhood of a Cooling Intrusive Sheet", Am. Jour. Sci., vol. 255, pp. 306-318.

1958, "The Solidification and Cooling of Intrusive Sheets from Dolerite: a Symposium", University of Tasmania.

1959, "Temperatures Outside a Cooling Intrusive Sheet", Am. Jour. Sci., vol 257, pp. 44-54.

Johnston, Bristow and Blav, 1951, "Diffusion of Ions in Some Simple Glasses", J. Am. Ceramic Soc., vol 34, #6.

Jost, W., 1952, "Diffusion in Solids, Liquids and Gases", Academic Press Inc., New York.

Kazakov and N. I Polevaya, 1958, "Some Preliminary Data on Elaboration of the Post-Precambrian Scale of Absolute Geochronology based on Glauconites", Translation of Geokhimiia, #4, p.374.

Krilov, A. Y., Baranovskaya etal., 1955, "Age of Various Intrusions of the Terskeialatai Range and the Significance of Geochemical Procession in Age Determinations by the Argon Method", 4th Session of the Comm. on the Determination of the Absolute Age of Geologic Formations.

Y. I. Silin, 1960, "The Application of Argon Dating to Clastic Sedimentary Rocks", Izvestiia, Ac. Sci. SSSR, No. 1, p. 56-66.

Lipson, J. 1958, "Potassium-Argon Dating of Sedimentary Rocks", Bull. G.S.A., vol 69, p. 137.

Long, LE., J. L. Kulp, and F. D. Eckelmann, 1959, "Chronology of Major Metamorphic Events in the Southeastern United States", Am. Jour. Sci., vol. 257, p. 585-603.

Lovering, T. S., 1935, "Theory of Heat Conduction Applied to Geological Problems", Bull, G.S.A., vol. 46, p. 69-94.

and E. N. Goddard, 1938, "Laramide Igneous Sequence and Differentiation in the Front Range, Colorado", G.S.A. Bull., vol. 49, p. 35-68.

1950, "Geology and Ore Deposits of the Front Range, Colorado", U.S.G.S. Prof. Paper 223,

"Geology and Ore Deposits of the Boulder County Tungsten District, Colorado", U.S.G.S. Prof. Paper 245, 1953.

Lowdon, J. A., 1960, "Age Determinations by the Geological Survey of Canada", Report I on Isotopic Ages, Paper 60-17.

McRitchie, 1950, "High-Temperature Resistance Furnace", J. Am. Ceramic Soc. 33, p. 25.

Mehnert, K. R., 1958, "Argon Determinations on K-Minerals VI - The Geological Development of the Black Forest Pre-cambrian by means of Age Determinations by the K-A Method", G.C.A. vol. 14, p. 105.

Newman, A. B., 1931, "The Drying of Porous Solids" "Diffusion Calculations", Trans., A. Inst. of Chem. Engineers, vol. 27, p. 310.

Nicolaysen, L. O., 1957, "solid Diffusion in Radioactive Minerals and the Measurement of Absolute Age", G.C.A. vol. 11, p. 41.

J. W. de Villiers, A. J. Burger, and F. W. E. Strelow, 1958, "New Measurements Relating to the Absolute Age of the Transvaal System and of the Bushveld Igneous Complex", Trans. of the Geol. Soc. of South Africa, vol. LXI.

Ovchinnikov, L. N., V. V. Kelarev. M. V. Panova, V. A. Dunaev, F. L. Shangareev and R. I. Osadchaya, 1959, "Retention of Argon in Micas", 8th Session of the Commission on the Determination of Absolute Age of Geologic Formations, Moscow.

Pahl, M., J. Hiby, F. Smits, W. Gentner, 1950, "Mass Spectrometric Determinations of Argon from Potash Salts", Zeitchrift fur Naturforshung, vol. 5a, p. 404.

Phinney, W. C., 1959, "Phase Equilibrium in the Metamorphic Rocks of St. Paul Island and Cape North, Nova Scotia", Ph.D. thesis, M.I.T.

Pinson, W. H., H. W. Fairbairn, R. F. Cormier, 1958, "Sr/Rb Age Measurements on Hornblende and Feldspar and the Age of Syenite at Chicoutimi, Quebec, Canada", Bull. G.S.A. vol. 69, p. 599.

Reichenberg, D., 1953, "Properties of Ion-Exchange Resin in Relation to their Structure, III. Kinetics of Exchange", J. Amer. Chem. Soc. 75, p. 589.

Reynolds, J. H., 1956, "High Sensitivity for Noble Gas Analysis", Rev. Sci. Inst., vol. 27, No11, p. 928.

1960, "A Determination of the Age of the Elements", Physical Review Letters, vol. 4, #1.

Reynolds, M. B., 1956, "Diffusion of Argon in a K-Ca Silica Glass", A.E.C. Report KAPL-1612, Schenectady, N.Y. (also in J. Am. Ceramic Soc. 1956).

Rubinstein, M. M., B. G. Chikvaidze, A. L. Khutzaidze and C. Y. Gelman, 1959, "Using Glauconite for Absolute Age Determination of Sedimentary Rocks by the Argon Method", Izvestiia, Ac. Sci. SSSR, Geol. Series, No. 12, pp. 76-83.

Sardarov, S. S., 1957, "New Reactor For Separating and Cleaning of Radiogenic Argon", Trans. Ac. Sci. Ser. Geol. #4, p. 108.

1957, "The Preservation State of Radiogenic Argon in Microclines", Geokhimmia #3.

Schneider, 1950, "Temperature-Controlled Resistance Furnace", Rev. Sci. Inst. 21, (1) p. 94.

Schreiner, G. D. L., 1957, "Comparison of the ^{87}Rb - ^{87}Sr Ages of the Red Granite of the Bushveld Complex from Measurements on the Total Rock and Separated Mineral Fractions", Bernard Price Institute of Geophysical Research, Johannesburg.

Smith, W. 1938, "Geology of the Caribou Stock in the Front Range, Colorado", Am. J. Sci. 5th Ser, vol. 36, p. 8-26.

Smits, F. and W. Gentner, 1950, "Argon Determinations on K-Minerals I - Determinations on Tertiary Potash Salts", G.C.A., vol. 1, p. 22.

J. Zahringer, 1955, "A Mass Spectrometer for very Small Amounts of Gas", Zeitschrift fur Angenwandte Physik, vol. 7, p. 313.

Starik, I. E., and L. A. Litvina, 1958, "Application of the Leaching Method in Evaluating the Suitability of Samples for Age Determination by the Argon Method", Geokhimiia #2.

V. V. Kurbatov, L. A. Litvina, 1959, "Concerning The Influence of Heat on the Structure of Mica and Microcline, and about the Preservation of Argon in Them", Zapiski Ve. Mineralogiia, Seria 2, Chast 88, Vipusk 6, ANSSSR.

Strickland, L., 1956, "Improvements in Methods of Extraction, Purification and Measurement of Radiogenic Argon in Minerals", Ph.D. Thesis, M.I.T.

Tilton, G. R., L. T. Aldrick and M. G. Inghram, 1954, "Mass Spectrometric Determination of Thorium", Analytical Chemistry, vol. 26, p. 894.

C. Patterson, H. Brown, M. Inghram, R. Hayden, D. Hess, and E. Larsen, Jr., 1955, "Isotopic Composition and Distribution of Lead, Uranium, and Thorium in a Precambrian Grnaite", Bull, G.S.A., vol. 66, pp. 1131-1198.

1956, "The Interpretation of Lead-Age Discrepancies, by Acid-Washing Experiments", Transactions, A.G.U., vol. 37, No. 2.

G. L. Davis, G. W. Wetherill, L. T. Aldrich, 1957, "Isotopic Ages of Zircon from Granites and Pegmatites", Transactions A.G.U., vol. 38, pp. 360-371.

LO. Nicolaysen, 1957, "The Use of Monazites for Age Determiaation", Geochim. et Cosmochim. Acta, vol. 11, pp. 28-40.

1958, "Isotopic Composition of Lead from Tektites", Geochim. et Cosmochim. Acta, vol. 14, No. 4, pp. 323-330.

G. W. Wetherill, G. L. Davis, C. A. Hopson, 1958, "Ages of Minerals from the Baltimore Gneiss near Baltimore, Maryland", Bull, G.S.A., vol. 69, pp. 1469-1474.

G. L. Davis, 1960, "Solid Diffusion as a Mechanism for Discordant Lead Ages", Abstract, A.G.U. Annual Meeting, Proceedings of Conference on "Geochronology of Rock Systesm", Annals of the N.Y. Academy of Science, in press.

Tomlinson, 1950, "Vacuum Furnace", Rev. Sci. Inst. 21 (6), p. 507.

Tuttle, O. F., N. L. Bowen, 1958, "Origin of Granite in the Light of Experimental Studies in the System $NaAlSi_3O_8$-$KAlSi_3O_8$-SiO_2-H_2O", G.S.A. Memoir 74.

Van Orstrand, 1944, "Flow of Heat from an Intrusive Body into Country Rock", A.I.M.E., Technical Publication No. 1677.

Wahlstrom, E. E., 1940, "Geology of the Audubon-Albion Stock", Bull. G.S.A., vol. 51, #12, p. 1789.

Wasserburg, G. J., 1954, "Ar^{40}-K^{40} Dating", in Nuclear Geology, John Wiley and Sons, Inc., New York.

and G. M. Wetherill, 1959, "Ages on the Precambrian of Death Valley, California", Abstract, Annual Meetings, A.G.U., 1959.

Webber, G. R., P. M. Hurley, and H. W. Fairbairn, 1956, "Relative Ages of Eastern Massachusetts Granites by Total leadRation in Zircon", Am. J. Sci. 254,

Weeks, W. F., 1956, "A Thermochemical Study of Equlibrium Relations During Metamorphism of Siliceous Carbonate Rocks", J. Geo., vol. 64, No. 3.

Wetherill, G. W., L. T. Aldrich, G. L. Davis, 1955, "A^{40}/K^{40} Ratios of Feldspars and Micas from the Same Rock", Geochim. et Cosmochim. Acta, vol. 8, pp. 171-172.

1956, "Discordant Uranium-Lead Ages, I", Transactions, A.G.U., vol. 37, No. 3.

1956, "An Interpretation of the Rhodesia and Witwatersrand Age Patterns", Geochimical Notes, Geochim. et Cosmochim Acta, vol. 9, Nos. 5/6, pp. 290-292.

G. R. Tilton, G. L. Davis, L. T. Aldrich, 1956, "New Determinations of the Age of the Bob Ingersoll Pegmatite Keystone, S. Dakota", Geochim. et Cosmochim. Acta, Vol. 9, Nos. 5/6, pp. 292-297.

Wones and Eugster, 1959, "Biotites on the join Phlogopite-Annite", 1958-1959 Annual Repot of the Director of the Geocpysical Laboratory, Washintgon, D.C.

Youden, W. J., 1951, "Statistical Methods for Chemists", John Wiley and Sons.

Zener, C., 1952, "Theory of Diffusion", "Imperfections in Nearly Perfect Crystals", Symposium, Shockley, chairman.

Biographical Sketch

The author was born in Lynn, Massachusetts in 1935. He was educated in the Lynn Public School system, graduating in 1952 from Lynn English High School. Undergraduate training in Geology at M.I.T. led to the S.B. degree, received in June, 1956. While an undergraduate the author was active with the M.I.T. Outing Club, serving as President in 1954. He was also a member of the M.I.T. Ski Team which won the Intercollegiate Championships in 1956. A year of study at California Institute of Technology led to a Master's degree in Geochemistry in 1957.

His professional experience includes three summers as a research Associate on the Geochronology project at M.I.T, a summer with a Gulf Oil Co. seismic crew, and a summer of exploration geophysics for Newmont Exploration, Ltd. The author held teaching and research assistantships during his graduate years at M.I.T. and C.I.T.

The author is a member of the Geochemical Society, the American Geophysical Union and the Geological Society of America.

He was married in 1956 to Joanna Smith of Conway, N.H., and has one daughter, Jolene Kaweah, born in 1957.

The author has accepted a Postdoctoral fellowship with the Department of Terrestial Magnetism, Carnegie Institution of Washington, for the coming year.